Cover Page

The handle http://hdl.handle.net/1887/35931 holds various files of this Leiden University dissertation

Author: Deventer, Sjoerd van
Title: Tracking the big ones : novel dynamics of organelles and macromolecular complexes during cell division and aging
Issue Date: 2015-10-21

Tracking the big ones: Novel dynamics of organelles and macromolecular complexes during cell division and aging

Sjoerd Jan van Deventer

If you are told that a bag full of marbles could be alive, you would never believe it.
Still, this is exactly what a cell is; a bag full of lifeless material that is very much alive!

Tracking the big ones: Novel dynamics of organelles and macromolecular complexes during cell division and aging

PROEFSCHRIFT

ter verkrijging van
de graad van Doctor aan de Universiteit Leiden,
op gezag van Rector Magnificus prof. mr. C.J.J.M. Stolker,
volgens besluit van het College van Promoties

te verdedigen op woensdag 21 oktober 2015
klokke 13:45 uur

door

Sjoerd Jan van Deventer

geboren te Apeldoorn op 25 september 1984

Promotiecommissie:

Promotor:	Prof. dr. J.J. Neefjes
Co-Promotor:	dr. F. van Leeuwen *Nederlands Kanker Instituut*
Overige leden:	Prof. dr. F. A. Ossendorp
	Prof. dr. H.S. Overkleeft
	Prof. dr. H. Ovaa
	dr. E. A. J. Reits *Universiteit van Amsterdam*
	dr. V. Menendez-Benito *Karolinska Institutet (Zweden)*

Table of contents

Scope of the Thesis

Although Heraclitus did most likely not think about proteins when he made his famous statement "Panta Rhei", this saying applies very well to proteins inside cells. Cellular proteins are highly dynamic due to continuous synthesis, degradation, modification, translocation and interactions with other cellular components [1–3]. Protein dynamics is an absolute requirement for life and aberrations of it are implicated in several diseases. Understanding the processes underlying protein dynamics is pivotal to understanding these diseases and developing effective treatments [2–4]. In this Thesis we address two important aspects of protein dynamics; protein synthesis and distribution upon cell division and dynamics of the protein degradation machinery.

Upon cell division, a cell needs to distribute its components in such a way that both of the new cells get enough starting material to support a successful life. This is accomplished by sharing the existing components of the mother cell (inheritance) and by the synthesis of new components. Synthesis of macromolecular complexes and organelles can occur *de novo*, or by growth and division of existing structures (template-based). The template-based synthesis of some of these essential cell structures makes the inheritance of the existing components particularly important. The mechanisms underlying the inheritance of organelles and macromolecular complexes have been successfully studied in budding yeast and are often found conserved in mammalian cells [5]. Budding yeast has the advantage of easy genetics and a distinguishable 'mother' and 'daughter' cell upon cell division and is therefore used as a model organism in this Thesis.

In this Thesis we applied a new tool, Recombination-Induced Tag Exchange (RITE) [6,7], to visualize novel aspects of inheritance and synthesis of organelles and macromolecular complexes in budding yeast. RITE is able to distinguish and simultaneously track old and new proteins and can thus be used to study the inheritance of existing (old) cell components and the synthesis of new components [6,7]. Using RITE, we made a comprehensive analysis of the inheritance and synthesis of all organelles and the major macromolecular protein complexes in cells. Our data resolves ongoing debates on the synthesis of certain organelles (*de novo* or template-based) and visualizes patterns of symmetric and asymmetric inheritance [8]. Asymmetric inheritance of organelles is of interest since it may define lineage differences and play a role in the differentiation of mammalian cells [9,10].

The dynamics of the protein degradation machinery is of interest since it affects the degradation of damaged proteins in aging cells. Damaged proteins tend to accumulate in aging cells and are implicated in several age-related diseases [3]. This suggests that insufficient degradation of damaged proteins is a dominant factor in cellular aging. An important mechanism for the degradation of damaged proteins is the ubiquitin-proteasome system (UPS) [11]. The activity of the UPS is found to decrease during the aging of several model organisms and this decrease is suggested to play a causative role in cellular aging [12–14]. Also, enhanced UPS activity seems to correlate with enhanced longevity [15,16]. These observations fueled a growing interest in the role of UPS activity in the aging process and raise the possibility of curing age-related diseases by enhancing this activity. In this Thesis we present data that suggest that not only the activity of the UPS, but also the localization of this activity may play a role in cellular aging. We tracked the localization of the degrading entity of the UPS (the proteasome) in starving budding yeast cells, a frequently used aging model. We observed a correlation between the localization of

the proteasome and the age of the cell and identified genetic factors controlling both proteasome localization and the fitness of aging cells [17].

One reason for insufficient UPS activity in aging cells may be a less 'fit' pool of proteasomes. Being a protein complex itself, the proteasome is also vulnerable to protein damage. Therefore, analogous to damaged proteins, one would expect damaged proteasomes to be cleared from the cell. The scope and mechanisms of such proteasome quality control however, remain to be determined. Earlier studies suggested that the proteasome is an extremely stable complex with a reported half-life ranging from 5 to 12 days [18–20]. Studies in rat liver suggest that proteasomes are degraded in the lysosomal compartment [20]. In this Thesis we present data supporting lysosomal degradation of proteasomes in budding yeast and HeLa cells, which are better suited model systems for further study then rat livers. Also, our findings in HeLa cells are consistent with a model in which damaged proteasomes are delivered to the lysosome by autophagy.

In summary, this Thesis addresses synthesis and distribution of proteins upon cell division and the dynamics of the protein degradation machinery. Application of RITE technology in budding yeast gave us the unique opportunity to track both the age of proteins and of cells, which yielded novel insights relevant for cell differentiation and cellular aging. In the study of a possible degradation mechanism for the proteasome, we extended our findings in yeast to a mammalian cell line.

Chapter 1:

General Introduction

General introduction

To survive as a single cell or to function within a multi-cellular organism, cells need to continuously adapt their internal processes to changing internal and external signals and stressors. Cellular processes can be modulated by controlling the local abundance and activity of proteins. This is achieved by continuous and highly regulated synthesis, degradation, folding, modification and translocation of proteins. Protein dynamics therefore lies at the heart of virtually all cellular process and aberrations of it are implicated in several diseases. To understand cellular processes and possibly treat these diseases, knowledge of the underlying protein dynamics is essential. [1–4] In this Thesis we address two important aspects of protein dynamics: protein synthesis and distribution upon cell division and dynamics of the protein degradation machinery.

Cell division: A matter of equal sharing?
When cells divide they give rise to two new cells. Cell division is as simple as that. However, as is often the case when things need to be divided, the exact distribution of components is a more complicated issue. The heritage of the original cell consists of both functional and damaged cellular components. Either type needs to be distributed adequately over the two new cells to support a successful life of the next generation. Adequate distribution of cellular components is an absolute prerequisite for life and therefore tightly regulated. The importance and tight regulation of this distribution is exemplified by the process of DNA replication and chromosome distribution during cell division.

'Adequate distribution of cellular components' does not necessarily mean 'equal distribution'. In fact, asymmetric sharing of cellular components appears to be an important aspect of cell divisions across the kingdoms of life. In single cell organisms asymmetric cell division is suggested to be important to generate phenotypic variation in a population, which allows this population to survive a variable environment. Moreover, asymmetric distribution of damaged cell components provides a way to restrict the consequences of aging in one cell at the expense of another. This prevents aging of the entire population, which may otherwise lead to mass extinction. In multicellular organisms asymmetrical distribution of cell components has been suggested to be essential for the creation of differentiated cells and the maintenance of germ lineages and stem cell populations. [9,10,21,22]

Asymmetric distribution of cellular components has both quantitative (one cells gets more than the other) and qualitative (one cell gets components with different characteristics) aspects. Quantitative aspects of asymmetrical inheritance are relatively easy to address and examples include asymmetric distribution of a nuclear transport factor [23] and of plasma membrane proton ATPase's [24]. Qualitative aspects of asymmetric distribution are usually caused by subtle changes in composition or small modifications of the protein (complex) leading to altered functionality. The functional significance of these subtle differences is often unknown, but may induce lineage differences. In budding yeast, for example, the asymmetric distribution of malfunctioning mitochondria defines an 'old' and a 'young' lineage [25,26]. Another example is formulated by the immortal DNA strand hypothesis, which suggests that stem cells retain a template copy of genomic DNA to avoid buildup of replication-induced mutations [27].

Asymmetric distribution of cell components and the potential lineage differences they induce are relatively easy to study in the budding yeast *Saccharomyces cerevisiae* [5]. This

unicellular eukaryotic organism produces two morphologically distinct cells upon cell division, a 'mother' and a 'daughter, that differ in age and define an 'old' and a 'young' cell lineage. Asymmetric distribution of cell components that consistently favor one of the two lineages may therefore be connected to the aging of the old lineage or the fitness of the young lineage [22]. The asymmetric distribution of cell wall components can be used to define both lineages. Upon cell division the mother cell keeps its own cell wall, whereas the cell wall of the emerging daughter cell (bud) is formed completely *de novo* [28]. When the daughter breaks away from the mother cell, chitinous scar tissue (the bud scar) is left on the mother cell. Every cell division leads to a new bud scar which allows tracking of the number of cell divisions a mother cell underwent [29]. This allows the study of the cumulative effects of multiple cell divisions with asymmetric distribution of cellular components.

Adequate distribution of cell components is of particular importance for organelles and macromolecular complexes since they are essential, often synthesized in a template-based manner and their size and complexity don't always allow rapid synthesis after cell division. Like chromosomes, the distribution of these large cell components is therefore actively controlled during cell division. This process is extensively studied in *S. cerevisiae* and involves three fundamental steps: cell polarization, transport and retention. Cell polarization is established by a complex signaling network that recruits formin proteins to the cell membrane at the future bud site. Formins act as a nucleation point for the assembly of unbranched actin cables. These cables function as the transport route for cell membrane and cell wall material which is deposited at the growing bud site. Later, these cables serve the transport of cellular organelles from the mother cell into the growing bud (Figure 1). The transport itself is mediated by class-V myosin motor proteins that recognize the different organelles by specific receptor molecules. Important exceptions are the nucleus and the nuclear ER, which depend on microtubules for their transport towards the daughter cell. Once at their destination, organelles need to be retained by tethering, e.g. to the cytoskeleton or the cell cortex, to prevent them from diffusion back into the mother cell. To make sure the mother cell keeps enough organelles for herself, some organelles are retained in the mother cell, as has been shown for peroxisomes [5]. Many of the key aspects of the mechanisms to distribute organelles upon cell division in yeast are conserved in mammalian cells and are reviewed by Jongsma *et al* [30].

To ensure that both new cells get sufficient amounts of organelles and macromolecular complexes, sharing the pre-existing components of the original cell (inheritance) is not enough. To support life in both new cells the pre-existing components need to be supplemented with synthesis of new components, which can either occur before or after cell division. Whether pre-existing (old) and newly synthesized components are equally shared between the two new cells, is unknown for most organelles and macromolecular complexes. One exception is the spindle pole body (SPB), the yeasts centrosome, for which it is reported that one cell inherits mainly old proteins and the other cell mainly new proteins [31]. This asymmetric distribution of old and new SPB proteins may imply functional differences between the two SPB's, which may induce lineage differences. Whether this qualitative asymmetric distribution is a curiosity of the SPB or a common topic for organelles and macromolecular complexes was unclear. A comprehensive analysis of the different organelles would greatly benefit from methods to simultaneously visualize old and new proteins.

Synthesis of new organelles and complexes can take place *de novo* or template-based. Template-based synthesis of an organelle or complex is a combination of growth by

Fig. 1

Figure 1: Organelle transport in dividing budding yeast
When a yeast cell divides, a daughter cell (bud) emerges from the mother cell. To equip the bud with all necessary organelles, a mother cell transports a portion of her organelles towards the emerging bud. For most organelles this transport is mediated by Myosin-V motor proteins that 'walk' along actin cables from the minus to the plus end. The directionality of this transport towards the bud is facilitated by the polar distribution of formin proteins, which position the formation of actin cables (and thus the plus end) at or near the emerging bud. To transport organelles, they are attached to the motor proteins by organelle-specific receptor molecules. In contrast to the actin-based transport of most organelles, the nucleus is transported along microtubules. Microtubules attach with their minus end to the nucleus at the spindle pole body and are oriented towards the bud by actin-based transport of their plus end. Pulling forces on the microtubules drag half of the nucleus towards the daughter cell and retain the other half in the mother cell.

addition of new components and division in two new organelles or protein complexes. A well-established example of this method is the formation of new mitochondria by growth and division [32]. Also the ER is thought to utilize this method as many of its constituents require functional ER for their synthesis. Macromolecular complexes like the proteasome or the ribosome on the other hand are formed completely *de novo* [33,34]. However, the contribution of *de novo* and template-based synthesis is much debated for other organelles and macromolecular complexes. Peroxisomes, for example, are proposed to form *de novo* using the ER as a platform for their synthesis [35,36], but also by growth and division [37]. As for their asymmetrical inheritance, the study of organelle and macromolecular complex synthesis would greatly benefit from methods to track old and new proteins simultaneously.

How to distinguish and track old and new proteins?
Several methods have been developed to distinguish and simultaneously track old (synthesized long ago) and new (recently synthesized) proteins. These methods can be divided into four categories: differential chemical labeling, differential isotope labeling, fluorescent timers, and photo-transformable fluorescent proteins.
Differential chemical labeling involves the expression of a protein with a tag that reacts

1

with different chemical probes. Sequential administration of these probes allows tracking of old (labeled with the first probe) and new (labeled with the second probe) proteins. Several (differential) chemical labeling methods tag the protein of interest with an enzyme and use modified (eg. containing a fluorescent group) substrate molecules as chemical probe. Commonly used examples are SNAP-, CLIP-, and Halo tags [38–40]. The protein of interest can also be tagged with a small peptide tag, like the tetra-cysteine sequence used for FlAsH-ReAsH labeling [41].

Differential isotope labeling is usually achieved by stable-isotope labeling by amino acids in cell culture (SILAC) during a defined time (pulse), followed by a chase in the presence of the 'normal' amino acids [42]. New and old proteins can now be distinguished by mass spectrometry by the mass differences caused by the isotopic labeled amino acids. Commonly used isotope labeled amino acids include ^{2}H leucine, ^{13}C lysine and ^{15}N arginine. Differential isotope labeling has been successfully used to track the inheritance of (very) old proteins in budding yeast and to reveal the long-lived proteome in rat brains [43,44].

A fluorescent timer is a protein tag that changes its fluorescent properties as a function of time. An example is dsRed, which undergoes a fluorescence shift during its slow maturation [45]. Newly synthesized dsRed-tagged proteins will first have green fluorescence, whereas the fluorescence of older proteins will have matured to red. This fluorescent timer was successfully used to address the distribution of old and new proteins of the yeast SPB upon cell division [31]. Another example is a series of mCherry derivatives developed by Subach *et al* that change their fluorescence over time from blue to red. As a result, newly synthesized proteins show blue fluorescence whereas older proteins show red fluorescence. These fluorescent timers were developed with a half-life for the shift in fluorescence of 0.25, 1.2 and 9.8h [46]. Unlike the other methods to distinguish and track old and new proteins, fluorescent timers entail a continuous flux from the new to the old population.

This limitation is largely overcome in the use of photo-transformable fluorescent proteins (PTFPs). PTFPs change their fluorescent properties upon exposure to light of a specific wavelength. A well-known example is photo-activatable GFP (PA-GFP), which only starts to fluoresce like a GFP molecule after exposure to intense 405 nm light [47]. PTFPs allow simultaneous tracking of new and old proteins by their fluorescent properties. The last ten years have shown a tremendous expansion of the collection of PFTPs, fuelling many new and exciting imaging techniques, like super resolution microscopy [48].

The different techniques to assess the (relative) age of proteins have led to valuable new insights in protein dynamics. However, with the exception of some differential chemical labeling methods, these techniques do not provide handles for selective purification or biochemical analysis of old and new proteins. Differential chemical labeling then has the drawback of the need for (expensive) chemicals. Also, presented techniques are not easily incorporated in (genetic) screenings. These limitations of the existing techniques are largely overcome by a novel technique that we present in this Thesis; Recombination-Induced Tag Exchange (RITE) [5]. RITE allows distinction and simultaneous tracking of old and new proteins and the used protein tags can be easily adjusted to the experimental needs.

Protein Quality Control counteracts accumulation of damaged proteins during aging

Another aspect of protein dynamics that is addressed in this Thesis is the dynamics of the protein degradation machinery in aging cells. In aging cells, damaged proteins tend to

accumulate, which is a hallmark of cellular aging and implicated in several age-related diseases. This suggests that the degradation of these proteins is insufficient and that protein degradation is a relevant factor in cellular aging. However, protein degradation is only one modality of a larger system that prevents the accumulation of damaged proteins: the Protein Quality Control (PQC) system. The cellular PQC system has two modalities, protein refolding and protein degradation, that often compete for the same damaged proteins [2].

Cellular proteins are continuously at risk for (partial) unfolding, e.g. as a result of post-translational modifications or altered concentrations of certain metabolites. Various cellular stresses, like osmotic stress or heat shock, can dramatically increase this risk. Not only are (partially) unfolded proteins less likely to function properly, they also tend to cluster with other (misfolded) proteins. This clustering is often caused by the exposure of hydrophobic patches as a result of protein unfolding and may lead to the formation of harmful aggregates. To maintain proper folding, cellular PQC employs a family of 'refolding' proteins; chaperones. Some chaperone proteins, like the small heat shock proteins, bind the (partially) misfolded proteins, thereby shielding their exposed hydrophobic patches and preventing aggregate formation. Other chaperones are also able to support the refolding of substrate proteins in an ATP-dependent process, like chaperones belonging to the HSP70 family [1,49]. How chaperones 'decide' when proteins are correctly folded, is unclear but probably relates to the absence of hydrophobic patches as detected by these various chaperones.

When a soluble protein cannot be refolded, the cellular PQC system can only destroy the protein to prevent the formation of aggregates. There are two 'degrading entities' to degrade these proteins; the proteasome and the lysosome. The proteasome is a multi-subunit protein complex containing protease activity, whereas the lysosome is a membrane enclosed compartment containing multiple proteases [50]. The proteasome and the lysosome have in common that they shield their catalytic activity from the rest of the cell to prevent unwanted degradation. Although safe, this necessitates the cell to 'present' the proteins to be degraded to the degrading entities. In case of the lysosome this is either mediated by direct import of the proteins to be degraded or by fusion with vesicles containing these proteins [51,52]. These vesicles can for example originate from autophagy or the endocytic machinery [52,53]. In case of the proteasome, substrate molecules are presented by the ubiquitin-proteasome system (UPS) [11].

The UPS is the primary degradation mechanism for the specific degradation of short-lived regulatory proteins and damaged soluble proteins. The UPS enables protein degradation in a time and place specific manner and is essential for virtually all cellular processes. The UPS is an extensive network of co-operating proteins (and protein complexes) and can be divided in a part that marks the proteins to be degraded (the ubiquitination machinery) and a protein complex that degrades the marked proteins, the 26S proteasome [11] (Figure 2).

The recognition signal for proteasomal degradation is a ubiquitin chain attached to the protein to be degraded. The covalent attachment of ubiquitin to the target protein is called ubiquitination. Ubiquitination is performed by an ATP-dependent enzymatic cascade involving three classes of enzymes; ubiquitin-activating enzymes (E1), ubiquitin-conjugating enzymes (E2) and ubiquitin-ligating enzymes (E3). Together they form an isopeptide bond between the ε-amino group of substrate lysines and the carboxyl group at the C-terminal glycine of ubiquitin. The presence of internal lysines in ubiquitin allows

the formation of poly-ubiquitin chains. The signal conveyed by the poly-ubiquitin chain is highly dependent on the internal lysines used to make the chain. A lysine 63 linked ubiquitin chain for example is a signal to be degraded by autophagy, whereas a chain of at least four ubiquitins linked via lysine 48 is the typical recognition signal for the 26S proteasome [11,54].

The 26S proteasome is the macromolecular protease responsible for the degrading capacity of the UPS. The 26S proteasome consists of one 20S core particle (CP) flanked by one or two 19S regulatory particles (RP). Within the 26S proteasome the 20S CP is the degradation functionality, whereas the 19S RP's are needed for recognition of ubiquitinated substrates and their translocation in the 20S CP [33].

The 20S CP consists of four stacked heptameric rings, together forming a barrel-shaped structure with an inner catalytic chamber. The catalytic activity in this chamber comes from three catalytic active subunits in each of the two inner, or β, rings. The two outer, or α, rings close the catalytic chamber leaving only a small entrance. To prevent untargeted degradation of proteins, the access through this 'gate' is restricted by the N-terminal tails of the α-subunits. This renders the 20S CP on its own largely inactive towards folded peptides. To activate the 20S CP it needs to associate with one of several proteasome activators, the most common of which is the 19S RP [33].

The 19S RP recognizes ubiquitinated proteins, de-ubiquitinates them to recycle ubiquitin,

Fig. 2
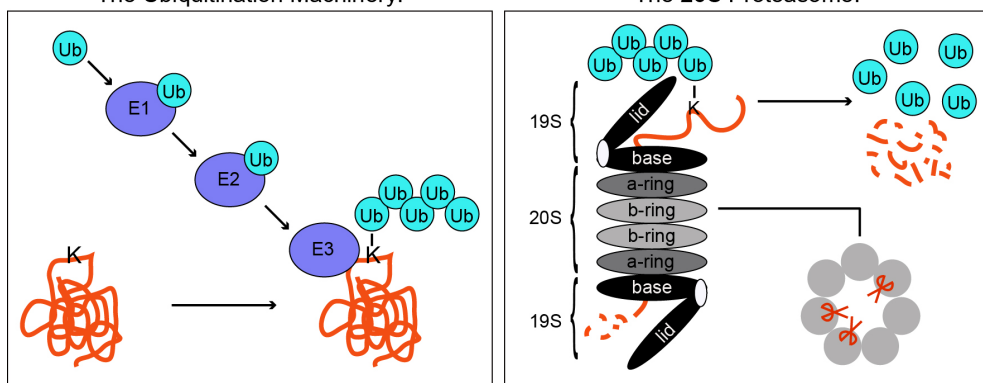
Figure 2: The ubiquitin-proteasome system
The ubiquitin-proteasome system (UPS) facilitates specific degradation of proteins and can be divided in two parts; the ubiquitination machinery and the 26S proteasome.
The ubiquitination machinery marks proteins for degradation by covalent attachment of ubiquitin (Ub). This is mediated by an extensive network of ubiquitin-activating (E1), ubiquitin-conjugating (E2) and ubiquitin-ligating (E3) enzymes. Together E1, E2 and E3 form an enzymatic cascade that attaches ubiquitin to an internal lysine residue (K) of the targeted protein. The presence of lysine residues in ubiquitin itself allows the formation of poly-ubiquitin chains. A chain of at least four ubiquitins attached via lysine 48 is the typical recognition signal for the 26S proteasome.
The 26S proteasome recognizes ubiquitinated substrates and degrades them into peptide fragments. The 26S is a proteins complex that can be subdivided in a central 20S particle and two flanking 19S particles. The 20S particle contains protein degrading activity inside a barrel-like structure formed by the stacking of four heptameric rings. The two inner (or β-) rings contain three catalytic active subunits each, which supply protein degrading activity to the 20S. The two outer (or α-) rings close the access to the degrading activity by blocking the entrance of the barrel-like structure with their N-terminal tails. This 'gate' can be opened by the 19S particle. The 19S particle consists of two sub-complexes; the base and the lid. The lid recognizes ubiquitinated substrates and removes the ubiquitin, whereas the base unfolds the substrates and transports them into the 20S barrel.

and then unfolds them before translocation into the 20S catalytic chamber where they are degraded. The 19S RP consists of a base and a lid complex. The lid complex is important for substrate recognition and de-ubiquitination and is loosely connected to the base by a 'hinge' subunit. Recognition of ubiquitinated proteins is mediated by two ubiquitin receptors; RPN10 and RPN13. De-ubiquitination is mediated by the RP resident RPN11, possibly aided by the proteasome associated dubs USP14 and UCH37. The base is attached to the 20S proteasome where it opens the 'gate' formed by the N-terminal tails of the α-subunits. Six AAA+ ATPase subunits in the base are required for unfolding and possibly translocation of the substrate protein [55]. In summary, the 26S proteasome is a multi-protein protease with a unit for substrate recognition and unfolding (the 19S) and a unit for degradation (the 20S).

The other degrading entity at the disposal of cellular PQC is the lysosome. Damaged cytosolic proteins, and even damaged organelles, are targeted to the lysosome by a process called autophagy. The autophagy lysosome system (ALS) was long considered a non-specific degradation mechanism for bulk degradation of cytoplasmic proteins and compartments [56]. However, over the years increasing specificity has been assigned to this process, like the identification of specific autophagy mechanisms for ribosomes and mitochondria [56,57].

Different ways of lysosomal targeting define three different forms of autophagy; macro-autophagy, micro-autophagy and chaperone-mediated autophagy (Figure 3). Macro-autophagy is most predominant and includes the formation of a double membrane, the phagophore, around cytosolic proteins or organelles that are destined for degradation. When the phagophore completely encloses its substrates it is called an autophagosome. The autophagosome then fuses with the lysosome, leading to the degradation of its contents. Substrates for macro-autophagy are recognized by autophagic adaptor proteins, like P62, which couple them to the growing phagophore [52]. Micro-autophagy is a more direct way of cargo delivery to the lysosome, as the lysosome acquires its substrates by their endocytosis. Central in the selection of cargo by the lysosome is the chaperone protein HSC70 [52,58]. The direct uptake of substrate proteins is also apparent in chaperone-mediated autophagy (CMA), though CMA uses a protein translocation complex instead of endocytosis to deliver substrates to the lysosome [51].

Apart from refolding and degradation, another important aspect of PQC mechanisms is the sequestration of damaged proteins in PQC compartments. Several different PQC compartments have been described with distinct composition, function and localization in the cell [59]. The JUxtaNuclear Quality control compartment (JUNQ), for example, is localized near the nuclear ER and contains soluble, ubiquitinated, damaged proteins as well as many chaperones and active proteasomes. Its proposed function is to enhance the efficiency of the PQC by sequestering (and thus concentrating) the important players. The Insoluble Protein Deposit compartment (IPOD) on the other hand resides near the lysosome and contains terminally aggregated proteins. Its function is thought to be the scavenging of potentially harmful misfolded proteins [60,61].

Apart from enhancing PQC efficiency and scavenging harmful proteins, sequestration of protein damage also facilitates asymmetric inheritance of damaged proteins. Association of these compartments with the cytoskeleton or organelles is proposed to restrict their presence to the older lineage upon cell division. In bacteria and fission yeast for example, aggregated proteins are sequestered at the old pole of a dividing cell [62,63]. In budding yeast on the other hand, protein aggregates are retained in the mother cell by association

Fig. 3
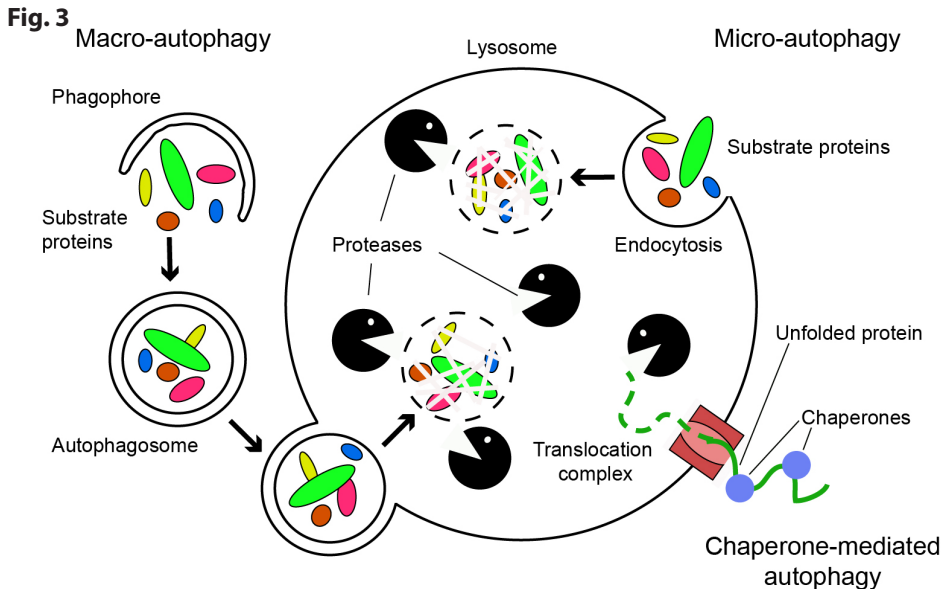
Figure 3: The autophagy lysosome system
The autophagy lysosome system (ALS) enables the degradation of proteins, complexes and even organelles in the lysosome. To this end, the lysosome is filled with proteases and other degrading enzymes. Substrates are targeted towards the lysosome by autophagy, which can be subdivided in three different classes; Macro-, Micro-, and Chaperone-mediated- autophagy.
Macro-autophagy entails the formation of a double membrane, the phagophore, around the cytosolic substrates. When the substrates are completely engulfed it is called an autophagosome. The autophagosome delivers its contents to the lysosome by fusing with the lysosomal membrane. Micro-autophagy is the direct endocytosis of substrates by the lysosome and their subsequent degradation. In chaperone-mediated autophagy, substrate proteins are recognized and unfolded by chaperones and transported across the lysosomal membrane by a translocation complex.
Together, the different modes of autophagy allow the ALS to (specifically) degrade a wide variety of substrates.

with the polarisome [64]. A recent study in mammalian cell lines, that are supposed not to have lineage differences, showed asymmetrical inheritance of JUNQ, possibly mediated by the intermediate filament vimentin [65].
In summary, cells prevent the accumulation of damaged proteins by the protein quality control (PQC) system. The PQC system initially tries to repair the damaged proteins, e.g. by employing chaperones to refold unfolded proteins. When repair fails, cells have two systems for the degradation of damaged proteins; the ubiquitin-proteasome system (UPS) and autophagy lysosome system (ALS). Together these systems prevent harmful accumulation of damaged proteins and thus support healthy cellular aging.

Yeast as a model system for cellular aging
The budding yeast *Saccharomyces cerevisiae* is an important model organism in age-related research. Because it is easy to quantify longevity in budding yeast and because it is easy to manipulate its genome. This has allowed the identification of dozens of factors affecting longevity and the identification of several mechanisms underlying aging [22]. The search for homologues of these factors in higher eukaryotes has made major contributions

to mammalian aging research. Most notable is the identification of the sirtuins, a family of NAD$^+$ dependent protein deacetylases. Decreasing its activity in yeast and several other lower eukaryotes results in decreased longevity, whereas increased activity correlates with increased longevity. In mammalian cells, sirtuins have less drastic effects, although they have been implicated in several age-related processes and diseases [66].

When we define cellular aging as the accumulation of cellular damage resulting in a gradual loss of the cells functionality, we can distinguish two modes of aging in budding yeast: chronological aging and replicative aging (Figure 4). In chronological aging damage accumulates over time in a non-dividing cell, which as a result will eventually lose its capacity to divide and then dies. To measure chronological life span, one monitors the viability of a population of non-dividing cells over time. A population of non-dividing cells is obtained by starving cells in a liquid culture and viability is defined as the ability to resume cell growth once fresh medium is added [22]. Replicative aging is the accumulation of cell damage in the mother cell, due to the asymmetric distribution of cell damage upon cell division. Each time a yeast cell divides, the mother cell retains all cell damage in order to give rise to the fittest daughter cells possible. The cumulative effect of 25-30 of these asymmetric divisions will lead to a terminal replicative senescence [67]. Replicative life span
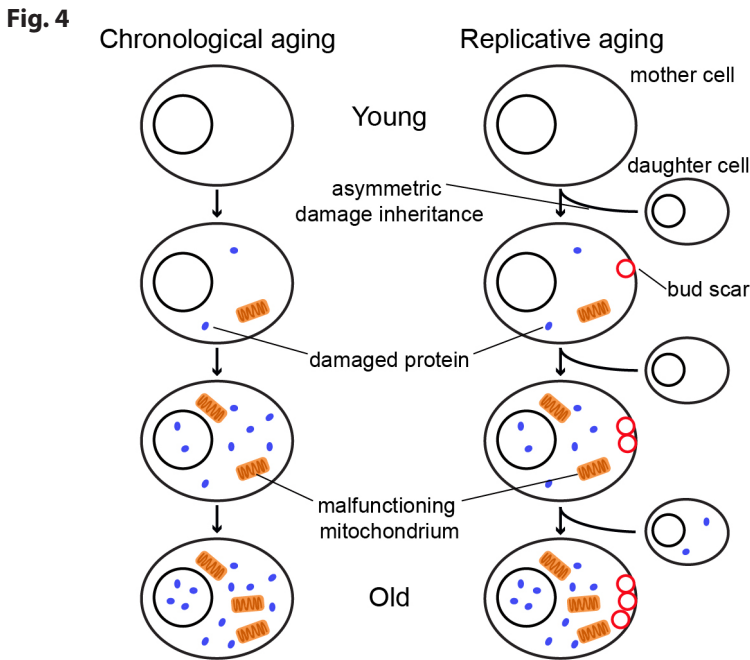
Figure 4: Chronological and replicative aging in budding yeast
Cellular aging is the gradual loss of the cells functionality and viability as a result of the accumulation of cellular damage. Many types of cell damage have been implicated in cellular aging, like protein damage and malfunctioning mitochondria. In budding yeast cell damage accumulates in two different ways; chronological aging and replicative aging. Chronological aging is the accumulation of cell damage as a function of time in non-dividing cells and can be assessed by measuring viability in time. Replicative aging is the accumulation of cell damage in mother cells as a result of asymmetric inheritance of cell damage. Upon cell division, the mother cell retains the cell damage to give rise to the fittest daughter cell possible. Replicative age can be assessed by counting the bud scars that are left on the cell wall of the mother cell, each time a daughter cell breaks away.

1

is defined as the amount of daughter cells one cell can produce and replicative age is the amount of cell divisions a cell underwent [22,68]. The replicative age of a yeast cell can be determined by counting the number of bud scars, which can be visualized by a staining with Calcofluor White [29].

Although replicative aging as a result of damage retention in the mother cell currently lacks a well-studied analogue in mammalian cells, the kind of damage (the aging factor) that is retained yields valuable information about the aging process. Several aging factors have been implicated in replicative aging in yeast [68]. Oxidized and aggregated proteins for example were found to accumulate with replicative age in mother cells and to show a mother-biased segregation upon cell division [69,70]. The retention of this protein damage in the mother cell is suggested to be the result of the association of protein aggregates with the actin cytoskeleton, which prevents their diffusion into the daughter cell [71]. These oxidized proteins may be the results of another aging-related factor; malfunctioning mitochondria. Malfunctioning mitochondria are found to accumulate in mother cells during replicative aging and suggested to be causative for this aging [25,72,73]. The mother-biased inheritance of malfunctioning mitochondria is suggested to be the result of an ingenious filtering mechanism [26]. A potential cause for the appearance of malfunctioning mitochondria is yet another aging factor; lost pH control of the vacuole (the yeast lysosome) in mother cells [74]. Although the role of the lysosomal pH in mammalian aging remains to be established, accumulation of damaged proteins and malfunctioning mitochondria are conserved aspects of cellular aging.

Chronological aging of budding yeast is a model system for the aging of post-mitotic cells and is studied in stationary phase yeast cultures [22]. A stationary culture is reached by growing rich liquid cultures to saturation, usually for 5-7 days at 30ºC. At the start of this period, yeast cells gain energy by fermentation of glucose to ethanol and are proliferating rapidly. When glucose gets limiting, proliferation is slowed down and the cells adjust their metabolism to utilize non-fermentable carbon sources, like ethanol. After this metabolic adjustment, the diauxic shift, cells make one or two very slow cell divisions before the non-fermentable carbon sources are depleted and the cells enter a starvation-induced quiescent state. The culture is now said to be in a stationary phase [75]. Upon the diauxic shift, cells start an extensive 'quiescence program' to prepare for a long survival in quiescence. An important part of this program is the adjustment of transcription and translation rates to the lower energy intake, reducing it to respectively ~20% and 0.3% of their original values. Another consequence is that this program makes the cell more resilient towards stress by up-regulation of genes involved in PQC and by thickening the cell wall. Furthermore, autophagy is induced under these conditions to scavenge damaged cell components and as a source of energy [75]. Also, several cellular proteins (like actin, proteasomes and several metabolic enzymes) get sequestered in so called storage compartments. These storage compartments are suggested to protect its constituents and provide a rapidly available pool of proteins once the growth conditions get more favorable [76–78]. Although the aging of mammalian post-mitotic cells is usually not starvation-induced, several factors and mechanisms are similar to yeast chronological aging, like the central role for TOR signaling and PQC mechanisms.

Replicative and chronological aging are intimately linked and many examples exist of chronological age affecting replicative life span and vice versa [79–81]. The tight link between both modes of aging is exemplified by the strong influence of replicative age on the chronological life span in a starving yeast culture. Based on their replicative age, two

populations of cells can be distinguished in stationary phase yeast cultures: Quiescent (Q) and Non-Quiescent (NQ) cells. Q cells are unbudded daughter cells formed after the diauxic shift that maintain their reproductive ability during long periods of starvation. NQ cells on the other hand, are replicative older cells with a reduced chronological life span [82]. NQ cells have a high load of reactive oxygen species and damaged proteins, which is consistent with the mother-biased inheritance of malfunctioning mitochondria and protein damage. Q cells on the other hand have low levels of both, possibly as a result of the observed up regulation of oxidative stress response genes [82–84].

These observations suggest that one can learn about age-related processes by observing phenotypic differences between cells of different replicative age in a starved yeast culture. In this Thesis we take this approach to study how a cell modulates its ubiquitin-proteasome system in response to aging.

How does the cell modulate its UPS in response to aging?
Selective degradation of damaged proteins by the UPS is an important PQC mechanism in the aging cell. Insufficient UPS activity leads to the accumulation of damaged proteins, which is a hallmark of cellular aging and implicated in several age-related diseases [3]. Insufficient UPS activity can be caused by limiting proteasome activity or limiting activity of the ubiquitination machinery. The accumulation of poly-ubiquitinated proteins that is often observed in aging cells, suggests that proteasome activity is limiting. Also, increased proteasome activity is found to be sufficient to reduce cytotoxicity upon oxidative stress and to increase longevity in budding yeast [85,86]. The concept of limiting proteasome activity as an important factor in aging and age-related diseases is getting increasing attention. This is exemplified by the growing interest for proteasome activators as potential therapeutics in the treatment of age-related diseases like Alzheimers disease [86]. Unfortunately for the cell, the chances of limiting proteasome activity increase during the aging process as a result of increased internal stress factors and an age-dependent decrease in said activity. The age-dependent decrease in proteasome activity is observed in several model organisms and is even suggested to be causative for this aging [14,85,87,88]. The age-dependent decrease of proteasome activity in human epidermal cells and the relatively high activity in fibroblast of healthy centenarians suggests that this phenomenon may also be relevant for mammalian cells [88,89]. Whether it is proteasome activity per se or whether there are other proteasome-related factors important during the aging process remains an open question.

The first indication of the involvement of another proteasome-related factor in the aging process came from a study in budding yeast. The proteasome in budding yeast is primarily localized in the nucleus when they grow in the presence of sufficient nutrients [90]. When yeast cells experience a limiting amount of glucose however, they export their proteasomes from the nucleus and sequester them in cytosolic foci termed Proteasome Storage Granules (PSG). These structures are stable when starvation is prolonged, but dissolve rapidly when nutrients are re-added, followed by the rapid import of proteasomes in the nucleus. PSGs are proposed to store proteasomes during starvation-induced quiescence, while allowing rapid release upon cell cycle re-entry [78]. Interestingly, proteasome localization is not the same for all yeast cells in a stationary phase culture. In this Thesis we show that the localization of the proteasome in starving budding yeast correlates with the replicative age of a cell. This may suggest that proteasome localization, like its activity, plays an important role in cellular aging.

1

A PQC system for the proteasome?

Although an age-dependent decline in proteasome activity is observed in several model systems for aging research, the cause of this decline remains obscure. Several factors are proposed to play a role, including decreased proteasome levels, altered proteasome conformation or an increasing number of damaged (less functional) proteasomes.

An age-dependent decrease in proteasome levels is observed in several model systems, often deduced from lower expression of proteasome subunits [12,87]. The reason for this counter-intuitive age-dependent decrease in proteasome levels is unclear. Conformational changes of proteasomes during aging were observed in a study in *Drosophila*, showing an age-dependent decline of the highly active 26S form of the proteasome in favor of the less active 20S form [14]. Since the 26S proteasome is stabilized by ATP, Vernace *et al* suggest that the decline in cellular ATP levels they observed in their aging cells is causative for this conformational change. This hypothesis may be supported by a similar shift from the 26S to the 20S form of the proteasome observed in yeast cells undergoing starvation [91]. Still, these data are merely a correlation at present.

A decreased proteasome activity due to an increased population of damaged proteasomes is consistent with several *in vitro* and *in vivo* studies showing decreased proteasome activity upon treatment with oxidizing agents like nitric oxide. However, none of these studies shows the actual damage to the proteasome [12,92]. Still, it is likely that proteasomes get (oxidatively) damaged during their life time given their extremely long reported half-life of 5-12 days [18–20]. Oxidative damage to the proteasome is even more likely in aging cells as many of these cells experience oxidative stress as a result of malfunctioning mitochondria. This (oxidative) damage may lead to reduced proteasome activity.

Given its central role in the protein quality control system, it is of vital importance to maintain a 'fit' population of proteasomes. To prevent the accumulation of damaged proteasomes during cellular aging, cells are therefore expected to employ quality control mechanisms on the proteasome. Degradation of the proteasome is reported in HeLa cells and rat livers and suggested to be mediated by the lysosome [18–20]. The way proteasomes are delivered to the lysosome and whether there is specificity towards damaged proteasomes, as PQC entails, is currently unknown.

The action of such a potential proteasome quality control mechanism would be of particular interest for long-lived non-dividing cells, like neurons. This type of cells cannot simply 'dilute' their malfunctioning proteasomes by cell division and since they are long-lived they will need exquisite UPS activity to maintain proteome fitness during their entire lifetime. The relevance of optimal UPS activity in these cells is highlighted by the appearance of protein aggregates, and thus insufficient PQC, in many neurodegenerative disorders. We believe that a deeper understanding of the proteasome quality control mechanisms may yield new therapeutical targets to increase UPS activity in the treatment of these and other age-related diseases.

Conclusion

In this Thesis we address two important aspects of protein dynamics: protein synthesis and distribution upon cell division and dynamics of the protein degradation machinery.

In Chapter 2, we present novel technology (Recombination-Induced Tag Exchange) to distinguish and simultaneously track old and new proteins. In Chapter 3 we used this technology to make a comprehensive analysis of the inheritance and synthesis of

organelles and macromolecular complexes in budding yeast. Thereby we resolved outstanding issues in organelle synthesis and uncovered symmetrical and asymmetrical patterns of inheritance. Asymmetrical inheritance of organelles and macromolecular complexes may induce lineage differences and could be involved in cell differentiation.

Next, we address two aspects of the dynamics of the protein degradation machinery that may be relevant for cellular aging: proteasome localization and degradation of the proteasome. In Chapter 4 we show that the localization of the proteasome, like its activity, may be a relevant factor in cellular aging and identify genetic factors affecting proteasome localization and longevity in budding yeast. In Chapter 5 we present data that is consistent with lysosomal degradation of damaged proteasomes, which may represent the first sketches of a quality control mechanism for the proteasome.

References

1. Hartl, F. U., Bracher, A. & Hayer-Hartl, M. Molecular chaperones in protein folding and proteostasis. Nature 475, 324–32 (2011).
2. Balch, W. E., Morimoto, R. I., Dillin, A. & Kelly, J. W. Adapting proteostasis for disease intervention. Science 319, 916–9 (2008).
3. Vilchez, D., Saez, I. & Dillin, A. The role of protein clearance mechanisms in organismal ageing and age-related diseases. Nat. Commun. 5, 5659 (2014).
4. Morimoto, R. I. Proteotoxic stress and inducible chaperone networks in neurodegenerative disease and aging. Genes Dev. 22, 1427–1438 (2008).
5. Fagarasanu, A., Mast, F. D., Knoblach, B. & Rachubinski, R. A. Molecular mechanisms of organelle inheritance: lessons from peroxisomes in yeast. Nat. Rev. Mol. Cell Biol. 11, 644–54 (2010).
6. Verzijlbergen, K. F. et al. Recombination-induced tag exchange to track old and new proteins. PNAS 107, 64–68 (2010).
7. Terweij, M. et al. Recombination-induced tag exchange (RITE) cassette series to monitor protein dynamics in Saccharomyces cerevisiae. G3 3, 1261–72 (2013).
8. Menendez-Benito, V. et al. Spatiotemporal analysis of organelle and macromolecular complex inheritance. PNAS 110, 175–180 (2012).
9. Li, R. The art of choreographing asymmetric cell division. Dev. Cell 25, 439–50 (2013).
10. Macara, I. G. & Mili, S. Polarity and differential inheritance-universal attributes of life? Cell 135, 801–12 (2008).
11. Glickman, M. H. & Ciechanover, A. The Ubiquitin-Proteasome Proteolytic Pathway : Destruction for the Sake of Construction. Physiol. Rev. 82, 373–428 (2002).
12. Carrard, G., Bulteau, A.-L., Petropoulos, I. & Friguet, B. Impairment of proteasome structure and function in aging. Int. J. Biochem. Cell Biol. 34, 1461–1474 (2002).
13. Dasuri, K. et al. Aging and dietary restriction alter proteasome biogenesis and composition in the brain and liver. Mech. Ageing Dev. 130, 777–83 (2009).
14. Vernace, V. A., Arnaud, L., Schmidt-glenewinkel, T. & Figueiredo-, M. E. Aging perturbs 26S proteasome assembly in Drosophila melanogaster. Faseb J 21, 2672–2682 (2012).
15. Kruegel, U. et al. Elevated proteasome capacity extends replicative lifespan in Saccharomyces cerevisiae. PLoS Genet. 7, e1002253 (2011).
16. Chen, Q., Thorpe, J., Dohmen, J. R., Li, F. & Keller, J. N. Ump1 extends yeast lifespan and enhances viability during oxidative stress: central role for the proteasome? Free Radic. Biol. Med. 40, 120–6 (2006).
17. Van Deventer, S. J., Menendez-Benito, V., van Leeuwen, F. & Neefjes, J. N-Terminal Acetylation And Replicative Age Affect Proteasome Localization And Cell Fitness During Aging. J. Cell Sci. (2014).
18. Tanaka, K. Half-Life of Proteasomes (Multiprotease Complexes) in Rat Liver '. Biochem. Biophys. Res. Commun. 159, 1309–1315 (1989).
19. Hendil, K. B. The 19 S multicatalytic "prosome" proteinase is a constitutive enzyme in HeLa cells. Biochem. Int. 17, 471–478 (1988).
20. Cuervo, M., Palmer, A., Rivett, J. & Knecht, E. Degradation of proteasomes by lysosomes in rat liver. Eur. J. Biochem. 227, 792–800 (1995).
21. Kysela, D. T., Brown, P. J. B., Casey Huang, K. & Brun, Y. V. Biological Consequences and Advantages of Asymmetric Bacterial Growth. Annu. Rev. Microbiol. 67, 417–435 (2013).
22. Kaeberlein, M. Lessons on longevity from budding yeast. Nature 464, 513–9 (2010).
23. Van den Bogaart, G., Meinema, A. C., Krasnikov, V., Veenhoff, L. M. & Poolman, B. Nuclear transport factor directs localization of protein synthesis during mitosis. Nat. Cell Biol. 11, 350–6 (2009).
24. Henderson, K. A., Hughes, A. L. & Gottschling, D. E. Mother-daughter asymmetry of pH underlies

aging and rejuvenation in yeast. Elife e03504 (2014).

25. McFaline-Figueroa, J. R. *et al*. Mitochondrial quality control during inheritance is associated with lifespan and mother-daughter age asymmetry in budding yeast. Aging Cell 10, 885–95 (2011).

26. Higuchi, R. *et al*. Actin dynamics affect mitochondrial quality control and aging in budding yeast. Curr. Biol. 23, 2417–22 (2013).

27. Yadlapalli, S. & Yamashita, Y. M. DNA asymmetry in stem cells - immortal or mortal? J. Cell Sci. 126, 4069–76 (2013).

28. Park, B. P. U., Mcvey, M. & Guarente, L. Separation of Mother and Daughter Cells. Methods Enzymol. 351, 468–477 (2002).

29. Pringle, B. J. R. S t a i n i n g o f B u d S c a r s a n d O t h e r Cell Wall C h i t i n with Calcofluor. Methods Enzymol. 194, 732–735 (1991).

30. Jongsma, M. L. M., Berlin, I. & Neefjes, J. On the move : organelle dynamics during mitosis. Trends Cell Biol. 1–13 (2014).

31. Pereira, G., Tanaka, T. U., Nasmyth, K. & Schiebel, E. Modes of spindle pole body inheritance and segregation of the Bfa1p-Bub2p checkpoint protein complex. EMBO J. 20, 6359–6370 (2001).

32. Cerveny, K. L., Tamura, Y., Zhang, Z., Jensen, R. E. & Sesaki, H. Regulation of mitochondrial fusion and division. Trends Cell Biol. 17, 563–9 (2007).

33. Tomko, R. J. & Hochstrasser, M. Molecular architecture and assembly of the eukaryotic proteasome. Annu. Rev. Biochem. 82, (2013).

34. Woolford, J. L. & Baserga, S. J. Ribosome biogenesis in the yeast *Saccharomyces cerevisiae*. Genetics 195, 643–81 (2013).

35. Hoepfner, D., Schildknegt, D., Braakman, I., Philippsen, P. & Tabak, H. F. Contribution of the endoplasmic reticulum to peroxisome formation. Cell 122, 85–95 (2005).

36. Van der Zand, A., Gent, J., Braakman, I. & Tabak, H. F. Biochemically distinct vesicles from the endoplasmic reticulum fuse to form peroxisomes. Cell 149, 397–409 (2012).

37. Motley, A. M. & Hettema, E. H. Yeast peroxisomes multiply by growth and division. J. Cell Biol. 178, 399–410 (2007).

38. Keppler, A., Pick, H., Arrivoli, C., Vogel, H. & Johnsson, K. Labeling of fusion proteins with synthetic fluorophores in live cells. PNAS 101, 9955–9 (2004).

39. Gautier, A. *et al*. An engineered protein tag for multiprotein labeling in living cells. Chem. Biol. 15, 128–36 (2008).

40. Los, G. V *et al*. HaloTag: A novel protein labeling technology for cell imaging and protein analysis. ACS Chem. Biol. 3, 373–382 (2008).

41. Gaietta, G. *et al*. Multicolor and electron microscopic imaging of connexin trafficking. Science 296, 503–7 (2002).

42. Mann, M. Functional and quantitative proteomics using SILAC. Nature 7, 952–958 (2006).

43. Thayer, N. H. *et al*. Identification of long-lived proteins retained in cells undergoing repeated asymmetric divisions. PNAS 111, 14019–26 (2014).

44. Toyama, B. H. *et al*. Identification of long-lived proteins reveals exceptional stability of essential cellular structures. Cell 154, 971–982 (2013).

45. Baird, G. S., Zacharias, D. a & Tsien, R. Y. Biochemistry, mutagenesis, and oligomerization of DsRed, a red fluorescent protein from coral. PNAS 97, 11984–9 (2000).

46. Subach, F. V *et al*. report on cellular trafficking. Nat. Chem. Biol. 5, 118–126 (2009).

47. Patterson, G. H. & Lippincott-Schwartz, J. A Photoactivatable GFP for Selective Photolabeling of Proteins and Cells. Science (80-.). 297, 1873–1878 (2002).

48. Zhou, X. X. & Lin, M. Z. Photoswitchable fluorescent proteins: ten years of colorful chemistry and exciting applications. Curr. Opin. Chem. Biol. 17, 682–90 (2013).

49. Lindquist, S. L. & Kelly, J. W. Chemical and biological approaches for adapting proteostasis to ameliorate protein misfolding and aggregation diseases: progress and prognosis. Cold Spring Harb. Perspect. Biol. 3, 1–34 (2011).

50. Ciechanover, A. Intracellular protein degradation: from a vague idea through the lysosome and the ubiquitin-proteasome system and onto human diseases and drug targeting. Bioorg. Med. Chem. 21, 3400–10 (2013).

51. Cuervo, A. M. & Wong, E. Chaperone-mediated autophagy: roles in disease and aging. Cell Res. 24, 92–104 (2014).

52. Feng, Y., He, D., Yao, Z. & Klionsky, D. J. The machinery of macroautophagy. Cell Res. 24, 24–41 (2014).

53. Luzio, J. P., Parkinson, M. D. J., Gray, S. R. & Bright, N. a. The delivery of endocytosed cargo to lysosomes. Biochem. Soc. Trans. 37, 1019–21 (2009).

54. Hershko, a & Ciechanover, a. The ubiquitin system for protein degradation. Annu. Rev. Biochem. 61, 761–807 (1992).

55. Liu, C.-W. & Jacobson, A. D. Functions of the 19S complex in proteasomal degradation. Trends Biochem. Sci. 38, 103–10 (2013).

56. Reggiori, F. & Klionsky, D. J. Autophagic processes in yeast: mechanism, machinery and regulation. Genetics 194, 341–61 (2013).

57. Kraft, C., Deplazes, A., Sohrmann, M. & Peter, M. Mature ribosomes are selectively degraded upon starvation by an autophagy pathway requiring the Ubp3p/Bre5p ubiquitin protease. Nat. Cell Biol. 10, 602–10 (2008).

58. Sahu, R. *et al*. Microautophagy of cytosolic proteins by late endosomes. 20, 131–139 (2012).

59. Sontag, E. M., Vonk, W. I. M. & Frydman, J. Sorting out the trash: the spatial nature of eukaryotic protein quality control. Curr. Opin. Cell Biol. 26, 139–46 (2014).

60. Kaganovich, D., Kopito, R. & Frydman, J. Misfolded proteins partition between two distinct quality control compartments. Nature 454, 1088–95 (2008).

61. Weisberg, S. J. et al. Compartmentalization of superoxide dismutase 1 (SOD1G93A) aggregates determines their toxicity. Proc. Natl. Acad. Sci. U. S. A. 109, 15811–6 (2012).

62. Lindner, A. B., Madden, R., Demarez, A., Stewart, E. J. & Taddei, F. Asymmetric segregation of protein aggregates is associated with cellular aging and rejuvenation. Proc. Natl. Acad. Sci. U. S. A. 105, 3076–81 (2008).

63. Coelho, M. et al. Fission yeast does not age under favorable conditions, but does so after stress. Curr. Biol. 23, 1844–52 (2013).

64. Liu, B. et al. The polarisome is required for segregation and retrograde transport of protein aggregates. Cell 140, 257–67 (2010).

65. Ogrodnik, M. et al. Dynamic JUNQ inclusion bodies are asymmetrically inherited in mammalian cell lines through the asymmetric partitioning of vimentin. Proc. Natl. Acad. Sci. U. S. A. 111, 8049–54 (2014).

66. Finkel, T., Deng, C.-X. & Mostoslavsky, R. Recent progress in the biology and physiology of sirtuins. Nature 460, 587–591 (2013).

67. Mortimer & Johnston. Life span of individual yeast cells. Nature 183, 1751–1752 (1959).

68. Nyström, T. & Liu, B. The mystery of aging and rejuvenation - a budding topic. Curr. Opin. Microbiol. 18, 61–7 (2014).

69. Aguilaniu, H., Gustafsson, L., Rigoulet, M. & Nyström, T. Asymmetric inheritance of oxidatively damaged proteins during cytokinesis. Science 299, 1751–3 (2003).

70. Tessarz, P., Schwarz, M., Mogk, A. & Bukau, B. The yeast AAA+ chaperone Hsp104 is part of a network that links the actin cytoskeleton with the inheritance of damaged proteins. Mol. Cell. Biol. 29, 3738–45 (2009).

71. Liu, B. et al. Segregation of protein aggregates involves actin and the polarity machinery. Cell 147, 959–61 (2011).

72. Erjavec, N. et al. Deletion of the mitochondrial Pim1/Lon protease in yeast results in accelerated aging and impairment of the proteasome. Free Radic. Biol. Med. 56, 9–16 (2013).

73. Lai, C., Jaruga, E., Borghouts, C. & Jazwinski, S. M. A Mutation in the ATP2 Gene Abrogates the Age Asymmetry Between Mother and Daughter Cells of the Yeast Saccharomyces cerevisiae. Genetics 87, 73–87 (2002).

74. Hughes, A. L. & Gottschling, D. E. An early age increase in vacuolar pH limits mitochondrial function and lifespan in yeast. Nature 492, 261–5 (2012).

75. Gray, J. V et al. Sleeping Beauty : Quiescence in Saccharomyces cerevisiae. Microbiol. Mol. Biol. Rev. 68, 188–202 (2004).

76. Sagot, I., Pinson, B., Salin, B. & Daignan-Fornier, B. Actin Bodies in Yeast Quiescent Cells : An Immediately Available Actin Reserve ? Mol. Cell. Biol. 17, 4645–4655 (2006).

77. Narayanaswamy, R., Levy, M., Tsechansky, M. & Stovall, G. M. Widespread reorganization of metabolic enzymes into reversible assemblies upon nutrient starvation. PNAS 106, 10147–10152 (2009).

78. Laporte, D., Salin, B., Daignan-Fornier, B. & Sagot, I. Reversible cytoplasmic localization of the proteasome in quiescent yeast cells. J. Cell Biol. 181, 737–45 (2008).

79. Delaney, J. R. et al. Dietary restriction and mitochondrial function link replicative and chronological aging in Saccharomyces cerevisiae. Exp. Gerontol. 48, 1006–1013 (2014).

80. Kennedy, B. K. Daughter cells of Saccharomyces cerevisiae from old mothers display a reduced life span. J. Cell Biol. 127, 1985–1993 (1994).

81. Murakami, C. et al. pH neutralization protects against reduction in replicative lifespan following chronological aging in yeast. Cell Cycle 11, 3087–3096 (2012).

82. Allen, C. et al. Isolation of quiescent and nonquiescent cells from yeast stationary-phase cultures. J. Cell Biol. 174, 89–100 (2006).

83. Aragon, A. D. et al. Characterization of differentiated quiescent and nonquiescent cells in yeast stationary-phase cultures. Mol. Biol. Cell 19, 1271–80 (2008).

84. Davidson, G. S. et al. The proteomics of quiescent and nonquiescent cell differentiation in yeast stationary-phase cultures. Mol. Biol. Cell 22, 988–98 (2011).

85. Kruegel, U. et al. Elevated proteasome capacity extends replicative lifespan in Saccharomyces cerevisiae. PLoS Genet. 7, e1002253 (2011)

86. Schmidt, M. & Finley, D. Regulation of proteasome activity in health and disease. Biochim. Biophys. Acta 1843, 13–25 (2014).

87. Lee, C., Klopp, R. G., Weindruch, R. & Prolla, T. A. Gene Expression Profile of Aging and Its Retardation by Caloric Restriction. Science (80-.). 285, 1390–1393 (1994).

88. Chondrogianni, N., Petropoulos, I., Franceschi, C., Friguet, B. & Gonos, E. . Fibroblast cultures from healthy centenarians have an active proteasome. Exp. Gerontol. 35, 721–728 (2000).

89. Bulteau, a.-L., Petropoulos, I. & Friguet, B. Age-related alterations of proteasome structure and function in aging epidermis. Exp. Gerontol. 35, 767–777 (2000).

90. Russell, S. J., Steger, K. A. & Johnston, S. A.

Subcellular Localization, Stoichiometry, and Protein Levels of 26 S Proteasome Subunits in Yeast. J. Biol. Chem. 274, 21943–21952 (1999).

91. Bajorek, M., Finley, D. & Glickman, M. H. Proteasome Disassembly and Downregulation Is Correlated with Viability during Stationary Phase. Curr. Biol. 13, 1140–1144 (2003).

92. Glockzin, S. Activation of the Cell Death Program by Nitric Oxide Involves Inhibition of the Proteasome. J. Biol. Chem. 274, 19581–19586 (1999).

Chapter Two

Chapter 2:

Recombination-Induced Tag Exchange to track old and new proteins

2

Kitty F. Verzijlbergen[1], Victoria Menendez-Benito[2], Tibor van Welsem[1], **Sjoerd J. van Deventer**[2], Derek L. Lindstrom[3], Huib Ovaa[2], Jacques Neefjes[2], Daniel E. Gottschling[3], Fred van Leeuwen[1]

[1] Division of Gene Regulation and
[2] Division of Cell Biology 2,
Netherlands Cancer Institute, Amsterdam, The Netherlands
[3] Division of Basic Sciences
Fred Hutchinson Cancer Research Center, Seatle, USA

Abstract

The dynamic behavior of proteins is critical for cellular homeostasis. However, analyzing dynamics of proteins and protein complexes *in vivo* has been difficult. Here we describe Recombination-Induced Tag Exchange (RITE), a novel genetic method that induces a permanent epitope-tag switch in the coding sequence after a hormone-induced activation of Cre recombinase. The time-controlled tag switch provides a unique ability to detect and separate old and new proteins in time and space, which opens up new opportunities to investigate the dynamic behavior of proteins. We validated the technology by determining exchange of endogenous histones in chromatin by biochemical methods and by visualizing and quantifying replacement of old by new proteasomes in single cells by microscopy. RITE is widely applicable and allows probing spatio-temporal changes in protein properties by multiple methods.

Introduction

Proteins are dynamic molecules. Their abundance is controlled by synthesis and degradation and they can be subject to post-translational processing, modification and demodification. In addition, most proteins are very mobile and undergo interactions with multiple other protein partners (1-4). However, little is known about the dynamics of proteins within macromolecular complexes *in vivo* (2, 4). Studying time-dependent changes in physical properties of proteins or protein turnover requires methods to distinguish resident (old) proteins from new proteins. Current methods that do so are usually based on fluorescent reporters or differential chemical labeling. For example, fluorescence recovery after photo bleaching relies on exchange of the old bleached protein by non-bleached proteins (1, 3, 4). Alternative methods involve time-dependent changes in fluorescence, non-specific pulse-chase labeling of proteins with labeled amino acids, or labeling with chemical dyes that specifically bind to short tags (5-7). Although suitable for detection of proteins by microscopy or mass spectrometry, a limitation of these methods is that they do not provide a handle for biochemical analysis of old and new proteins and their complexes. To solve this problem and to eliminate the requirement for chemical labels or UV light we developed Recombination-Induced Tag Exchange (RITE), a novel method in which a genetic epitope tag is switched by transient induction of a site-specific recombinase. As a consequence, old and newly synthesized proteins are differentially tagged, which enables monitoring of protein dynamics by multiple techniques, as illustrated here. In contrast to inducible expression strategies (8-12), differential tagging by a time-controlled site-specific protease (13), or the labeling methods described above, RITE allows parallel detection and purification of old and new proteins under physiological conditions and over long periods of time.

We used RITE to probe the stability of chromatin. Photo-bleaching experiments using histones tagged with fluorescent reporters suggest that chromatin is a static complex (14). However, recent work suggests that chromatin is more dynamic than previously anticipated (15). For example, ectopically induced histones can be incorporated into chromatin of non-dividing yeast cells and gene activation of certain promoters is accompanied by transient loss of histones (8-12, 16). In metazoans, the histone H3 variant H3.3 can be assembled into chromatin by a replication-independent transcription-

coupled process (17-19). We took advantage of RITE to determine whether endogenously expressed canonical histones undergo replication-independent exchange. RITE can also be used to visualize proteins by microscopy. To demonstrate this we applied RITE to the proteasome, a highly conserved and essential macromolecular complex critical for degradation of proteins by proteolysis (20). Using fluorescent RITE we could visualize the replacement of old by new proteasomes in the nucleus and cytoplasm of dividing cells.

Results

Recombination-Induced Tag Exchange (RITE) outline

RITE can be applied by integration of a RITE cassette downstream of any gene of interest, resulting in a C-terminal tag situated between two LoxP sites with an orphan tag downstream. Upon a transient time-controlled activation of the site-specific Cre-recombinase, recombination between the tandem LoxP sites results in exchange of the 'old' tag by an orphan 'new' tag in the coding sequence leading to an epitope-tag switch (Fig. 1). After switching, all newly synthesized mRNAs will encode for proteins containing the new epitope tag. The LoxP recombination sites are part of the coding sequence, which eliminates the need for introns and allows the tag cassette to be introduced directly at the 3' end of any gene of interest to generate a switchable tag. As a consequence, the differentially tagged proteins are encoded by a single gene and under control of the endogenous promoter. Recombination can be induced using a constitutively expressed Cre recombinase fused to the human estrogen binding domain (EBD). This fusion protein is sequestered by heat shock proteins and inactive (21). The nuclear activity of Cre-EBD can be rapidly activated by the addition of β-estradiol, which releases the fusion protein from heat shock proteins (21). A major advantage of RITE is that the genetic switch is permanent.
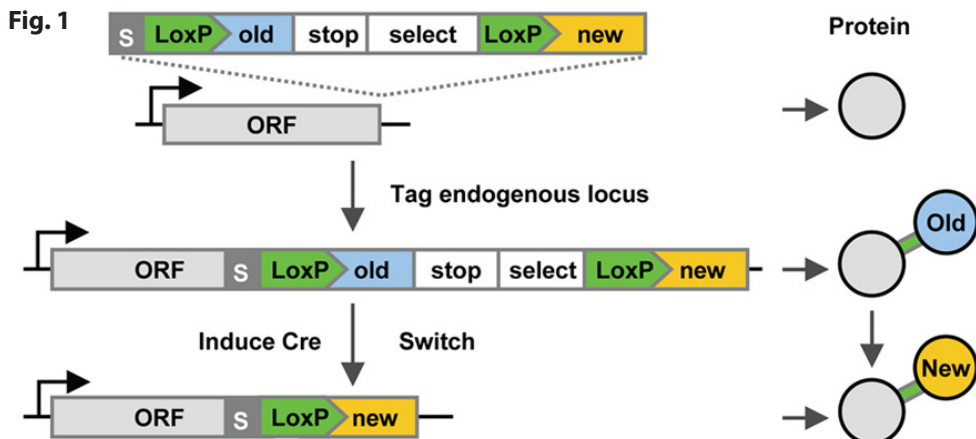
Fig. 1

Fig. 1. Outline of Recombination-Induced Tag Exchange (RITE). RITE cassettes contain two epitope tags (old and new) the first of which is in between two LoxP sites. Integration of a RITE cassette downstream of an open reading frame (ORF) results in a protein tagged with an 'old' tag (blue). The 'old' tag is preceded by an invariant flexible spacer (S) and a short peptide encoded by the LoxP sequence (LoxP), and is followed by a transcriptional terminator (stop) and a selectable marker (select). Upon induction of Cre recombinase, site-specific recombination between the tandem LoxP sites in the genome results in loss of the 'old' tag and fusion of the ORF to the 'new' tag. After the switch, newly synthesized proteins will contain the 'new' tag (yellow), whereas existing proteins will contain the 'old' tag. Old and new proteins are expressed from the same gene by the native promoter.

Therefore, after the switch both old and new proteins can be followed in the original cells and their descendants under any condition of interest. We applied this strategy in haploid yeast cells and integrated RITE cassettes by homologous recombination at endogenous gene loci.

Application of RITE to Histone H3

First RITE was applied to histone H3 to investigate the stability of histones within chromatin. One of the two histone H3 genes was tagged with a RITE cassette containing two small epitope tags, HA and T7 (H3-HA→T7) (Fig. 2A). The second histone H3 gene was deleted. As a consequence, in this strain all histone H3 proteins were tagged (Fig. 2A). Yeast cells expressing the tagged histones are viable (Fig. 2B). Since histone H3 is essential, this demonstrates that the tagged H3 proteins are functional. After addition of the hormone β-estradiol, which has no detectable effect on growth or transcription (22), most of the cells had undergone recombination within two hours (Fig. 2C). To confirm that the genetic switch at the DNA level yields differentially tagged proteins, switched starved cells (see below) were released in fresh media and harvested at several time points after re-entry into the cell cycle. Immunoblot analysis demonstrated replacement of old histone H3-HA protein by new H3-T7 in dividing cells (Fig. 2D). The replacement of one tagged protein by the other is in contrast to previously used 'inducible-expression' strategies, which involve
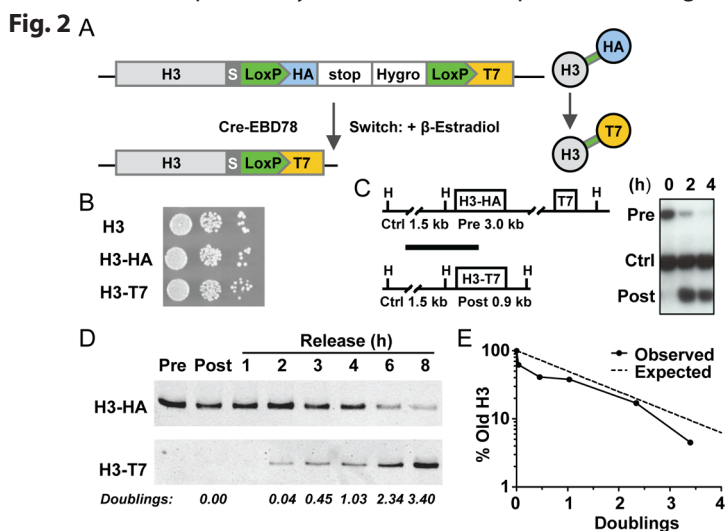
Fig. 2 A

Fig. 2. Application of RITE to endogenous histone H3. (A) One of the two genes encoding histone H3 in yeast (HHT2) was tagged with a RITE cassette (H3-RITE) containing short epitope tags: HA (old) and T7 (new). The other gene encoding histone H3 (HHT1) was deleted. A Hygromycin resistance gene (Hygro) was used to select against illegitimate recombinants. The tag switch was under control of a constitutively expressed hormone-dependent Cre recombinase (Cre-EBD78). (B) Growth of wild-type and H3 RITE-tagged (before [HA] and after [T7] the switch) yeast cells spotted in a ten-fold dilution series. (C) The efficiency of recombination in the cell population was determined by Southern blot analysis of genomic DNA digested with HindIII (H) before (Pre) and after (Post) addition of the hormone β-estradiol. An invariant fragment was used as a control (Ctrl). (D) Detection of old (HA) and new (T7) histone H3 by quantitative immunoblot analysis of whole cell lysates of equal numbers of starved switched cells released into fresh media. The number of population doublings was calculated by staining the cells with NHS-TER (see supplementary methods). (E) The percentage of old H3-HA plotted against the number of population doublings. The measured HA/T7 ratios of the blot in panel D were converted into H3-HA percentages by using standard curves of samples with known percentages of H3-HA and H3-T7 (see supplementary methods).

ectopic expression of a tagged (new) version of a protein by an inducible promoter in the presence of an endogenous copy. Because of ongoing synthesis of the endogenous gene copy, endogenous histones represent old as well as new proteins. As a consequence, the induced and endogenous proteins quickly reach a new steady state. Tagging a single endogenous gene with a RITE cassette eliminates this problem and allows simultaneous tracking of old and new proteins over many cell divisions.

Immunodetection of protein turnover in replicating and non-replicating cells

Quantification of the immunoblot shown in Fig. 2D showed that replacement of old H3-HA by new H3-T7 occurred at a rate faster than expected when only dilution due to replication is taken into account, suggesting histone turnover by replication-independent mechanisms (Fig. 2E). The fact that RITE introduces a permanent genetic switch after a transient signal allowed direct comparison of histone exchange in different cell cycle stages. To minimize new histone mRNA and protein expression during the recombination process the tag switch was performed in nutrient-starved cells, here referred to as G0 (Fig. 3A). Switched H3-HA→T7 cells were released into fresh medium containing nocodazole to arrest the cells after passage through one S-phase in G2/M (Fig. 3A and Fig. S2). During S-phase, like the DNA, the amount of histones gets duplicated and incorporated into the chromatin. As expected, cells at the estimated start of the G2/M cell cycle block (t=3 h) showed an approximately equal abundance of old H3-HA and new H3-T7 (Fig. 3B-C). To investigate replication-independent histone exchange, the switched H3-HA→T7 cells were released into fresh media containing α-factor to arrest the cells in G1, to prevent passage through S-phase (Fig. 3A). New H3-T7 was detected at the start of the cell block (t=2 h) and increased further during the next three hours (t=5 h). Moreover, the abundance
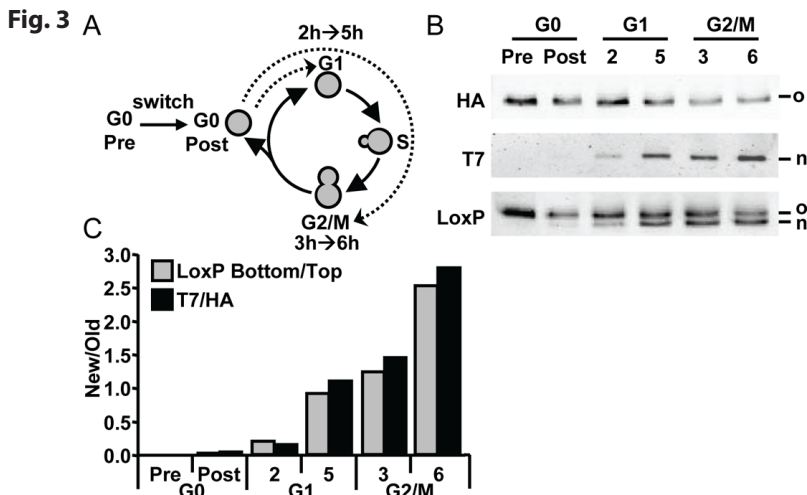
Fig. 3

Fig. 3. Global histone exchange determined by immunodetection. (A) Yeast strains were grown to saturation (here referred to as G0) in complete medium and recombination was induced overnight (switch) by addition of hormone (Fig. S1). Cells were released in fresh media and arrested in G1 (alpha factor) or G2/M (nocodazole). Samples were taken at the estimated start of the arrest (2 h G1 and 3 h G2/M) and three hours later. (B) Quantitative immunoblot analysis of old and new histone H3 in whole-cell lysates using antibodies against HA (old, blue), T7 (new, yellow) or an antibody raised against the spacer-LoxP sequence (LoxP) recognizing 'old' and 'new' proteins simultaneously. (C) Relative H3-T7/H3-HA ratios (New/Old) were calculated based on the ratio of the top band (H3-HA) and bottom band (H3-T7) of the LoxP blot (absolute values) and the ratio of HA and T7 signals (arbitrary units).

Fig. 4
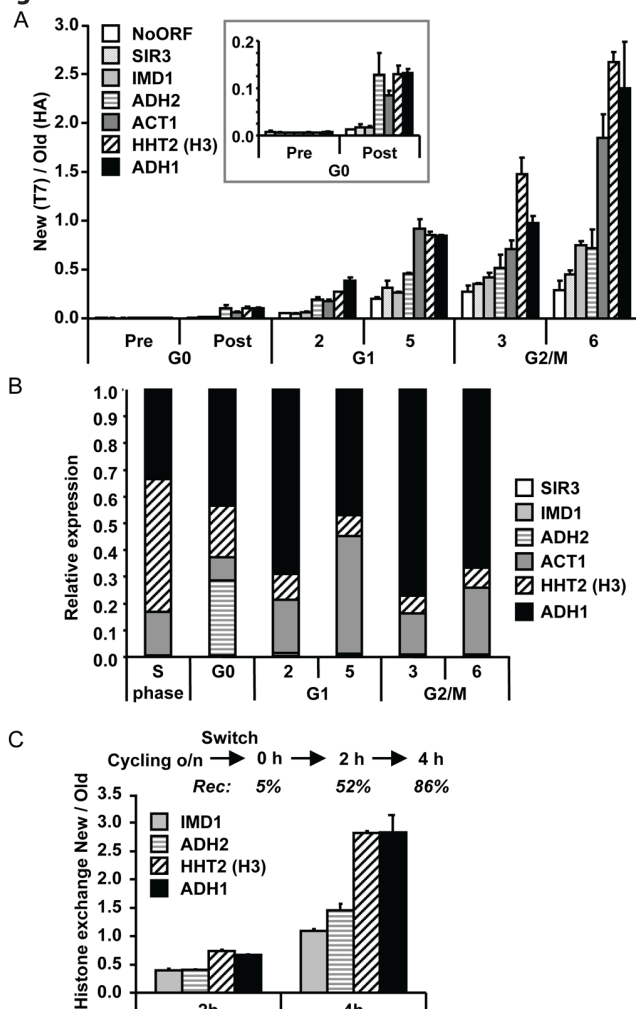
Fig. 4. Replication-independent transcription-coupled histone turnover quantified by affinity purification. (A) Analysis of chromatin-bound histones by ChIP of HA (old) and T7 (new) histone H3 quantified by real-time quantitative PCR (qPCR). Histone exchange (ratio of new/old) was determined for promoters of the indicated genes and an intergenic region on chromosome V (No-ORF). The genes are ranked by estimated transcription frequency in log-phase, from low (white) to high (black) frequency. The result shown is the average of two individual experiments (± SEM). The box is a zoom-in of the G0 time points. (B) Relative mRNA expression levels were determined by reverse-transcriptase qPCR (RT-qPCR). An S-phase sample of the same H3-RITE strain was used as a reference sample. A wild-type strain without a RITE tag showed very similar expression profiles (Fig. S4). (C) Histone turnover in H3-T7→HA cells without any arrest was determined by induction of Cre-recombinase in log-phase cells (OD660=0.25). The percentage of cells that had undergone recombination (Rec) is indicated for each time-point (determined by a colony plating assay). Histone replacement at promoters was determined by ChIP (HA/T7).

of new histone H3-T7 after five hours in G1 was similar to that of cells arrested in G2/M, which had undergone one round of genome duplication and therefore contain at least 50% new H3-T7 and 50% old H3-HA (Fig. 3B-C). Thus, yeast cells that had been arrested in G1 for the duration of around three cell doubling times had replaced approximately half of the old H3-HA protein by new H3-T7 in the absence of DNA replication.

Affinity purification of old and new histones in chromatin

Since soluble histones represent a minor fraction of the total histone pool (23), these results suggested that the G1-arrested cells had incorporated new histone H3-T7 into chromatin. To address this question we took advantage of the possibility of using the epitope tags for affinity purification of chromatin fragments containing old and new histones. Following chromatin immunoprecipitation (ChIP) the ratio of new H3-T7 over old H3-HA was determined by real-time quantitative PCR (qPCR) for promoter regions of a set of genes with different transcriptional properties and for an intergenic region (Fig.

4A). Histone exchange in chromatin was already detectable in switched G0 cells prior to release. After supplementation of fresh medium containing α-factor, exchange increased in the transition to the G1 arrest, and increased further during the arrest (2 and 5 h G1). Strikingly, five hours after release into the G1 block, the replacement of old H3-HA by new H3-T7 was quantitatively similar at different loci to that of cells that had just duplicated their genome and histone content (3 h G2/M). This confirms that cells arrested in G1 had undergone rapid replication-independent exchange of chromatin-bound histones (Fig. 4A). However, histone exchange was not restricted to the G1 phase. Cells arrested in G2/M (from 3 h until 6 h) and even cells arrested by nutrient depletion (G0 pre until G0 post) accumulated new H3-T7 during the arrest, albeit slower (Fig. 3B and 4A). Identical results were obtained with a strain in which the old and new tags were swapped (H3-T7→HA; Fig. S3), showing that the characteristics of new histone deposition were not determined by the specific epitope tags. We conclude that replication-independent histone exchange is a common feature of arrested cells but the rate of exchange can vary between cell cycle phases.

RITE allowed a direct and quantitative comparison between G1 and G2/M cells, which demonstrated that cells arrested in G1 replaced half of the old histones by new histones within five hours by replication-independent mechanisms. Analysis of mRNA expression levels during the different phases of the cell cycle showed that the rate of histone exchange was coupled to the level of transcription at each time point or to previous transcription events (Fig. 4B, Fig. S4). Analysis of the inducible GAL1 promoter showed that induction of transcription caused an increase in histone exchange (Fig. S4), suggesting that transcription leads to histone exchange. In addition, transcription-coupled histone exchange also occurred in coding regions, at rates similar to the rates found at promoters (Fig. S5). Transcription-coupled histone exchange might be a specific property of arrested cells that cannot replace histones by replication-dependent mechanisms. To investigate this possibility, histone exchange in chromatin was determined in log-phase cells that had been grown for many generations without a growth arrest (Fig. 4C). In these cycling cells new histone H3-HA was also incorporated more efficiently in highly transcribed genes (Fig. 4C), suggesting that transcription-coupled histone exchange occurred on top of replication-dependent histone deposition. In addition, monitoring of old and new histones during successive cell divisions showed that transcription-coupled histone deposition was maintained during at least three cell divisions (Fig. S6). Thus, biochemical purification of old and new histones revealed that chromatin is a very dynamic macromolecular complex in dividing as well as non-dividing cells and that transcription is a key determinant of chromatin instability.

Fluorescent RITE to monitor proteasome replacement in time and space

The methods discussed above probe protein dynamics in pools of cells. To visualize the behavior of old and new proteins in single cells, a fluorescent RITE cassette was constructed that switches from a green fluorescent protein (GFP) tag to a monomeric red fluorescent protein (mRFP) tag (Fig. 5A). To illustrate the use of fluorescent RITE, a constituent protein of another macromolecular complex, the proteasome, was tagged. Specifically, we constructed a yeast strain where the only endogenous PRE3 gene, encoding a catalytic β-subunit of the proteasome, was tagged with the GFP→mRFP RITE cassette. This strain has a normal growth rate, indicating that the RITE-tagged subunit is functional, since deletion or mutation of PRE3 is lethal. We note that yeast cells expressing

Fig. 5
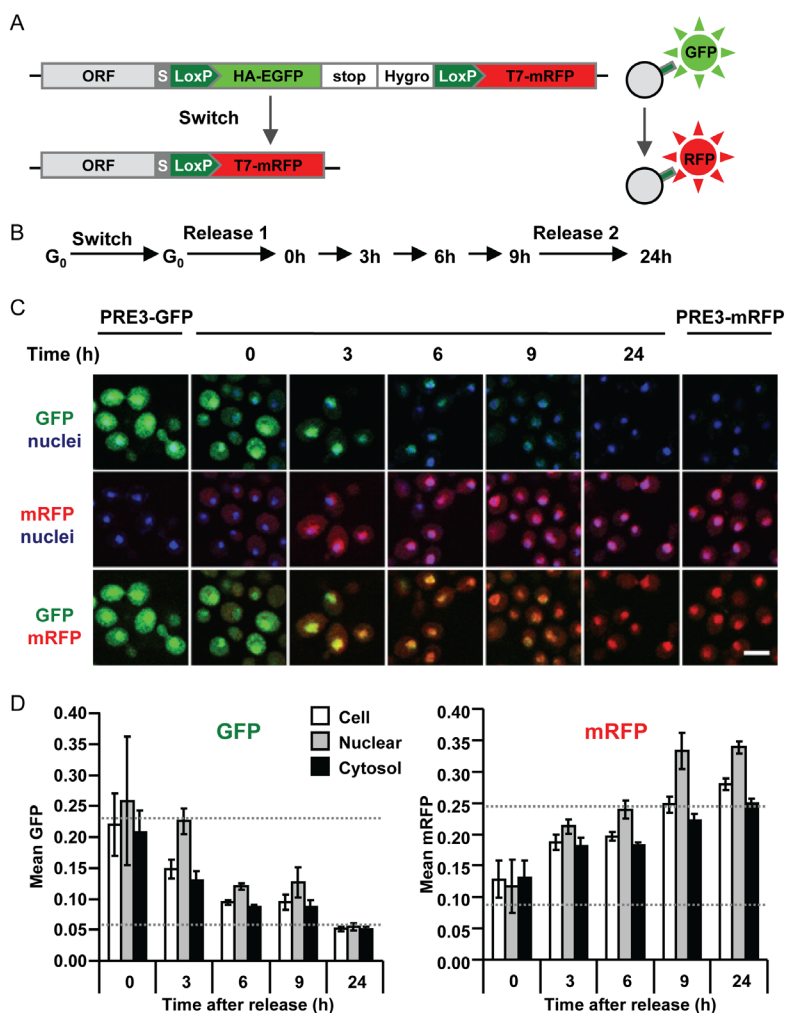
Fig. 5. Spatio-temporal analysis of old and new proteasomes by microscopy. (A) Schematic representation of fluorescent RITE. (B) PRE3-GFP→mRFP cells were grown to saturation (G0) and recombination was induced overnight (switch). Subsequently, cells were released in fresh media (release 1) and samples were taken at the indicated time points. Nine hours after the first release, cells were again supplemented with fresh media (release 2). Time points 3, 6, 9, and 24 h correspond to approximately 0.3, 2, 3, and 8 cell divisions, respectively. (C) Representative confocal microscopy images of PRE3-GFP→mRFP grown as indicated in panel B and of control strains (PRE3-GFP and PRE3-mRFP). Hoechst was used as a nuclear counterstaining (blue). Scale bar represents 4 μm. (D) The GFP and mRFP fluorescent intensities of micrographs from panel C were quantified and the value shown for each time-point is an average of the mean fluorescence intensity in the nuclei, cytoplasm and total surface of 400 cells (± SD). Dashed lines indicate GFP and mRFP signals in control cells expressing GFP or mRFP only (the bottom dashed lines indicate background levels)

H3-GFP→mRFP were inviable, indicating that not every protein can be safely tagged with the larger GFP→mRFP RITE cassette. To visualize the replacement of old by new proteasomes by microscopy, recombination was induced in G0 (Fig. 5B), during which very little proteasome synthesis occurs. Since the proteasome is a stable complex, many old proteasomes (Pre3-GFP) remain that are slowly replaced by new proteasomes (Pre3-

mRFP) (Fig. 5C). When the cells were released in fresh media the old proteasomes were more swiftly replaced by new proteasomes due to dilution during cell division (Fig. 5C). In yeast and mammalian cells the proteasome is present in both the nucleus and the cytosol (24). Quantification of GFP and mRFP signals showed that in the switched yeast cells, the appearance of new proteasome and loss of old proteasome followed similar kinetics in the two compartments (Fig. 5D). Thus fluorescent RITE enables visualization of replacement of old by new proteins in living cells in time and space during cell cycle arrests and during successive cell divisions.

2

Discussion

Here we show that RITE is a versatile method to study different parameters of protein dynamics such as protein turnover and exchange of subunits in macromolecular complexes. In contrast to other methods such as pulse-chase labeling, inducible expression, methods based on differential fluorescence, or TimeStamp (3, 5, 6, 13, 25), RITE provides the unique possibility to simultaneously monitor old and new proteins and to do so by multiple techniques. RITE has important additional advantages over existing technologies. It does not require addition of UV light, chemicals or labels, circumventing the need for expensive ultra sensitive mass spectrometry technologies. Furthermore, since no heterologous inducible promoters are required to differentially express old and new proteins, tagged genes are regulated by their endogenous promoter and the switch can occur without perturbation under any condition of interest. Protein replacement of the stable proteasomes and histones could be assessed over long time periods in dividing and non-dividing cells, indicating that RITE is suitable to study the dynamics of long-lived proteins, which are typically difficult to study with more traditional methods. RITE should also be applicable to shorter lived proteins, however. Although it takes about two hours until the majority of the cells has switched, switched cells can already be detected as early as fifteen minutes after activation of Cre. RITE may be less suitable for studies of very short-lived proteins.

The differential tagging of histone H3 showed that endogenously expressed canonical histones undergo turnover within chromatin in a transcription-dependent manner. Our results are in agreement with previous histone H3 turnover studies using time-controlled induced expression of a tagged ectopic histone copy in yeast (8-12, 16, 26). The direct comparison to replication-dependent assembly of new histones indicates that replication-independent histone exchange occurs at a high rate. This was unexpected when one considers the regulated expression of histones. We note that while H3 mRNA indeed peaks in S-phase when chromatin is duplicated, its expression is lower but still substantial outside of S-phase (Fig. 4B). This supports the idea that canonical histones are synthesized outside of S-phase for replication-independent histone exchange. Especially in starved cells, H3 mRNA is relatively abundant (Fig. 4B). The high rate of histone exchange suggests that post-translational modifications in chromatin are continuously being erased in dividing and non-dividing cells. Thus, replication-independent histone exchange might provide cycling and non-cycling cells with a means to replace old histones that have acquired damage or that need to be epigenetically re-set.

Using fluorescent RITE, replacement of old by new proteasomes in time and space was determined by microscopy. The amount of old proteasomes decreased at a very similar rate in the cytosolic and nuclear compartments, suggesting an even segregation during cell division and/or a fast re-equilibration between proteasomes in both compartments.

Likewise, the appearance of new proteasome in both compartments followed similar kinetics, indicating that the translocation of new proteasome subunits into the nucleus is a relatively fast phenomenon (Fig. 5D).

RITE is a widely applicable tool to dissect novel mechanisms and functions of protein dynamics. For example, RITE-tagged genes of interest and the Cre recombinase can be efficiently introduced into the collection of yeast deletion strains by one round of genetic crossing, which allows genome-wide genetic screens for identification of factors involved in protein dynamics. RITE can also be applied to investigate whether new and aging proteins have different properties such as age-related post-translational modifications or whether they show differential segregation between mother and daughter cells. Finally, although we have validated RITE in budding yeast, with minor modifications RITE technology may be adapted for use in higher eukaryotes. The RITE cassettes are universally applicable and conditional versions of Cre recombinase have already been developed for many cell systems or even whole organisms (27).

Materials and Methods

Yeast strains and growth conditions

Yeast strains and growth conditions are described in Table S1 and the supplementary methods. RITE cassettes contain an invariant short peptide spacer sequence (GGSGGS) that was found to be required for viability of strains carrying tagged histones. The spacer and ITSYNVCYTKLS peptide encoded by the LoxP DNA sequence are present in front of the epitope tags both before and after the switch. RITE cassettes were PCR amplified and targeted to the 3' end of the endogenous genes by homologous recombination to tag the C-terminus and ensure regulation by the endogenous promoter. The hormone-dependent Cre-EBD (Cre-EBD78) was described previously (22). A constitutively expressed copy was stably integrated in the yeast genome. For RITE experiments, yeast cells were grown overnight in YPD in the presence of Hygromycin B (200 μg/ml, Invitrogen). The cells were then diluted 1:10 into fresh YPD and incubated for 30-36 hours. Recombination was induced by the addition of 1μM β-estradiol (E-8875 Sigma-Aldrich). Subsequently, cells were diluted 1:25 in fresh YPD media to release the cells back into the cell cycle. Cells enter G1 arrest upon addition of 0.5 ng/μl of α-factor and G2/M arrest upon addition of 15 μg/ml Nocodazole (Sigma-Aldrich). Detailed protocols for ChIP, RT-PCR, immunoblot, Southern-blot, FACS, and microscopy are described in the supplementary methods and Table S2.

Acknowledgements

References

1. Gorski SA, Dundr M, Misteli T (2006) The road much traveled: trafficking in the cell nucleus. Curr. Opin. Cell Biol. 18:284-290.

2. Russel D *et al*. (2009) The structural dynamics of macromolecular processes. Curr. Opin. Cell Biol. 21:97-108.

3. Reits EA, Neefjes JJ (2001) From fixed to FRAP: measuring protein mobility and activity in living cells. Nat. Cell Biol. 3:E145-E147.

4. D'Angelo MA, Hetzer MW (2008) Structure, dynamics and function of nuclear pore complexes. Trends Cell Biol. 18:456-466.

5. Adams SR, Tsien RY (2008) Preparation of the membrane-permeant biarsenicals FlAsH-EDT2 and ReAsH-EDT2 for fluorescent labeling of tetracysteine-tagged proteins. Nat. Protoc. 3:1527-1534.

6. Mann M (2006) Functional and quantitative proteomics using SILAC. Nat. Rev. Mol. Cell Biol. 7:952-958.

7. Subach FV *et al*. (2009) Monomeric fluorescent timers that change color from blue to red report on cellular trafficking. Nat. Chem. Biol. 5:118-126.

8. Schermer UJ, Korber P, Horz W (2005) Histones Are Incorporated in trans during Reassembly of the Yeast PHO5 Promoter. Mol Cell 19:279-285.

9. Linger J, Tyler JK (2006) Global replication-independent histone H4 exchange in budding yeast. Eukaryot Cell 5:1780-1787.

10. Dion MF *et al*. (2007) Dynamics of replication-independent histone turnover in budding yeast. Science 315:1405-1408.

11. Rufiange A *et al*. (2007) Genome-wide replication-independent histone h3 exchange occurs predominantly at promoters and implicates h3 k56 acetylation and asf1. Mol Cell 27:393-405.

12. Jamai A, Imoberdorf RM, Strubin M (2007) Continuous histone H2B and transcription-dependent histone H3 exchange in yeast cells outside of replication. Mol Cell 25:345-355.

13. Lin MZ, Glenn JS, Tsien RY (2008) A drug-controllable tag for visualizing newly synthesized proteins in cells and whole animals. Proc. Natl. Acad. Sci. U S A 105:7744-7749.

14. Kimura H, Cook PR (2001) Kinetics of core histones in living human cells: little exchange of H3 and H4 and some rapid exchange of H2B. J. Cell Biol. 153:1341-1353.

15. Henikoff S (2008) Nucleosome destabilization in the epigenetic regulation of gene expression. Nat. Rev. Genet. 9:15-26.

16. Kim HJ *et al*. (2007) Histone chaperones regulate histone exchange during transcription. EMBO J.

17. Mito Y, Henikoff JG, Henikoff S (2005) Genome-scale profiling of histone H3.3 replacement patterns. Nat Genet 37:1090-1097.

18. Wirbelauer C, Bell O, Schubeler D (2005) Variant histone H3.3 is deposited at sites of nucleosomal displacement throughout transcribed genes while active histone modifications show a promoter-proximal bias. Genes Dev 19:1761-1766.

19. Chow CM *et al*. (2005) Variant histone H3.3 marks promoters of transcriptionally active genes during mammalian cell division. EMBO Rep. 6:354-360.

20. Finley D (2009) Recognition and processing of ubiquitin-protein conjugates by the proteasome. Annu. Rev. Biochem. 78:477-513.

21. Logie C, Stewart AF (1995) Ligand-regulated site-specific recombination. Proc. Natl. Acad. Sci. U S A 92:5940-5944.

22. Lindstrom DL, Gottschling DE (2009) The Mother Enrichment Program: A Genetic System for Facile Replicative Life Span Analysis in *Saccharomyces cerevisiae*. Genetics 183:413-422.

23. Gunjan A, Verreault A (2003) A Rad53 kinase-dependent surveillance mechanism that regulates histone protein levels in *S. cerevisiae*. Cell 115:537-549.

24. Reits EA *et al*. (1997) Dynamics of proteasome distribution in living cells. EMBO J. 16:6087-6094.

25. Yen HC *et al*. (2008) Global protein stability profiling in mammalian cells. Science 322:918-923.

26. Choi ES, Shin JA, Kim HS, Jang YK (2005) Dynamic regulation of replication independent deposition of histone H3 in fission yeast. Nucleic Acids Res 33:7102-7110.

27. Branda CS, Dymecki SM (2004) Talking about a revolution: The impact of site-specific recombinases on genetic analyses in mice. Dev. Cell 6:7-28.

2

Supplemental Figures:

Fig. S1
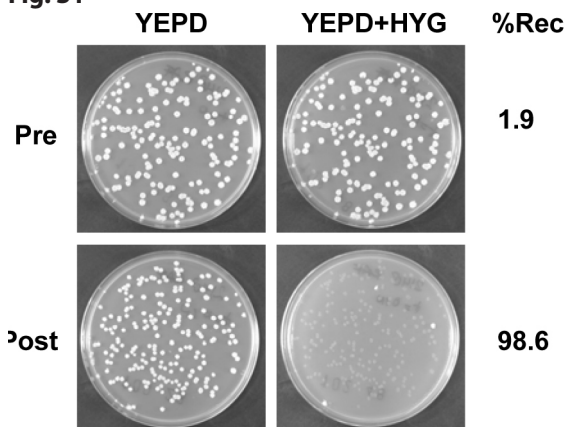
Figure S1. The efficiency of Cre-recombination in G0 cells determined by a plating assay. The efficiency of recombination in the cell population in G0 cells was determined by plating the yeast cells on non-selective media (YEPD) and subsequent replica plating to media containing Hygromycin (YEPD+HYG). The fraction of Hygromycin sensitive colonies indicates the fraction of recombined/switched cells (%Rec) before (Pre) and after (Post) activation of Cre-recombinase by addition of the hormone β-estradiol.

Fig. S2
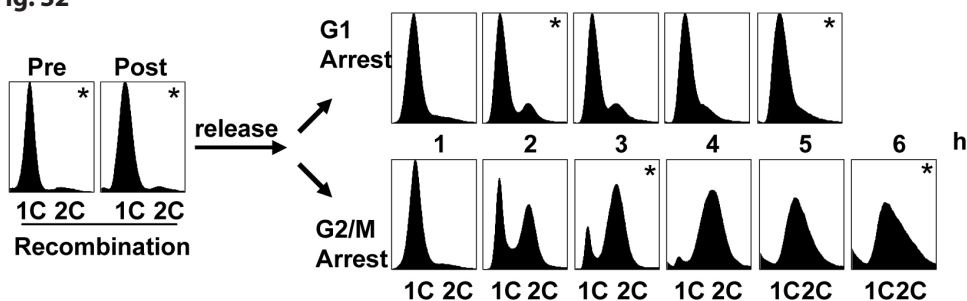
Figure S2. Cell cycle progression and arrest monitored by flow cytometry.
FACS analysis of DNA content to monitor release of starved cells from G0 (1C) into the G1 (1C) and G2/M (2C) blocks. Asterisks indicate the analyzed time points.

Fig. S3
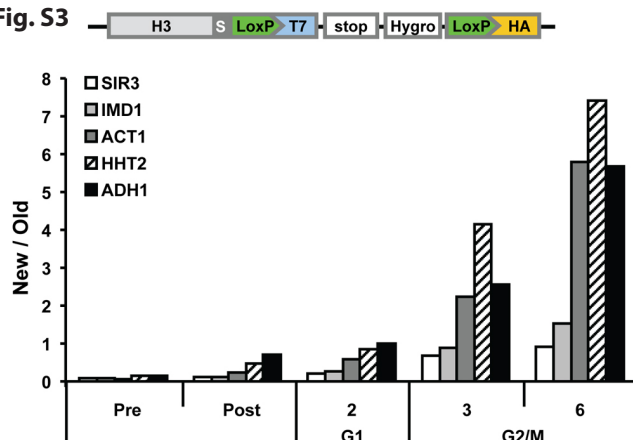
Figure S3. Histone exchange is independent of the order of the RITE tags
Starved switched cells (see Fig. 3) containing a 'swapped-tag' cassette that switches from T7 to HA (H3-T7→HA) were released into fresh media and arrested in G1 or G2/M. ChIP of T7 and HA was quantified by qPCR for the genes indicated. The 5 h G1 arrest time-point was not analyzed because this BAR1 wild-type strain degrades α-factor and escapes from the arrest after four hours.

Fig. S4

2
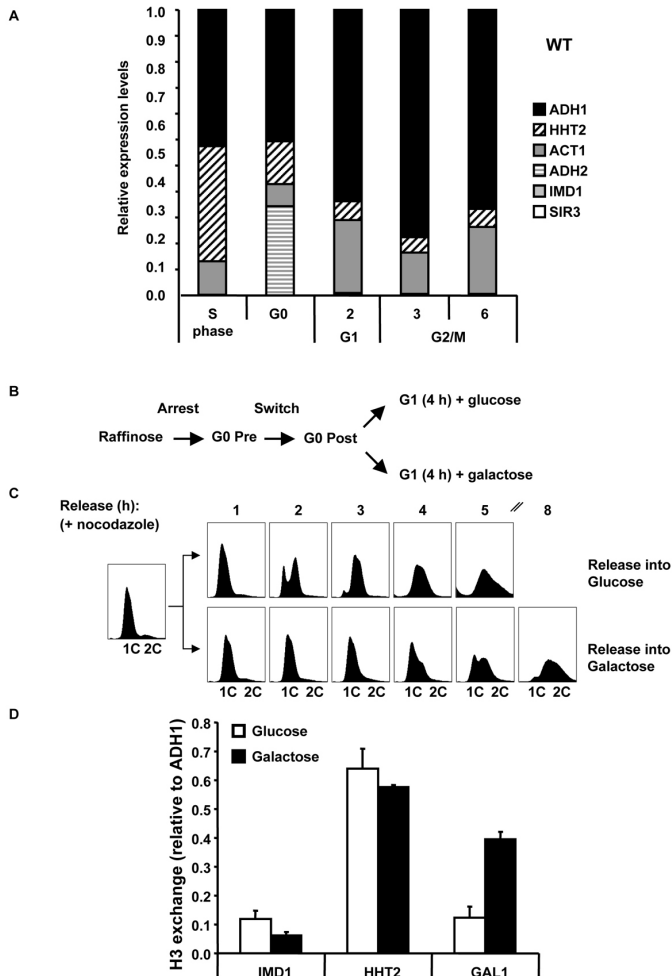
Figure S4. Histone exchange correlates with mRNA expression levels. (A) To confirm that the RITE tags did not affect gene expression, mRNA was isolated from a wild-type strain (NKI2036) and relative expression levels were calculated at each indicated time. The relative expression levels are identical to those of the RITE tagged strain (Fig. 4B). The relative mRNA expression patterns correlated very well with the observed histone exchange rates. For example, ADH2 was active under low glucose conditions in starved cells and repressed in cells released in glucose-rich media. Indeed, ADH2 belonged to the genes with high exchange in arrested cells or shortly after release and then dropped to the low exchange at later time points (Fig.s 3C and 3D). ACT1, which was induced in cells arrested by α-factor, specifically peaked late in the G1 arrest (Fig. 3C). Finally, relative exchange at HHT2 was highest early in the G2/M arrest. Although HHT2 expression was low in G2/M, cells at this time point have just exited S-phase, during which transcription of histone genes was induced (Fig. 3D). Therefore, the presence of new H3-T7 might be a mark of previous transcription events. (B) To analyze the causal effect of transcription on histone exchange, cells were starved and switched in medium containing raffinose and subsequently released into medium containing glucose or galactose, to repress or induce the GAL1 gene, respectively. Cells were arrested in G1 for 4 hrs. (C) FACS analysis of cells starved in raffinose media and released in media containing nocodazole (G2/M arrest) and either glucose or galactose. Starved cells released in media with galactose re-entered more slowly into the cell cycle and showed lower overall new histone expression at this time point. Therefore, subsequent exchange ratios were determined relative to ADH1. (D) Histone exchange (ChIP T7/HA) at GAL1, HHT2 and IMD1.Upon activation of GAL1, deposition of new H3-T7 was increased at the GAL1 promoter indicating that transcription enhanced histone exchange.

Fig. S5
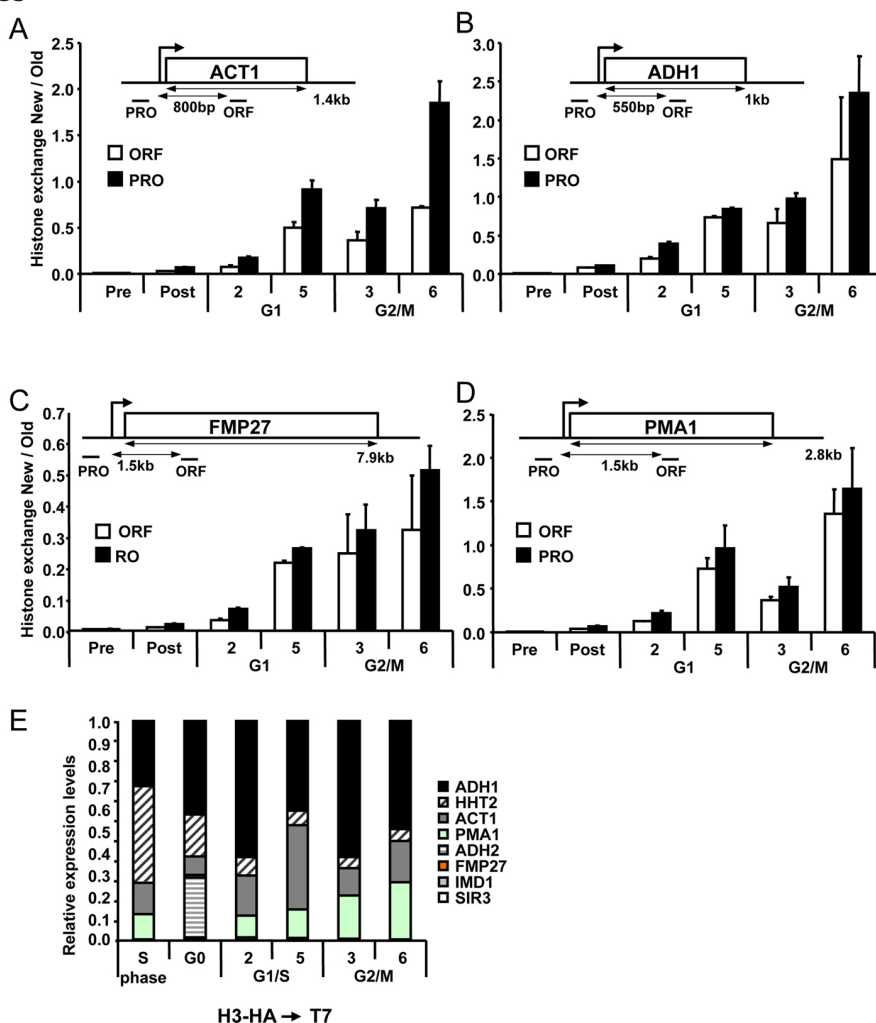
Figure S5. Histone exchange occurs at promoters and coding sequences. (A-D) RITE-ChIP showed that new H3-T7 was readily incorporated in promoters by a transcription-coupled process. However, histone exchange at promoter regions, which represent less than a quarter of the yeast genome, was insufficient to explain the global deposition of new H3-T7 (~50% of the total H3 pool) observed by immunoblots (Fig. 3B). Therefore histone exchange in coding sequences was also determined. Histone exchange at promoters (PRO) was determined as in Fig. 3C and compared to exchange in coding sequences (ORF) of ACT1 and ADH1, and in addition of two long genes FMP27 and PMA1 to exclude effects of proximal promoter sequences. The location of the analyzed regions and the distance between promoter and ORF regions is indicated. (E) Relative mRNA expression levels in the H3-HA→T7 strains as shown in Fig. 3D but now including the expression of PMA1 and FMP27. Ectopically expressed histones in yeast have been shown to be predominantly incorporated in promoter regions largely irrespective of the level of transcription, whereas the lower level of exchange in ORFs correlated with transcription rates (1-7). Using RITE we found by ChIP that exchange of endogenous histones in ORFs was nearly as high as in promoters and this notion was supported by the global turnover of bulk histones that we detected by immunoblot (Fig. 3B). In addition, the rate of exchange of endogenous histones in ORFs as well as promoters correlated with transcription levels. Thus, transcription-coupled replication-independent exchange of histones occurred in promoters and coding regions.

Fig. S6
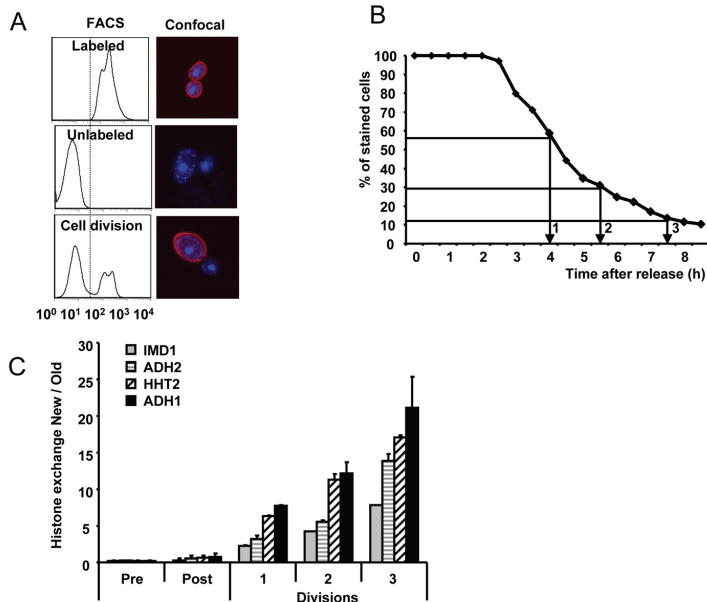
Figure S6. Histone exchange in successive cell divisions. Starved switched H3-T7→HA cells were released into fresh media and harvested after one, two, and three rounds of cell division. To count cell divisions we developed a convenient and stable fluorescent cross linker, NHS-TER, which labels the yeast cell wall. Upon cell division, daughter cells or buds synthesize cell wall *de novo* and emerge as unlabeled cells whereas the mother cells retain the label (8) (A). Thus, the fraction of unlabeled cells, which can be quantitatively determined by FACS, is a measure of the number of cell doublings. (B) The cell wall of the starved cells was labeled with NHS-TER prior to induction of Cre recombinase to quantitatively determine the number of cells in the population that had undergone cell division. Mother cells retain the old cell wall and daughter cells make cell wall *de novo*, as confirmed by confocal microscopy (right panel; blue is Hoechst DNA staining). The percentage of unlabeled cells identified by FACS (left panel) indicates the percentage of new-born daughter cells in the population and corresponds to the percentage of chromatin that is new. (B) Starved H3-T7→HA cells stained with NHS-TER prior to Cre-induction were released after the switch into fresh media and samples were taken at the indicated time points to capture cells after 1, 2, and 3 cell divisions. The number of cell divisions in the population was confirmed by FACS. The percentage of cells that had undergone a cell division (d) relates to the percentage of unlabeled cells (u) by 100*u=d/(100+d). (C) Histone replacement at promoters in samples described in panel B was determined by ChIP (HA/T7).

Supplementary References:

1. Linger J, Tyler JK (2006) Global replication-independent histone H4 exchange in budding yeast. Eukaryot Cell 5:1780-1787.
2. Dion MF, Kaplan T, Kim M, Buratowski S, Friedman N *et al*. (2007) Dynamics of replication-independent histone turnover in budding yeast. Science 315:1405-1408.
3. Rufiange A, Jacques PE, Bhat W, Robert F, Nourani A (2007) Genome-wide replication-independent histone h3 exchange occurs predominantly at promoters and implicates h3 k56 acetylation and asf1. Mol Cell 27:393-405.
4. Kim HJ, Seol JH, Han JW, Youn HD, Cho EJ (2007) Histone chaperones regulate histone exchange during transcription. EMBO J.
5. Jamai A, Imoberdorf RM, Strubin M (2007) Continuous histone H2B and transcription-dependent histone H3 exchange in yeast cells outside of replication. Mol Cell 25:345-355.
6. Kaplan T, Liu CL, Erkmann JA, Holik J, Grunstein M *et al*. (2008) Cell cycle- and chaperone-mediated regulation of H3K56ac incorporation in yeast. PLoS Genet. 4:e1000270.
7. Gat-Viks I, Vingron M (2009) Evidence for gene-specific rather than transcription rate-dependent histone H3 exchange in yeast coding regions. PLoS Comput. Biol. 5:e1000282.
8. Park PU, McVey M, Guarente L (2002) Separation of mother and daughter cells. Methods Enzymol. 351:468-477.

Supplemental Table 1:

Strain:	Relevant genotype	Reference
BY4705	MATα ade2Δ::HisG his3Δ200 leu2Δ0 lys2Δ0 met15Δ0 trp1Δ63 ura3Δ0	(1)
BY4724	MATa lys2Δ0 ura3Δ0	(1)
BY4742	MATα his3Δ1 leu2Δ0 lys2Δ0 ura3Δ0	(1)
NKI2036	MATa his3Δ200 leu2Δ0 lys2Δ0 met15Δ0 ura3Δ0 Δhhf1-hht1::LEU2	This study
NKI2148	MATa his3Δ200 leu2Δ0 lys2Δ0 met15Δ0 ura3Δ0 Δhhf1-hht1::LEU2 HIS3::Ptdh3_CRE_EBD78 bar1Δ::HisG hht2::HHT2-LoxP-HA-HYG-LoxP-T7	This study
NKI2158	MATa his3Δ200 leu2Δ0 lys2Δ0 met15Δ0 ura3Δ0 Δhhf1-hht1::LEU2 CYC1term::Ptdh3_CRE_EBD78_HIS3 hht2::HHT2-LoxP-T7-HYG-LoxP-HA	This study
NKI4004	MATa his3Δ200 leu2Δ0 lys2Δ0 met15Δ0 ura3Δ0 Δhhf1-hht1::LEU2 hht2::HHT2-LoxP-HA-HYG-LoxP-T7	This study
NKI4009	MATa his3Δ200 leu2Δ0lys2Δ0 met15Δ0 ura3Δ0 Δhhf1-hht1::LEU2 hht2::HHT2-LoxP-T7	This study
Y7092	MATα can1Δ::STE2pr-Sp_his5 lyp1Δ his3Δ1 leu2Δ0 ura3Δ0 met15Δ0 LYS2	(2)
NKI4101	MATα can1Δ::STE2pr-Sp_his5 lyp1Δ his3Δ1 leu2Δ0 ura3Δ0 met15Δ0 LYS2 pre3::PRE3-V5-loxP-HA-yEGFP-HYG-loxP-T7-mRFP	This study
NKI4103	NKI4101 + lyp1Δ::NATMX-GPD_CRE_EBD78	This study
NKI4104	MATα can1Δ::STE2pr-Sp_his5 lyp1Δ his3v1 leu2Δ0 ura3v0 met15Δ0 LYS2 lyp1Δ::NATMX-GPD_CRE_EBD78 pre3::PRE3-V5-loxP-T7-mRFP	This study

1. Brachmann CB, Davies A, Cost GJ, Caputo E, Li J *et al*. (1998) Designer deletion strains derived from *Saccharomyces cerevisiae* S288C: a useful set of strains and plasmids for PCR-mediated gene disruption and other applications. Yeast 14:115-132.
2. Tong AH, Boone C (2006) Synthetic genetic array analysis in *Saccharomyces cerevisiae*. Methods Mol. Biol. 313:171-192.

Supplemental Table 2:

Gene name:	Primer name:	Primer Sequence:
ADH1	ADH1 PRO II fwd	CCGTTGTTGTCTCACCATATCC
ADH1	ADH1 PRO II rev	GTTTCGTGTGCTTCGAGATACC
ADH1	ADH1 ORF II fwd	TAGGTTCTTTGGCTGTTCAATACG
ADH1	ADH1 ORF II rev	CGGAAACGGAAACGTTGATGACACCG
HHT2	HHT2 QFor1	GTGCCAAACGACCACAGTTG
HHT2	HHT2 QRev1	GGGCGTGCCAATAGTTTCAC
HHT2	HHT2 QFor2	AAGCCCCAAGAAAACAATTAGC
HHT2	HHT2 QRev2	AAGCCCCAAGAAAACAATTAGC
ACT1	ACT1 Qfor	CTCTTTTTATCTTCCTTTTTTTCCTCTCT
ACT1	ACT1 Qrev	CGTGAAAAATCTAAAAGCTGATGTAGTAG
ACT1	ACT1 QforORF	TCGTTCCAATTTACGCTGGTT
ACT1	ACT1 QrevORF	CGGCCAAATCGATTCTCAA
ADH2	ADH2 PRO II fwd	AACACCGGGCATCTCCAAC
ADH2	ADH2 PRO II rev	AAGTCGCTACTGGCACTC
ADH2	ADH2 ORF I fwd	ACACCCACGACGGTTCTTTC
ADH2	ADH2 ORF I rev	CAAGATTGGCGCGACTTCAG
IMD1	QFOR IMD1	TTTCGTGGGCTAGTACATTTTACCT
IMD1	QREV IMD1	TGATAAGAAAAGTAAGGCAAGGAATAGA
IMD1	Q IMD1 for-2	TTTGCAGGCTTCCCTGTCA
IMD1	Q IMD1 rev-2	TGATGGCACCCACCAACTTT
SIR3	SIR3 Qfor	CGAAAACGCTATTCTTTCCAAAA
SIR3	SIR3 Qrev	CCCCTGTAAGGAAGGTGATGAA
SIR3	SIR3 ORF Qfor 1	GACGGCCGAGAGAATTTTGTAT
SIR3	SIR3 ORF Qrev 1	CTTCAAGCCCACCATCATCA
PMA1	PMA1 PRO Qfor1	TGGTGGGTACCGCTTATGCT
PMA1	PMA1 PRO Qrev1	TGTTAGACGATAATGATAGGACATTTGA
PMA1	PMA1 ORF Qfor1	AAATCTTGGGTGTTATGCCATGT
PMA1	PMA1 ORF Qrev1	CCAAGTGTCTAGCTTCGCTAACAG
FMP27	FMP27 PRO Qfor1	AGGGAGACATGAAAAAGGGTCTT
FMP27	FMP27 PRO Qrev1	TCTCTGAGATGTCTAGGCCCTTTTA
FMP27	FMP27 ORF Qfor1	TGGACAGCATTGCCATAGAAGA
FMP27	FMP27 ORF Qrev1	TGTACTAATTCACTCAACATAACCATTGTT
NoORF	NoORF Qfor	GGCTGTCAGAATATGGGGCCGTAGTA
NoORF	NoORF Qrev	CACCCCGAAGCTGCTTTCACAATAC

Supplementary Methods

Yeast strains and plasmids

All *S. cerevisiae* strains used in this study are derived from S288C strains BY4705, BY4727, BY4741, BY4742 (1) and are listed in Table 1. Plasmids pRS400, pFvL99 and pFvL100 were used for gene replacements by KanMX4, NatMX4, and HpHMX4, respectively (2, 3). To generate pFvL99 and pFvL100, the PacI-BsmI KanMX4 insert of pRS400 was replaced by a PacI-BsmI fragment of pAG25 or pAG32 (4), respectively. The drug resistance cassettes were amplified using the standard pRS primers. RITE cassettes were constructed by restriction enzyme based cloning of PCR fragments in a modular fashion to generate the following basic construct: NotI-spacer-LoxP-KpnI-Tag1-Spe1-stop-ADH1term-BamHI-HygroMX-XbaI-LoxP-SalI-Tag2-BsrGI-stop. The following modules were used: spacer: GGTGGATCTGGTGGATCT, LoxP: ATAACTTCGTATAATG¬TATGCTATACGAAG-TTATCA, HA: TACCCATACGATGTT¬CCTGACTATGCG, T7: ATGGCAAGCATGAC-TGGTGGACAGCAAATGGGT, HphMX: 1.8 kb fragment amplified from pFvL100 AGATTGTACTGA¬GAGTGCAC….. CGGTGTGAA¬ATACCGCACAG, ADH1 terminator: amplified from pFA6a-3HA-KanMX (5) CTTCTAA¬ATAAGCGA…… GGGATAACAGGGTAA. The encoded short peptide spacer sequence (GGSGGS) was found to be required for viability of strains carrying tagged histones. The 34bp LoxP DNA sequence is part of the coding region (resulting in the peptide sequence ITSYNVCYTKLS) and is present in front of the epitope tags both before and after the switch. RITE cassettes were PCR amplified and targeted to the 3' end of the endogenous genes by homologous recombination to tag the C-terminus and ensure regulation by the endogenous promoter. The hormone-dependent Cre-EBD was described previously (6). We used a derivative of this construct (Cre-EBD78) which is constitutively expressed and contains several mutations to make the recombinase more tightly dependent on β-estradiol (7). A TDH3 promoter fragment, Cre-EBD78, and a CYC1 terminator sequence were cloned into pRS303 (1) to generate pTW040, which was linearized with Eco47III or MluI to integrate the construct at the HIS3 locus or CYC1 locus, respectively.

Galactose induction

To perform a galactose induction the cells were grown to saturation in YP containing 3% raffinose. Since the cells cycle a little slower in raffinose than in glucose twice the amount of cells was grown for the same amount of time as previously. In order to release the cells into the cell cycle, one half of the culture was resuspended in YPD, the other half in YP + 1% raffinose + 2% galactose. Both media contained 0.5 ng/μl of α-factor. To determine the speed of release in either media, the cells were grown identical to previously, but released into media containing 15 μg/ml Nocodazole. Cells were harvested every hour for FACS analysis of DNA content.

Polyclonal antibody production

A polyclonal antibody was obtained by immunizing rabbits using the peptide GGSGGSITSYNVC*YTKLS against the spacer and LoxP sequence (the asterisk indicates the cysteine present as a sulfhydryl necessary for conjugation). For immunization 2 mg of the peptide was covalently conjugated to Imject Mariculture Keyhole Limpet Hemocyanin (mcKLH) (Pierce) as a carrier protein. The concentration of the conjugated hapten was determined using Bradford (Bio-Rad). Per immunization 100μg in 1ml PBS was injected. Each rabbit received 3 boosts with 1 month intervals, two rabbits were immunized. Each antibody was tested for specificity using a WT, an HA and a T7 tagged strain.

Southern Blotting

For Southern blotting $5x10^8$ cells were spun and frozen at -80ºC. A histone H3 (HHT2) specific probe was made by PCR amplification using the primers: HHT2_HindIII_for: GAATCTTTCTGTGACGCTTGG and HHT2_HindIII_rev GGGGAAGAACAGTTGGAAGG, resulting in a 650bp amplicon covering the region 576144 to 576794. When used on genomic DNA which was digested using the HindIII enzyme, the three bands recognized are specific for before the switch (3000bp), after the switch (931bp) or as an internal control (1538bp). Radioactive Southern blotting was performed using 50μCi of 32P-dCTP; incubation was done overnight at 65ºC.

Quantitatve Immunoblotting

For immunoblotting $5x10^7$ cells were spun, washed once with cold 1xTE+0.2mM PMSF, pellet was frozen (3). Whole-cell extracts were obtained from approximately $5x10^7$ cells by the classical glass beads breakage method using 200μl of glass beads and SUMEB (8) complemented with PMSF (1 mM), benzamidine (5 mM), pepstatin (1 μg/ml), leupeptin (1 μg/ml) and DTT (1 μM). The resulting lysate was separated onto a 16% polyacrylamide gel and blotted onto 0.45 μm nitrocellulose membrane. Membranes were blocked with 2% Nutrilon (Nutricia) in PBS. Primary antibody incubations were performed overnight in Tris-buffered saline-Tween with 2% Nutrilon, anti-HA (12CA5), anti-T7 (Abcam, 1:1000) and a polyclonal antibody obtained against the LoxP peptide (1:2500). Secondary antibody incubations were performed for 45 minutes using LI-COR® Odyssey IRDye® 800CW (1:12.000).

Immunoblots were subsequently scanned on a LI-COR Odyssey® IR Imager (Biosciences) using the 800 channel. Signal intensities were determined using Odyssey LI-COR software version 3.0. Ratios of T7/HA were converted into %HA values by using a standard curve of samples with known amounts of H3-HA and H3-T7. These samples were generated by mixing cells expressing either only H3-HA (NKI4004) or H3-T7 (NKI4009) in various ratios of cell numbers. Blots of the standard curve and the experimental samples were processed simultaneously.

Reverse-transcription
Ranking of genes based on estimated transcription frequencies was based on genome-wide mRNA expression and stability data from Holstege *et al*. (9). Total yeast RNA was prepared from 5×10^7 cells of each of the indicated growth condition using the RNeasy kit (Qiagen) according to the manufacturer's protocol (10). RNA samples were treated with RNase free DNAse (Qiagen), and cDNA was made by using Super-Script II reverse transcriptase (Invitrogen). To obtain an S-phase sample, cells were synchronized for three hours in G1 using 0.5 ng/µl α-factor, released after two washes with YPD (containing 0.1mg/ml ProNase E if strain was bar1Δ) and isolated every 0.5 h. By FACS analysis it was determined that 0.5 h after release the maximum amount of cells were in S-phase.

Chromatin immunoprecipitation
ChIP was performed as described previously (3, 10, 11). Approximately 1×10^9 cells were fixed with 1% formaldehyde for 15 minutes room temperature. The formaldehyde was quenched with 125mM glycine by shaking 5 minutes at room temperature. Cells were washed once in cold TBS + 0.2 mM PMSF, pellet was frozen at -80ºC.The chromatin was sheared using a bioruptor (Diagenode) for 6 minutes with 30 seconds intervals at high. The obtained fragments have an average size of 500bp, as determined on a 2% TAE gel stained with ethidium bromide and quantified using TINA software. The isolated chromatin of the equivalent of 5×10^7 cells was immunoprecipitated overnight at 4ºC using magnetic Dynabeads (Invitrogen) which were previously incubated with antibody o/n at 4ºC.

Real-time PCR
ChIP DNA and cDNA was quantified in real-time PCR using the SYBR® Green PCR Master Mix (Applied Biosystems) and the ABI PRISM 7500 as described previously (2, 10). An input sample was used to make a standard curve, which was then used to calculate the IP samples, all performed in the 7500 fast system software. As a measurement for exchange, the amount DNA of the T7-IP was divided over the HA-IP. Primers used for qPCR are listed in Table S2.

Staining cells with N-hydroxysuccinimide-Tetra-Ethylrhodamine (NHS-TER)
A 20% aqueous solution of an isomeric mixture of 5(6)-carboxyrhodamine (Rhodamine WT) was obtained from Abbey Color, Philadelphia, PA. The free acid was precipitated with concentrated hydrochloric acid (two equivalents) as described (12). The precipitate was collected by centrifugation, and resuspended in 1M HCl. This procedure was repeated twice and the precipitate was frozen and freeze-dried to remove residual traces of water. The free acid was converted in an active N-hydroxysuccinimide (NHS) ester by condensation with N-hydroxysuccinimide mediated by the agent di-isopropylcarbodiimide (DIC). This is a relatively simple and very economical procedure compared to other fluorescent labeling approaches. To stain yeast cells, cultures were washed twice with PBS. Cells resuspended in PBS, NHS-TER was added (0.8 mg NHS-TER per 10^8 cells) and incubated at room temperature for 15 minutes. Cells were washed 8 times with PBS and then resuspended in YPD medium. For each time point 10^7 cells were fixed for FACS analysis or confocal microscopy. The samples were fixed with 4% formaldehyde in PBS for 10 minutes at room temperature and washed with water. Cells were briefly sonicated. For confocal microscopy the pellet was resuspended in 1 ml water and cells were stained with Hoechst (1 µg/ml) as a DNA stain. The pellet was resuspended in 50 µl water and 2 µl of this solution was mounted in Vectashield mounting medium on a concanavalin-A coated cover slip. Confocal analyses were performed using a Leica TCS SP2 confocal system, equipped with Diode 405 and 561 lasers. Images were taken using a 63x 1.4 objective. Emission windows 415-540 and 571-700 and Kalman averaging were used. For FACS analysis the cells were resuspended in 500 µl water.

FACS analysis of DNA content and cell doubling
The DNA content was measured using SYTOX Green in flow cytometry as described previously (2, 13), detection was done using a 530/30 filter. For FACS analysis of DNA content 1×10^7 cells were spun briefly at maximum speed, resuspended in 1ml of 70% ethanol, and kept at -20ºC. NHS-TER stained cells were detected using a 585/42 filter of the FACS calibur (Becton-Dickinson). For each measurement 100.000 cells were counted. Analysis was performed using FCS express 2. To determine the percentage stained cells (mother) versus unlabeled cells (daughter), NHS-TER stained cells were harvested at indicated time points. Additionally, cells were also counted using a count chamber and a wide field microscope. The signal in channel FL2 was divided into two regions based on a 100% and an unlabeled control, these regions were applied to all samples. The number The percentage of

labeled cells (L) was used to calculate the number of population doublings (Dp) by: L=100*0.5^Dp.

Microscopy

5×10^6 cells were pelleted, washed once with water and fixed with 4% formaldehyde for 10 minutes at room temperature. Cells were then washed with water and nuclei were stained with Hoechst 33342 (Invitrogen, UK, 1 μg/ml) for 15 minutes at room temperature. Cells were then washed and resuspended in 100 μl water. Resuspended cells were mixed with one volume Vectashield mounting solution (Vector Laboratories) and mounted onto ConA-coated cover slips. The images were made using a Leica AOBS LSCM (Leica Microsystems), using a 405nm, a 488 and a 563nm laser to visualize Hoechst, GFP, and mRFP, respectively. Images were analyzed using customized Cell Profiler (open-source cell image analysis software). For each time point, 4 different micrographs, each of them containing approximately 100 yeast cells were quantified using the pipeline described below.

Confocal microscopy pipeline

Can be found at: www.pnas.org/content/107/1/64

2

Chapter Three

Chapter 3:

Spatiotemporal analysis of organelle and macromolecular complex inheritance

Victoria Menendez-Benito[1], **Sjoerd J. van Deventer**[1], Victor Jimenez-Garcia[1], Marina Roy-Luzarraga[1], Fred van Leeuwen[2], Jacques Neefjes[1]

3

[1] Division of Cell Biology 2 and
[2] Division of Gene Regulation,
Netherlands Cancer Institute, Amsterdam, The Netherlands

Abstract

Following mitosis, daughter cells must inherit a functional set of essential proteins and organelles. We applied a genetic tool to simultaneously monitor the kinetics and distribution of old and new proteins marking all intracellular compartments in budding yeasts. Most organelles followed a general pattern whereby preexisting proteins are symmetrically partitioned followed by template-based incorporation of new proteins. Peroxisomes belong to this group, supporting a model of biogenesis by growth and division from preexisting peroxisomes. We detected two exceptions: the nuclear pore complex (NPC) and the spindle pole body (SPB). Old NPCs are stably inherited during successive generations but remained separated from new NPCs, which are incorporated *de novo* in mother and daughter cells. Only the SPB displayed asymmetrical distribution, with old components primarily inherited by daughter cells and new proteins equally incorporated in both cells. Our analysis resolves conflicting models (peroxisomes, NPC) and reveals unique patterns (NPC, SPB) of organelle inheritance.

Introduction

Compartmentalization of specialized proteins into membrane-bound organelles and macromolecular machines constitutes an essential strategy to control biological processes such as DNA replication and protein degradation. When cells divide, the information and components required to build these intracellular compartments must be transmitted to progeny. One approach to achieving this is to share the preexisting maternal compartments between mother and daughter cells in a process known as "inheritance." The molecular mechanisms controlling inheritance of intracellular compartments have been extensively studied in the budding yeast *Saccharomyces cerevisiae* (1), as mothers can be distinguished from daughter cells. Budding yeasts divide asymmetrically, producing two cells (mother and bud) that are different in size, metabolism, and age. During mitosis in yeast, most organelles are transported from mother to bud along actin cables. This transport is mediated by class-V myosin proteins that recognize a specific receptor for each intracellular compartment, including the vacuole, mitochondria, peroxisomes, Golgi apparatus, and cortical endoplasmic reticulum (ER) (2). Two important exceptions are the nucleus and the perinuclear ER, which are transported by microtubules (3). Following transfer into the bud, some organelles such as cortical ER (4), mitochondria (5), and peroxisomes (6) become anchored at the bud tip, and this retention regulates the total amount of maternal components that enters the bud.

In addition to sharing preexisting compartments derived from the mother, new proteins are synthesized to support cellular growth. In principle, new components may either be incorporated into preexisting compartments or generate new copies without a template (*de novo*). Some membrane-bound compartments may only be generated in a template-based manner. For instance, many of the constituent proteins of the ER require a mature and functional translocon and chaperone system for their own synthesis. This may also be expected for other organelles such as mitochondria, which incorporate proteins made by cytosolic ribosomes. Other organelles may use the ER as a platform to generate essential components in a *de novo* fashion. Recent studies describing *de novo* formation of peroxisomes (7–10) and Golgi (11) have reopened the debate regarding organelle

biosynthesis by division and partitioning.

Another unresolved issue pertaining to protein inheritance is whether mother and daughter cells have an equal proportion of new and old components. Several examples of asymmetrical segregation have been documented. Specifically, damaged proteins accumulate in mother cells by an active retention mechanism for protein aggregates (12). Plasma membrane transporters are also distributed asymmetrically, with the old pool predominantly remaining in the mother cell (13). Recently, a nuclear transport factor was discovered that preferentially segregates to the bud, thereby redirecting translation into the daughter cell (14). It is unclear whether these examples specify specialized cases or general mechanisms for discrimination and differential segregation of old and new proteins. In such a model, newly made proteins, which may be less damaged but also less validated in functional terms, would concentrate in daughter cells. A different premise would be that old and new proteins are shared during cell division, resulting in two new cells with proteomes reset to the same molecular age.

Here we address these questions using a unique fluorescence-based system called "recombination-induced tag exchange" (RITE) (15, 16). RITE is specifically designed to distinguish and simultaneously monitor endogenous expression of old and newly synthesized proteins. Combining RITE with yeast genetics allows a global analysis of the inheritance of protein components of all intracellular compartments. Old and new proteins are homogeneously distributed within each compartment and are equally segregated between mother and daughter cells. We describe two exceptions where old and new components either remain separated in distinct domains (nuclear pore complex; NPC) or are asymmetrically inherited (spindle pole body; SPB). Our comprehensive analysis of inheritance of intracellular compartments defines general rules of equal partitioning of constituent proteins and some exceptions where daughters found a different solution to obtaining their essential biological share.

3

Results

Generation of a Collection of Yeast Strains for Intracellular Compartment Tracing.

We have recently developed a system to distinguish old and new proteins, named RITE. It consists of an inducible Cre-recombinase (which can be activated at will with β-estradiol) and a DNA tagging cassette that can be introduced in the genetic locus of the gene of interest (Fig. 1). Here we used a RITE DNA cassette with a GFP tag flanked by two LoxP recombination sites and followed by a red fluorescent protein (RFP) tag. This allows us to distinguish proteins produced before Cre activation (GFP-labeled) from newly synthesized proteins (RFP-labeled) following the "genetic switch" in single cells.

We generated a collection of RITE haploid *S. cerevisiae* by tagging proteins representative of each intracellular compartment (Fig. S1A). The target proteins were selected on the basis of the following characteristics: (i) essential cellular function, (ii) conservation among eukaryotes, (iii) slow turnover rate, and (iv) lack of effects on cell viability resulting from C-terminal GFP or RFP fusion. With the exception of the nucleolar marker, we chose proteins integrated in the membrane of organelles to exclude exchange by dynamic diffusion. The Yeast GFP Fusion Localization Database (http://yeastgfp.yeastgenome.org) was a source for selection of candidate genes allowing the GFP modification (17, 18). The RITE cassette was incorporated at the endogenous locus of target genes, yielding physiological expression of RITE-tagged proteins without competition from untagged

Fig. 1
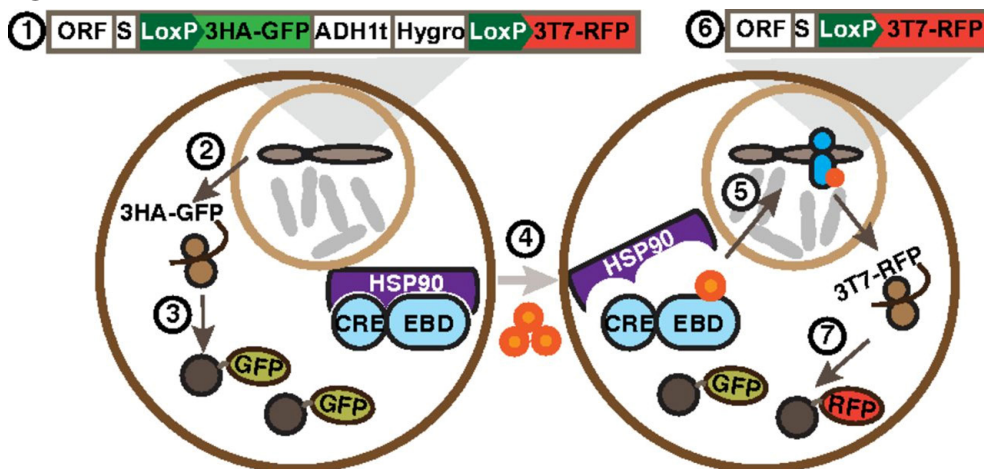
Figure 1: Schematic representation of RITE.
(1) In-frame insertion of RITE DNA with the ORF of the target gene. RITE DNA contains two tags (3HA-GFP and 3T7-RFP) separated by two LoxP recombination sites, an invariant flexible spacer (S), a transcriptional terminator (ADH1t), and a hygromycin resistance gene (Hygro). (2 and 3) As a result, the protein of interest is tagged with LoxP-3HA-GFP. (4–6) RITE yeasts express Cre-recombinase fused to the estrogen-binding domain (Cre-EBD), which is kept inactive binding to Hsp90. β-Estradiol releases Cre-EBD that then enters the nucleus for DNA recombination, resulting in a tag switch to LoxP-3T7-RFP. (7) The genetic switch yields proteins tagged with LoxP-3T7-RFP.

proteins.

To monitor protein inheritance, the genetic switch was induced during the postdiauxic shift (PDS) (Fig. S1 B–D). The PDS is naturally reached when the glucose in the media is consumed, resulting in adjustment of metabolism, low protein synthesis, the ability to remain viable for long periods of time, and very slow proliferation (one doubling over a period of days) (19). Once the genetic switch was completed, fresh medium was added to synchronously induce the first cell division within 3–4 h (Fig. S1D). We measured the levels of mRNA for the GFP-labeled proteins (GFP-mRNA) for each RITE strain (Fig. S2 and Table S1). GFP-mRNAs were unstable after the genetic switch and degraded during the PDS or within 30 min after release into fresh media. Therefore, (old) GFP-mRNAs do not contribute to the synthesis of new proteins during the first cell division in released cells. To monitor protein inheritance, we visualized old (GFP) and new (RFP) proteins by time-lapse microscopy and analyzed their final distribution at anaphase (3 h postrelease). For the study of highly dynamic organelles, such as the Golgi, the genetic switch was performed in log phase (Fig. S1 E–G).

RITE allowed us to perform a pulse–chase type of experiment in intact cells, where old and new proteins can be monitored by fluorescent microscopy. Unlike classical pulse–chase protocols, RITE can be combined with cell division, as done here, and with genetic screens (20).

Old and New Proteins Are Homogeneously Distributed in Most Organelles.
Tracing organelle markers for nucleolus, ER, mitochondria, vacuoles, and Golgi with RITE revealed even distribution between mother and bud. New proteins were uniformly

incorporated along with old proteins, as shown by the overlapping distribution of GFP and RFP (Fig. 2A). Quantification of GFP fluorescence intensity revealed that daughter cells inherited half of the old maternal proteins (Fig. 2B). Likewise, incorporation of new material reached comparable levels in mother and bud pairs, as deduced from the RFP fluorescence signal. The distribution of GFP and RFP was confirmed by immunofluorescence, as shown

Fig. 2
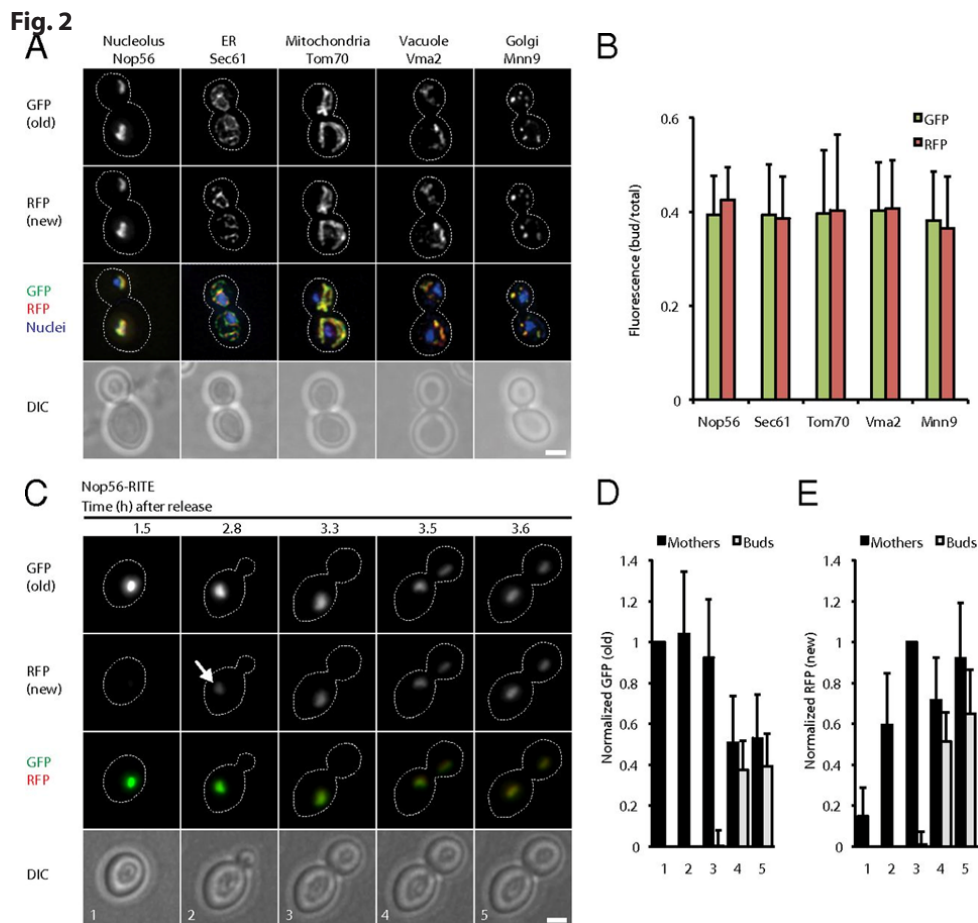
Figure 2: Nucleolus, ER, mitochondria, vacuole, and Golgi segregate symmetrically during cell division.
(A) Representative images of RITE strains 3 h postrelease. For the Golgi, the genetic switch was performed in log phase. (B) Quantification of old (GFP) and new (RFP) proteins at 3 h postrelease, measured as indicated in Materials and Methods. Values are average ± SD, determined from 25, 52, 32, 35, and 30 dividing cells, respectively (n). (C) Selected frames from time-lapse recordings of Nop56-RITE starting at 1 h postrelease. Images were taken at 10-min intervals over 3.5 h. The selected frames correspond to the following cell-cycle stages: (1) start, (2) bud emergence, (3) bud growth, (4) nuclear division, and (5) anaphase. The time (h) elapsed since the release is indicated by the numbers above the frames. The arrow indicates the area where new (RFP) Nop56 appears. (D and E) Quantification of old (GFP) and new (RFP) Nop56 in time-lapse recordings, imaged as indicated in C. For each dividing cell, frames were selected for the different cell-cycle stages (1–5), and GFP (D) and RFP (E) were measured in mother and daughter cells. GFP measurements were normalized to GFP in the mother cell in the first frame (1), and RFP measurements were normalized to RFP in the mother cell at bud-growth stage (3). Values are average ± SD (n = 26 cells). For all of the images, dashed lines represent the cell outlines based on DIC images. (Scale bars, 2 µm.) DIC, differential interference contrast.

for Vma2-RITE (Fig. S3). Time-lapse microscopy revealed similar dynamics of old and new proteins during cell division for these organelles (Fig. 2C and Fig. S4). With the exception of the Golgi, the total pool of old (GFP) proteins remained constant during cell division. When organelles segregated into the bud, old (GFP) proteins were redistributed between mother and daughter cells and remained thereafter (Fig. 2 C and D and Fig. S4 A–C). New (RFP) proteins were first detected in the mother cell, before organelle transfer, and continued increasing in mother and daughter cells during mitosis. The ER marker Sec61 appeared simultaneously in mother and daughter cells after organelle transfer (Fig. S4A). In the Golgi, old (GFP) Mnn9 disappeared following the genetic switch, probably due to the dynamic nature of the Golgi (20, 21). Time-lapse experiments showed exchange by new (RFP) Mnn9 at early phases of division (Fig. S4D).

In summary, nucleoli, ER, mitochondria, vacuole, and Golgi exhibit ordered partitioning and template-based growth, resulting in equal sharing of old and new organelle content between generations.

Peroxisomes Are Duplicated in a Template-Based Manner Before Segregation.

Peroxisomes are duplicated and subsequently segregated during each cell division. The duplication of peroxisomes has been a subject of debate, and two conflicting models have been proposed: *de novo* formation (7–10) and template growth from existing peroxisomes (21).

Fig. 3
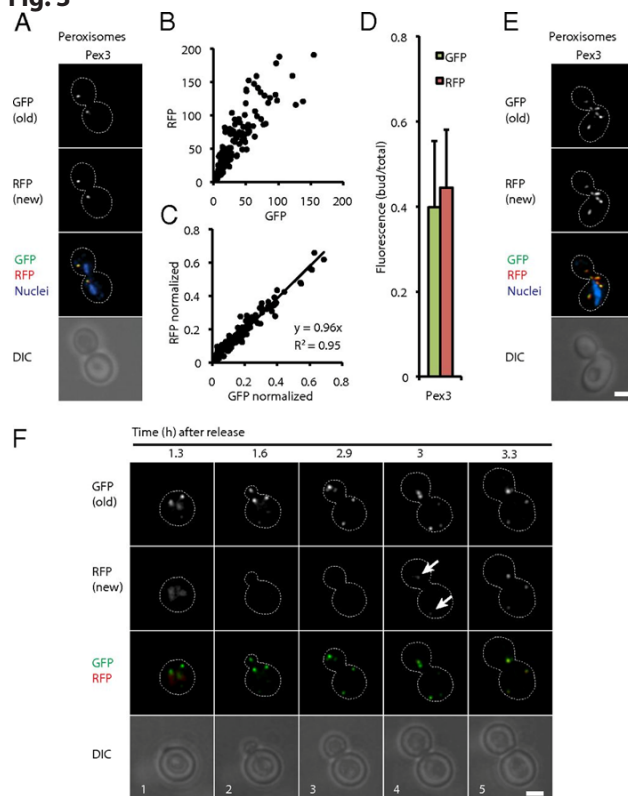
Figure 3: Peroxisomes are duplicated in a template-based manner and are equally segregated between mother and daughter cells. (A) Representative images of Pex3-RITE at 3 h postrelease. (B and C) Quantification of old (GFP) and new (RFP) Pex3 per individual peroxisome, showing total fluorescence intensities (B) and normalized values (C). Each dot represents an individual peroxisome (n = 120 peroxisomes, 22 dividing cells). (D) Quantification of old (GFP) and new (RFP) Pex3 at 3 h postrelease. Values are average ± SD (n = 30 dividing cells). (E) Representative images of Pex3-RITE, 3 h after inducing the genetic switch during cell division. (F) Selected frames from time-lapse recordings of Pex3-RITE, starting 1 h postrelease. Images were taken at 10-min intervals over 3.5 h. The selected frames correspond to the following cell-cycle stages: (1) start, (2) bud emergence, (3) bud growth, (4) nuclear division, and (5) anaphase. The time (h) elapsed since the release is indicated by the numbers above the frames. The arrows indicate the areas where new (RFP) Pex3 appears. For all of the images, dashed lines represent the cell boundaries based on DIC images. (Scale bars, 2 μm.)

We tagged an early integral peroxisomal membrane protein, Pex3 (22), with the RITE cassette and monitored the incorporation of newly synthesized Pex3 in peroxisomes. In the majority of cases (~99% of peroxisomes analyzed), newly synthesized (RFP) Pex3 was only present in peroxisomes containing preexisting (GFP) Pex3 (Fig. 3A). Quantification of GFP and RFP fluorescence intensities revealed that peroxisomes contained different quantities of Pex3. However, the relative amounts of old versus new Pex3 per peroxisome after one cell division was constant, as indicated by the linear correlation between GFP and RFP (Fig. 3 B and C). Old and new Pex3 were equally shared after cell division (Fig. 3D). Similar results for peroxisomal growth and segregation were found in experiments where the genetic switch was performed in log phase (Fig. 3E). Finally, the dynamics of Pex3 were visualized after a genetic switch in PDS by time-lapse imaging (Fig. 3F). Transfer of peroxisomes to the bud started early in mitosis and the total pool of old (GFP) Pex3 remained constant. By contrast, new (RFP) Pex3 was detected later and increased toward the end of anaphase. Importantly, new (RFP) Pex3 appeared (and remained) only in peroxisomes that were already labeled with Pex3-GFP. *De novo* synthesis of peroxisomes would have shown peroxisomes with exclusively new (RFP) Pex3, which was not observed. Rather, all peroxisomes contained both old and new Pex3 after cell division, supporting a template-based model of peroxisome duplication. Early transfer of peroxisomes to the daughter cell and template-based growth of peroxisomes resulted in equal distribution of old and new Pex3 in mitosis.

3

## Old and New NPCs Are Equally Segregated Without Mixing.

The nuclear envelope is a specialized case in organelle inheritance. In yeast, unlike mammalian cells, the nuclear envelope does not break down during mitosis but segregates alongside the chromosomes followed by fission (23). It is unclear whether the components of the nuclear envelope are freely distributed between mother and daughter cells. In particular, the segregation of NPCs is controversial, with two opposing models currently dominating the field. On the basis of photobleaching experiments it has been suggested that preexisting NPCs are retained by the mother cell, whereas only new NPCs are incorporated into the bud (24). By contrast, experiments with nucleoporins tagged with a photoconvertible fluorescent protein suggested that maternal NPCs migrate into the daughter cell (25).

We tagged two nucleoporins, Nup57 and Nup188, with RITE. These represent a central channel protein and a structural component of the NPC, respectively (26). The RITE assay showed that both preexisting (from maternal origin) and newly synthesized nucleoporins were present in mother and daughter cells (Fig. 4A). Quantification of old and new nucleoporins revealed an equal distribution among mothers and buds (Fig. 4B). Although maternal nucleoporins were shared with the bud, old and new nucleoporins did not mix, resulting in alternating regions formed by only old NPCs and only new NPCs (Fig. 4C). Strikingly, the old NPCs excluded new (RFP) Nup57 or Nup188 across generations, indicating that, once assembled, NPCs are very stable macromolecular complexes (Fig. 4D). We followed the dynamics of Nup57 inheritance by time-lapse microscopy (Fig. 4 E–H). At nuclear division, ~40% of old (GFP) Nup57 was transferred from the mother to the daughter cell and remained constant thereafter (Fig. 4 E and F). New (RFP) Nup57 appeared in the mother cell before nuclear division (Fig. 4E). As RFP has a lower quantum yield than GFP, new Nup57 may be more poorly detected. Therefore, we generated a strain with Nup57 tagged with T7 (nonfluorescent) that could be switched to HA-GFP (Fig. 4 G

and H). New (GFP) Nup57 appeared in the mother cell early after the switch (2 h), at the initiation of the cell cycle, and reached maximum levels before nuclear division. At nuclear division, ~40% of new (GFP) Nup57 was transferred to the daughter cell. Importantly, synthesis and incorporation of new Nup57 continued beyond nuclear division in both mother and daughter cells.

In conclusion, our data support a model where preexisting NPCs are highly stable and segregate equally between mother and daughter cells (25), whereas new NPCs are assembled *de novo* in both cells throughout cell division.

Fig. 4
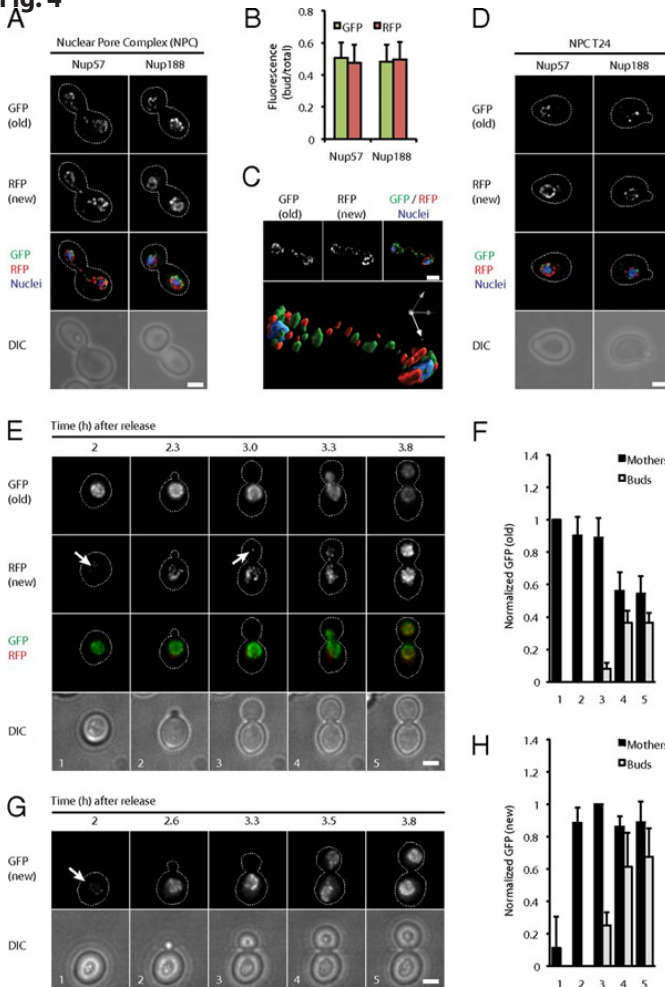
Figure 4 Old and new nucleoporins segregate equally between mother and daughter cells without mixing. (A) Representative images of Nup57-RITE and Nup188-RITE at 3 h postrelease. (B) Quantification of old (GFP) and new (RFP) Nup57 and Nup188 at 3 h postrelease. Values are average ± SD (n = 20 and 26 dividing cells). (C) Representative image of Nup57-RITE at 3 h postrelease. The image was acquired using structured illumination; a z projection (Upper) and the corresponding 3D-rendering model (Lower) are shown. Arrows represent the x-y-z axes. (D) Representative images of Nup47-RITE and Nup188-RITE 24 h (six cell divisions) postrelease. (E) Selected frames from time-lapse recordings of Nup57-RITE starting 1 h postrelease. Images were taken at 10-min intervals over 3.5 h. The selected frames correspond to the following cell-cycle stages: (1) start, (2) bud emergence, (3) bud growth, (4) nuclear division, and (5) anaphase. The time (h) elapsed since the release is indicated by the numbers above the frames. The arrows indicate the area where new (RFP) Nup57 appears. (F) Quantification of old (GFP) Nup57 in time-lapse recordings, imaged as indicated in E. For each dividing cell, frames were selected for different cell-cycle stages (1–5) and GFP was measured in mother and daughter cells. GFP measurements were normalized to GFP in the mother cell in the first frame (1). Values are average ± SD (n = 32 cells). (G) Nup57 was tagged with an alternative RITE cassette consisting of an epitope switch from T7 (nonfluorescent) to HA-GFP. Time-lapse imaging was performed and is represented as indicated in E. Arrows indicate the location of newly formed Nup57 (GFP). (H) Quantification of new (GFP) Nup57 in time-lapse recordings, imaged as indicated in G. For each dividing cell, frames were selected for different cell-cycle stages (1–5) and GFP was measured in mother and daughter cells. GFP measurements were normalized to GFP in the mother cell at bud-growth stages (3). Values are average ± SD (n = 30 cells). For all of the images, dashed lines represent the cell boundaries based on DIC images. (Scale bars, 2 μm.)

RITE Reveals a Unique Pattern for SPB Duplication and Inheritance.

One known exception to equal sharing between subsequent generations is the SPB—the centrosome in yeast (27–29). The SPB is a large protein complex embedded in the nuclear envelope (30). Each cell cycle, the SPB duplicates and each resulting SPB migrates to opposite sites of the nucleus to form the mitotic spindle. SPB duplication has been described as a conservative process that generates one old and one new SPB, followed by migration of the old SPB to the daughter cell (27). However, a later study suggested that the SPB is a dynamic complex that grows and exchanges subunits during cell division (28). Thus, the duplication process may be more complex than previously reported.

The RITE technology allowed monitoring SPB duplication and inheritance by tagging two different core SPB proteins, Spc42 and Spc110. The old (GFP) SPB components were asymmetrically distributed toward the bud, with only a small proportion remaining in mother cells (Fig. 5A). Remarkably, new proteins were incorporated into both SPBs. Quantification of the fluorescence intensity of old and new SPB subunits showed that most old subunits (~90%) were inherited by the daughter cell, whereas new subunits were incorporated to approximately the same extent into both SPBs (Fig. 5B). An alternative RITE construct with an epitope switch from GFP to mCherry (30) showed identical results (Fig. S5).

We followed the dynamics of SPB duplication by time-lapse imaging Spc42-RITE (Fig. 5C). The duplication started when a small proportion of old (GFP) Spc42 was separated from the original SPB and formed a small SPB. During the cell cycle, both SPBs continuously grew, incorporating new (RFP) Spc42. Notably, the total amount of old (GFP) Spc42 remained constant during the SPB growth, which is different from the exchange process described earlier (28).

Our data suggest that the SPB is duplicated following a unique pattern that is neither conservative nor semiconservative and that is followed by the transfer of the older SPB to the younger cell (Fig. 5D).

3

Discussion

The process of sharing copies of DNA in a correct manner in cell division has been recognized as essential for cell viability for a long time. Correct sharing of compartments and multiprotein complexes is also vital for successful progeny but is poorly described in many instances. How intracellular compartments grow and segregate during cell division has been visualized with inducible expression strategies and fluorescent reporters and by monitoring steady-state levels. These experiments have improved our understanding of protein inheritance but have also produced controversial results. We visualized compartment and multiprotein complex inheritance in a more global manner using a "genetic color switch" in yeast. This genetic switch is an *in vivo* pulse–chase assay with the advantage of a readout on protein destiny by fluorescent microscopy, which allows spatiotemporal analysis of the fate of old and new proteins. The fact that a genome-wide GFP-knockin library in yeast is available in the public domain allows accurate prediction of genes that can safely be modified by the RITE cassette (17, 18). Knocking in this genetic color switch within a collection of genes that represent essential and stable components of each intracellular compartment allowed a comprehensive analysis of the spatiotemporal fate of intracellular compartments during cell division.

Fig. 5
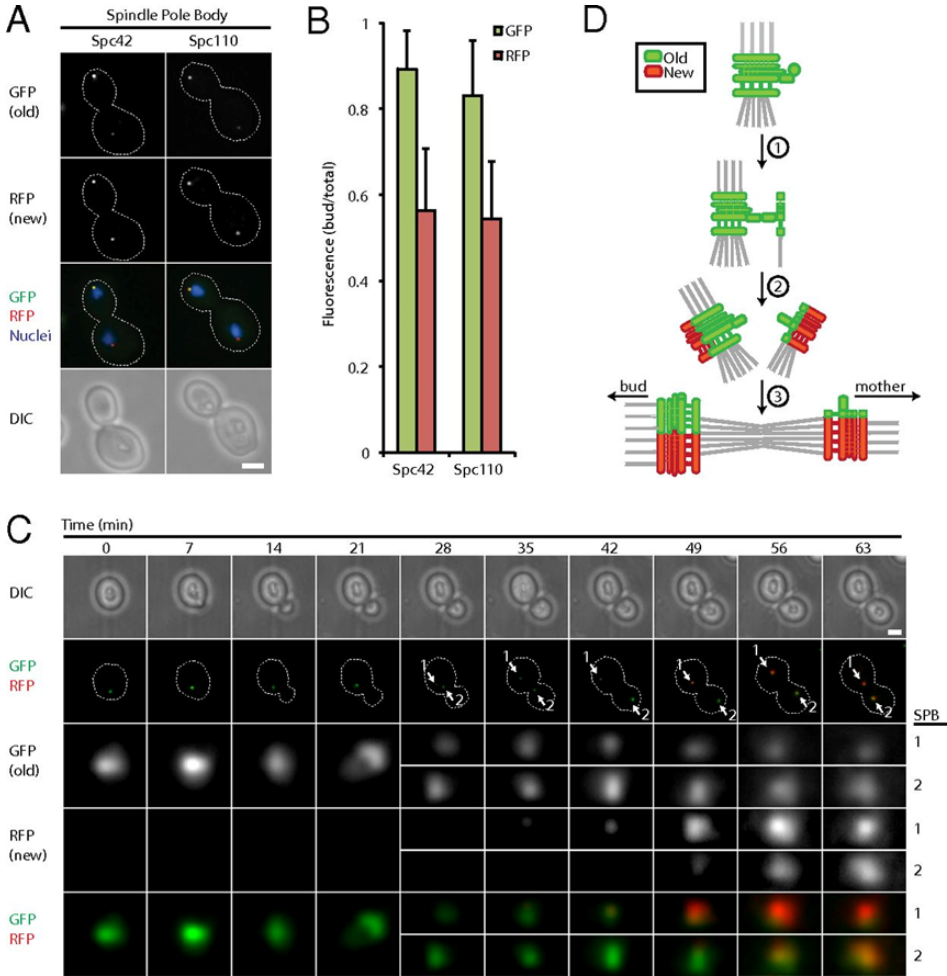
Figure 5: The SPB duplicates by a nonconservative mechanism followed by asymmetrical segregation between mother and daughter cells.
(A) Representative images of Spc42-RITE and Spc110-RITE at 3 h postrelease. (B) Quantification of old (GFP) and new (RFP) Spc42 and Spc110 at 3 h postrelease. Values are average ± SD (n = 30 dividing cells). (C) Selected frames from time-lapse recordings of Spc42-RITE. The time (h) elapsed since the release is indicated by the numbers above the frames. The new (1) and old (2) SPBs are indicated by arrows, and zoomed-in (8×) in the lower panels. For all of the images, dashed lines represent the cell boundaries based on DIC images. (Scale bars, 2 μm.) (D) Model of SPB duplication and inheritance

Using this technology, we showed that most organelles grow by homogeneous incorporation of new proteins into preexisting templates. These include several membrane-associated compartments (ER, mitochondria, vacuole, the Golgi apparatus) and the nucleolus. This growth pattern was also observed for peroxisomes. We noted that newly synthesized Pex3 was incorporated into preexisting peroxisomes, whereas peroxisomes exclusively containing new Pex3 were not observed. New Pex3 stayed connected to preexisting peroxisomes, resulting in a similar proportion of old and new Pex3. Collectively, our observations support template-based growth as the dominant

pathway for peroxisomal biogenesis, as observed for most other compartments, resolving a long-standing controversy in the field.

Although mother and daughter cells share and mix most of their organelles, some exceptions were observed relating to two stable macromolecular complexes within the nuclear envelope: the NPC and the SPB. Both old and new NPCs were present in mother and daughter cells, but the complexes remained spatially separated. Although shared between mother and daughter, NPCs are very stable complexes that do not renovate their subunits even after many divisions. New NPCs are assembled *de novo* using new nucleoporins. The SPB is a large and also stable multiprotein complex, yet, unlike the NPC, the already-assembled SPB allows incorporation of new proteins, an observation differing from previous descriptions (27, 29). Pereira and coworkers (27) exploited the slow maturation of RFP to follow old Spc42, reasoning that new Spc42-RFP acquires fluorescence only during the next cell cycle. To monitor new Spc42, they used inducible expression driven by the GAL promoter. We could—using RITE—follow SPB duplication without changing the endogenous regulation of SPB synthesis, which may explain the discrepancy in observations.

Based on our data, we propose a model for SPB biogenesis (Fig. 5D). First, a small proportion of maternal SPB components splits to initiate the duplication process. Newly synthesized proteins are added to this template to build the new SPB. Simultaneously, new proteins are also incorporated into the original SPB that consequently increases in size. Finally, as the cell cycle progresses, the original SPB—containing most of the preexisting components—migrates into the daughter cell. Consequently, the size of the SPB in mother cells may eventually become smaller than in daughter cells (which contains most of the old—and an equal number of new—SPB components). There are at least two options that could explain these results: One is to compensate for the difference in SPB size with synthesis and/or degradation in mother and daughter cells after cytokinesis. Alternatively, the shrinkage of the SPB in the mother yeast may be irreversible, which may ultimately restrict the lifetime of old yeast.

We have used a unique technology to study the fate and inheritance of all organelles and some large protein complexes. Mother cells usually share their content with daughter cells during cell division, with some exceptions where maternal components are kept separated from the new proteins or where old quality-controlled and functional components may be preferentially inherited by daughter cells.

Materials and Methods

Plasmids, yeast strains, growth conditions, RT-quantitative PCR, sample preparation for microscopy analysis, and immunofluorescence are described in SI Materials and Methods. The genetic switch was induced by adding β-estradiol (E-8875; Sigma-Aldrich) to a final concentration of 1 μM.

Fixed samples were analyzed with a Leica DMI 60000B wide-field fluorescence microscope equipped with a structural light unit (Angstrom Optigrid, Quorum Technologies) and using a Leica HCX PlanApo 63×/1.4–0.6 oil objective. Images were taken as z stacks (20 sections at 0.2-μm intervals). When indicated, the unit for structural illumination was used (40 sections at 0.1-μm intervals). Images were deconvolved using Volocity (Improvision/ PerkinElmer) software (99% confidence limit per 25 iterations) with calculated point-spread functions for each wavelength. Three-dimensional structures were obtained using

high-resolution volume rendering (Volocity). For quantification, we used Volocity software to measure the integrated GFP and RFP intensities and the background fluorescence (minimal fluorescence intensity) for each cell and marker. The relative (bud/total) GFP intensity was calculated for each mother–bud pair as follows: $GFP_{bud/total} = (GFP_b - GFP_0)/[(GFP_b - GFP_0) + (GFP_m - GFP_0)]$, where b is the bud, 0 is the background, and m is the mother. This formula was also used to calculate the $RFP_{bud/total}$. For quantification of peroxisomes, the GFP intensities of each individual peroxisome were normalized as follows: $GFP = (GFP_p - GFP_0)/SUM\_GFP$, where p is the peroxisome, 0 is the background, and SUM_GFP is the sum of the GFP intensities (background-subtracted) of all of the peroxisomes within the mother–bud pair. This formula was also applied to calculate normalized RFP intensities.

Time-lapse fluorescent microscopy was performed with a DeltaVision wide-field microscope (Olympus IX70; Applied Precision). Images were acquired at 32 °C as z stacks (10 sections at 0.4-µm intervals) and analyzed using softWoRx software (Applied Precision).

References

1. Fagarasanu A, Mast FD, Knoblach B, Rachubinski RA. Molecular mechanisms of organelle inheritance: Lessons from peroxisomes in yeast. Nat Rev Mol Cell Biol. 2010;11(9):644–654.

2. Bretscher A. Polarized growth and organelle segregation in yeast: The tracks, motors, and receptors. J Cell Biol. 2003;160(6):811–816.

3. Shaw SL, Yeh E, Maddox P, Salmon ED, Bloom K. Astral microtubule dynamics in yeast: A microtubule-based searching mechanism for spindle orientation and nuclear migration into the bud. J Cell Biol. 1997;139(4):985–994.

4. Finger FP, Hughes TE, Novick P. Sec3p is a spatial landmark for polarized secretion in budding yeast. Cell. 1998;92(4):559–571.

5. Boldogh IR, Ramcharan SL, Yang HC, Pon LA. A type V myosin (Myo2p) and a Rab-like G-protein (Ypt11p) are required for retention of newly inherited mitochondria in yeast cells during cell division. Mol Biol Cell. 2004;15(9):3994–4002.

6. Fagarasanu M, Fagarasanu A, Tam YY, Aitchison JD, Rachubinski RA. Inp1p is a peroxisomal membrane protein required for peroxisome inheritance in *Saccharomyces cerevisiae*. J Cell Biol. 2005;169(5):765–775.

7. Hoepfner D, Schildknegt D, Braakman I, Philippsen P, Tabak HF. Contribution of the endoplasmic reticulum to peroxisome formation. Cell. 2005;122(1):85–95.

8. Tam YY, Fagarasanu A, Fagarasanu M, Rachubinski RA. Pex3p initiates the formation of a preperoxisomal compartment from a subdomain of the endoplasmic reticulum in *Saccharomyces cerevisiae*. J Biol Chem. 2005;280(41):34933–34939.

9. Kragt A, Voorn-Brouwer T, van den Berg M, Distel B. Endoplasmic reticulum-directed Pex3p routes to peroxisomes and restores peroxisome formation in a *Saccharomyces cerevisiae* pex3Delta strain. J Biol Chem. 2005;280(40):34350–34357.

10. van der Zand A, Gent J, Braakman I, Tabak HF. Biochemically distinct vesicles from the endoplasmic reticulum fuse to form peroxisomes. Cell. 2012;149(2):397–409.

11. Bevis BJ, Hammond AT, Reinke CA, Glick BS. *De novo* formation of transitional ER sites and Golgi structures in Pichia pastoris. Nat Cell Biol. 2002;4(10):750–756.

12. Liu B, *et al*. The polarisome is required for segregation and retrograde transport of protein aggregates. Cell. 2010;140(2):257–267.

13. Eldakak A, *et al*. Asymmetrically inherited multidrug resistance transporters are recessive determinants in cellular replicative ageing. Nat Cell Biol. 2010;12(8):799–805.

14. van den Bogaart G, Meinema AC, Krasnikov V, Veenhoff LM, Poolman B. Nuclear transport factor directs localization of protein synthesis during mitosis. Nat Cell Biol. 2009;11(3):350–356.

15. De Vos D, *et al*. Progressive methylation of ageing histones by Dot1 functions as a timer. EMBO Rep. 2011;12(9):956–962.

16. Verzijlbergen KF, *et al*. Recombination-induced tag exchange to track old and new proteins. Proc Natl Acad Sci USA. 2010;107(1):64–68.

17. Ghaemmaghami S, *et al*. Global analysis of protein expression in yeast. Nature. 2003;425(6959):737–741.

18. Huh WK, *et al*. Global analysis of protein localization in budding yeast. Nature. 2003;425(6959):686–691.

19. Gray JV, *et al*. "Sleeping beauty": Quiescence in *Saccharomyces cerevisiae*. Microbiol Mol Biol Rev. 2004;68(2):187–206.

20. Verzijlbergen KF, *et al*. A barcode screen for epigenetic regulators reveals a role for the NuB4/HAT-B histone acetyltransferase complex in histone turnover. PLoS Genet. 2011;7(10):e1002284.

21. Motley AM, Hettema EH. Yeast peroxisomes multiply by growth and division. J Cell Biol. 2007;178(3):399–410.

22. Fujiki Y, Matsuzono Y, Matsuzaki T, Fransen M. Import of peroxisomal membrane proteins: The interplay of Pex3p- and Pex19p-mediated interactions. Biochim Biophys Acta. 2006;1763(12):1639–1646.

23. Mekhail K, Moazed D. The nuclear envelope in genome organization, expression and stability. Nat Rev Mol Cell Biol. 2010;11(5):317–328.

24. Shcheprova Z, Baldi S, Frei SB, Gonnet G, Barral Y. A mechanism for asymmetric segregation of age during yeast budding. Nature. 2008;454(7205):728–734.

25. Khmelinskii A, Keller PJ, Lorenz H, Schiebel E, Knop M. Segregation of yeast nuclear pores. Nature. 2010;466(7305):E1.

26. Hoelz A, Debler EW, Blobel G. The structure of the nuclear pore complex. Annu Rev Biochem. 2011;80:613–643.

27. Pereira G, Tanaka TU, Nasmyth K, Schiebel E. Modes of spindle pole body inheritance and segregation of the Bfa1p-Bub2p checkpoint protein complex. EMBO J. 2001;20(22):6359–6370.

28. Yoder TJ, Pearson CG, Bloom K, Davis TN. The *Saccharomyces cerevisiae* spindle pole body is a dynamic structure. Mol Biol Cell. 2003;14(8):3494–3505.

29. Hotz M, *et al*. Spindle pole bodies exploit the mitotic exit network in metaphase to drive their age-dependent segregation. Cell. 2012;148(5):958–972.

30. Barral Y, Liakopoulos D. Role of spindle asymmetry in cellular dynamics. Int Rev Cell Mol Biol. 2009;278:149–213.

3

Supplemental Information:

SI Materials and Methods

Plasmids.
A plasmid containing a GFP→mRFP (red fluorescent protein) recombination-induced tag exchange (RITE) cassette was constructed by restriction enzyme-based cloning of PCR fragments to generate the following construct: NotI-spacer-LoxP-KpnI-3xHA-yEGFP-SpeI-ADH1t-BamHI-HygroMX-XbaILoxP-SalI-3xT7-mRFP-BsrGI, as previously described (1). A plasmid containing a T7→GFP RITE cassette was constructed by swapping GFP from pKT127 (2) into pTW081 (3) using HindIII/ BsrGI restriction and ligation to yield the following construct: NotI-spacer-LoxP-KpnI-T7-ADH1t-HygroMX-LoxP-HA-yEGFPBsrGI. A plasmid to generate mCherry→GFP RITE strains has been previously described (4). For constitutive expression of hormone-regulated Cre, Cre-EBD78 (5), the module NATMX_GPD_Cre-EBD78_CYCt was amplified by a three-step overlap PCR from the plasmids pFvL099 and pTW040 (6) and targeted to the lyp1Δ locus by homologous recombination.

Yeast Strains and Growth Conditions.
The GFP→mRFP and T7→GFP RITE strains are derivatives of Y7092 (7) with the following genotypes: MATα his3Δ1 leu2Δ0 ura3Δ0 met15Δ0 can1Δ::STE2pr-Sp_his5 lyp1Δ::NATMX_TDH3pr_Cre-EBD78_CYC1tx::X-RITE, where x is the target gene. The SPC42-mCherry→GFP strain was made by successive transformations of pFA6a-GFP-S65T-KanMX6 (8) and pYB1511(4) in a BY4733his3::HIS3_GPD_ CRE_EBD78 strain. The genotype of the SPC42-mCherry→GFP strain is his3Δ200 leu2Δ0met15Δ0 trp1Δ63 ura3Δ0 his3::HIS3_GPD_CRE_EBD78spc42:: SPC42-LoxP-mCherry-NatNT2-LoxP-GFP-S65T-KanMX6 (2). Yeast cells were grown at 30 °C in rich medium [yeast extract peptone dextrose (YEPD)]. Hygromycin B (200 µg/mL; Invitrogen) was included when growing GFP→mRFP and T7→GFP RITE strains and removed before induction of the genetic switch.

RNA Isolation and RT-Quantitative PCR.
Total yeast RNA was purified from 3×10^7 cells using an RNeasy Kit (Qiagen) according to the manufacturer's protocol. RNA samples were treated with RNase-free DNase (Qiagen), and cDNA was made with Super-Script II reverse transcriptase (Invitrogen). GFP- and ADH1-cDNA was quantified by real-time PCR using Power SYBR Green PCRMaster Mix (Applied Biosystems) and a 7500 Fast Real-Time PCR System. The primers used for quantitative (q)PCR were:
yEGFP_ORF_fwd, 5'-TTTCTGTCTCCGGTGAAGGT-3';
yEGFP_ORF_rev, 5'-GGCATGGCA GACTTGAAAAA-3';
ADH1_ORF_II_fwd, 5'-TAGGTTCTTTGGCTGTTCAATACG-3';
and ADH1_ORF_II_rev, 5'-CGGAAACGGAAACGTTGATGACACCG-3'.

Sample Preparation for Microscopy Analysis.

For analysis of fixed samples, cells were fixed with 4% (vol/vol) formaldehyde, stained with 1 μg/mL Hoechst 33342 (Invitrogen), and mounted with Vectashield solution (Vector Laboratories) onto Con A-coated coverslips. For live-cell imaging, cells were diluted in synthetic liquid media and plated in a Ludin chamber type I (for round coverslips with 18-mm diameter) with a Con A-coated coverslip.

Immunofluorescence.

Cells were fixed for 30 min at 30 °C in 4% (vol/vol) formaldehyde, washed with SP buffer (0.1 M KPO_4, pH 7.5, 1.2 M sorbitol), and resuspended in SP buffer. To remove the cell wall, cells were incubated for 15 min at 30 °C with gentle shaking in SP buffer containing 0.1% (vol/vol) β-mercaptoethanol and lyticase (10 U per 10^7 cells) (Sigma). Spheroplasts were then washed two times in SP buffer and permeabilized in blocking solution [0.1% (vol/vol) Triton-X, 3% (vol/vol) BSA in PBS]. Spheroplasts were immunostained in suspension, using rabbit polyclonal antibodies specific for GFP (anti-GFP immunostaining) or RFP (anti-RFP immunostaining) (9), followed by incubation with Alexa 647-conjugated anti-rabbit antibody (Molecular Probes).

References:

1. De Vos D, *et al*. (2011) Progressive methylation of ageing histones by Dot1 functions as a timer. EMBO Rep 12(9):956–962.
2. Sheff MA, Thorn KS (2004) Optimized cassettes for fluorescent protein tagging in *Saccharomyces cerevisiae*. Yeast 21(8):661–670.
3. Verzijlbergen KF, *et al*. (2010) Recombination-induced tag exchange to track old and new proteins. Proc Natl Acad Sci USA 107(1):64–68.
4. Hotz M, *et al*. (2012) Spindle pole bodies exploit the mitotic exit network in metaphase to drive their age-dependent segregation. Cell 148(5):958–972.
5. Lindstrom DL, Gottschling DE (2009) The mother enrichment program: A genetic system for facile replicative life span analysis in *Saccharomyces cerevisiae*. Genetics 183(2):413–422.
6. Stulemeijer IJ, *et al*. (2011) Dot1 binding induces chromatin rearrangements by histone methylation-dependent and -independent mechanisms. Epigenetics Chromatin 4(1):2.
7. Tong AH, Boone C (2006) Synthetic genetic array analysis in *Saccharomyces cerevisiae*. Methods Mol Biol 313:171–192.
8. Wach A, Brachat A, Alberti-Segui C, Rebischung C, Philippsen P (1997) Heterologous HIS3 marker and GFP reporter modules for PCR-targeting in *Saccharomyces cerevisiae*. Yeast 13(11):1065–1075.
9. Rocha N, *et al*. (2009) Cholesterol sensor ORP1L contacts the ER protein VAP to control Rab7-RILP-p150 Glued and late endosome positioning. J Cell Biol 185(7):1209–1225.

Fig. S1
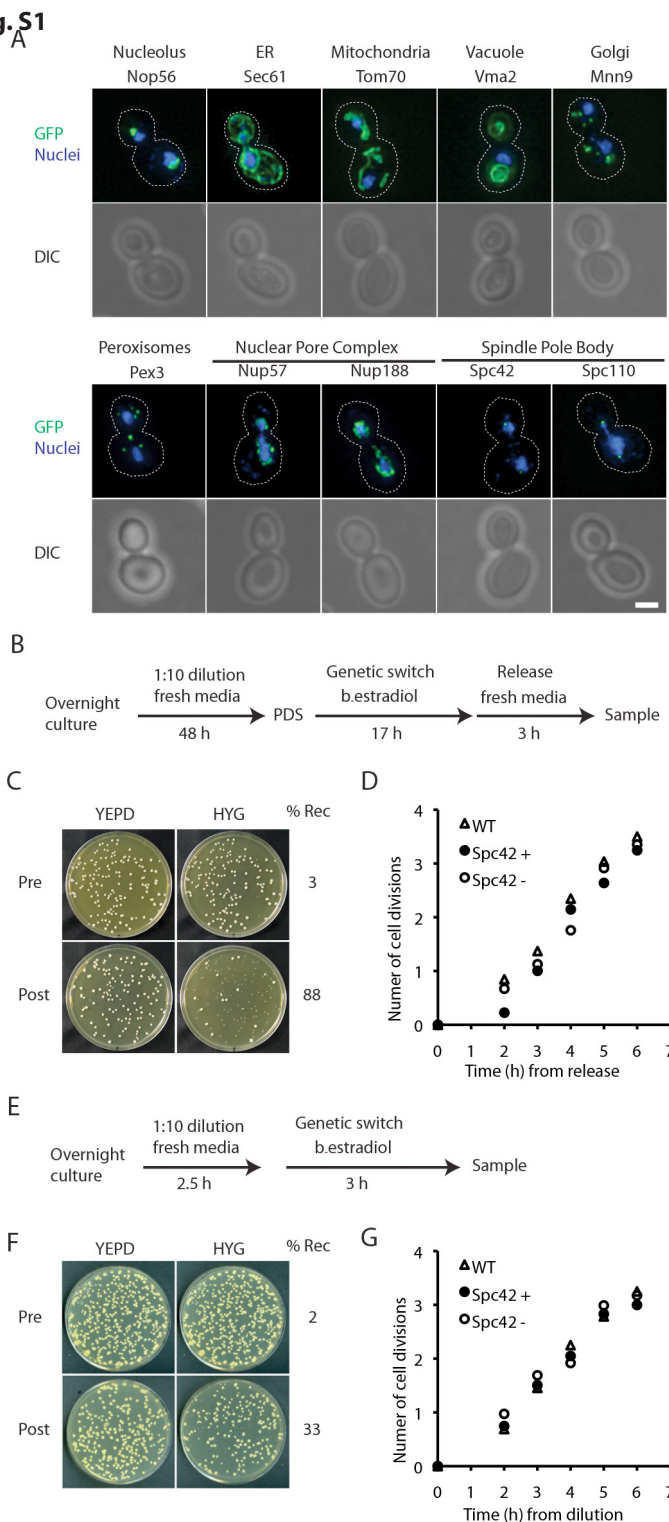
Fig. S1. RITE strains and assays.

(A) Intracellular localization of RITE-tagged proteins in *Saccharomyces cerevisiae*. Dashed lines represent the cell boundaries based on DIC images. ER, endoplasmic reticulum. (Scale bar, 2 μm.) DIC, differential interference contrast. (B–D) Genetic switch during the postdiauxic shift (PDS). (B) Schematic representation of the procedure. (C) Recombination efficiency during the PDS stage. Cells were plated before (Pre) and 17 h after (Post) the genetic switch and replica-plated in control media (YEPD, yeast extract peptone dextrose) or media with hygromycin (HYG). The fraction of hygromycinsensitive colonies indicates the recombination efficiency (Post) and the spontaneous recombination (Pre). (D) Growth rate during the release in fresh media of WT, Spc42-RITE– (without β-estradiol), and Spc42-RITE+ (with β-estradiol). (E–G) The genetic switch in log phase. (E) Schematic representation of the procedure. (F) Recombination efficiency in log phase, before (Pre) and 3 h after (Post) the genetic switch. (G) Growth rate of WT, Spc42-RITE– (without β-estradiol), and Spc42-RITE+ (with β-estradiol). For Spc42-RITE+ cells, β-estradiol was added at 2.5 h, as indicated in E.
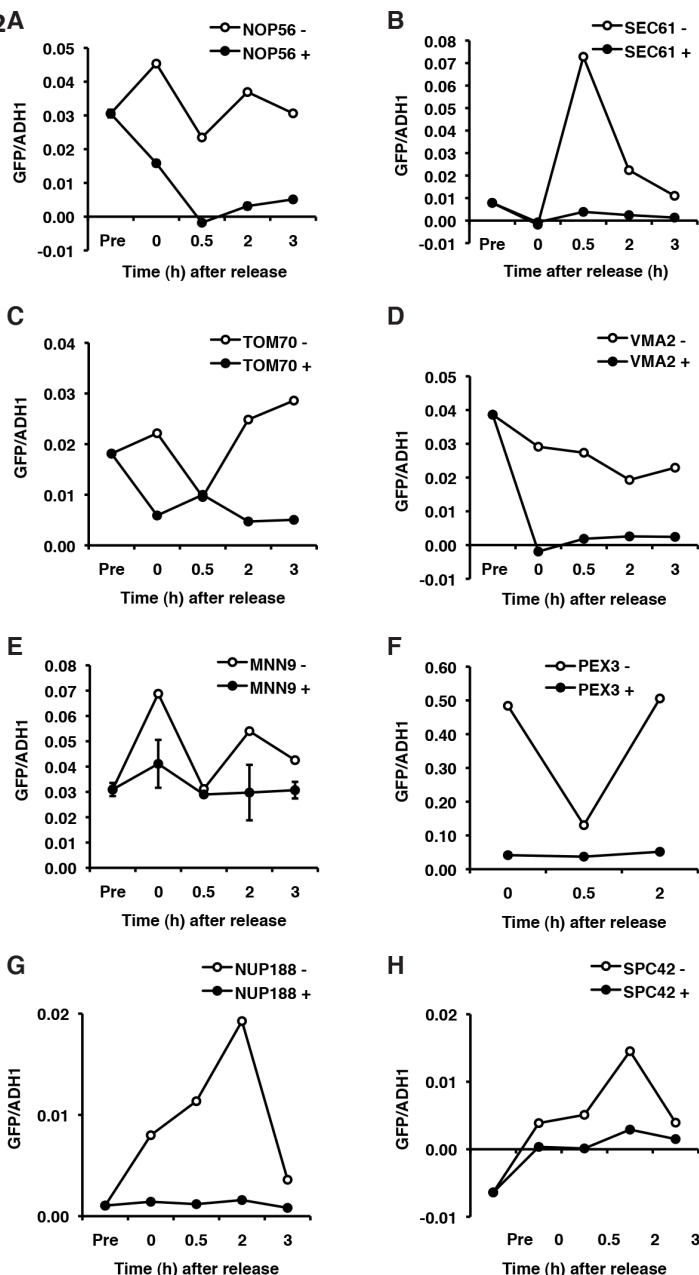
Fig. S2. mRNAs for the GFP-labeled proteins (GFP-mRNA) are degraded after the genetic switch.
For each RITE strain used in this study, GFP-mRNA levels were measured by RT-qPCR and normalized to the expression of ADH1 before the switch in PDS (Pre) and at several time points after the release (0, 0.5, 2, and 3 h) by RT-qPCR. GFP RT-qPCR background levels were measured using the Y7092 strain (WT), normalized to the expression of ADH1, and subtracted. Plots show representative curves of biological duplicates for Nop56-RITE (A), Sec61-RITE (B), Tom70-RITE (C), Vma2-RITE (D), Mnn9-RITE (E), Pex3-RITE (F), and Nup188 (G) and Spc42 (H) cells, treated with β-estradiol (+) or without treatment (−). The recombination efficiency was determined in the same experiment for all clones using a plating assay, and the results are shown in Table S1.

Fig. S3
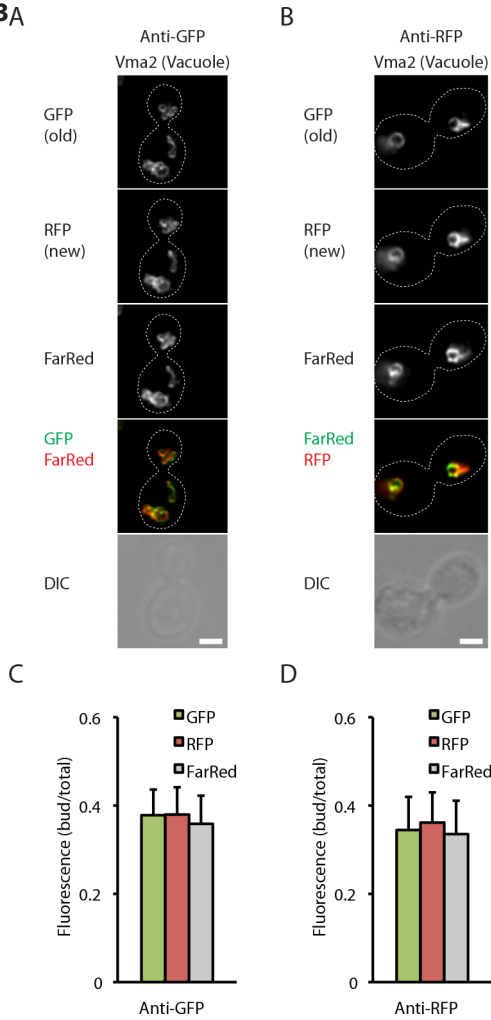
**Fig. S3. Segregation of old and new Vma2 proteins shown by immunofluorescence.**
Representative images of Vma2-RITE strains 3 h postrelease, immunostained with antibodies specific for
GFP (A) and RFP (B) and detected with Alexa 647-conjugated antibody (FarRed). Dashed lines represent the
cell boundaries based on DIC images. (Scale bars, 2 µm.) (C) Quantification of GFP, RFP, and FarRed-labeled
GFP in cells stained as shown in A. Values are average ± SD (n = 35 dividing cells). (D) Quantification of GFP,
RFP, and FarRed-labeled RFP in cells stained as shown in B. Values are average ± SD (n = 35 dividing cells).

Fig. S4
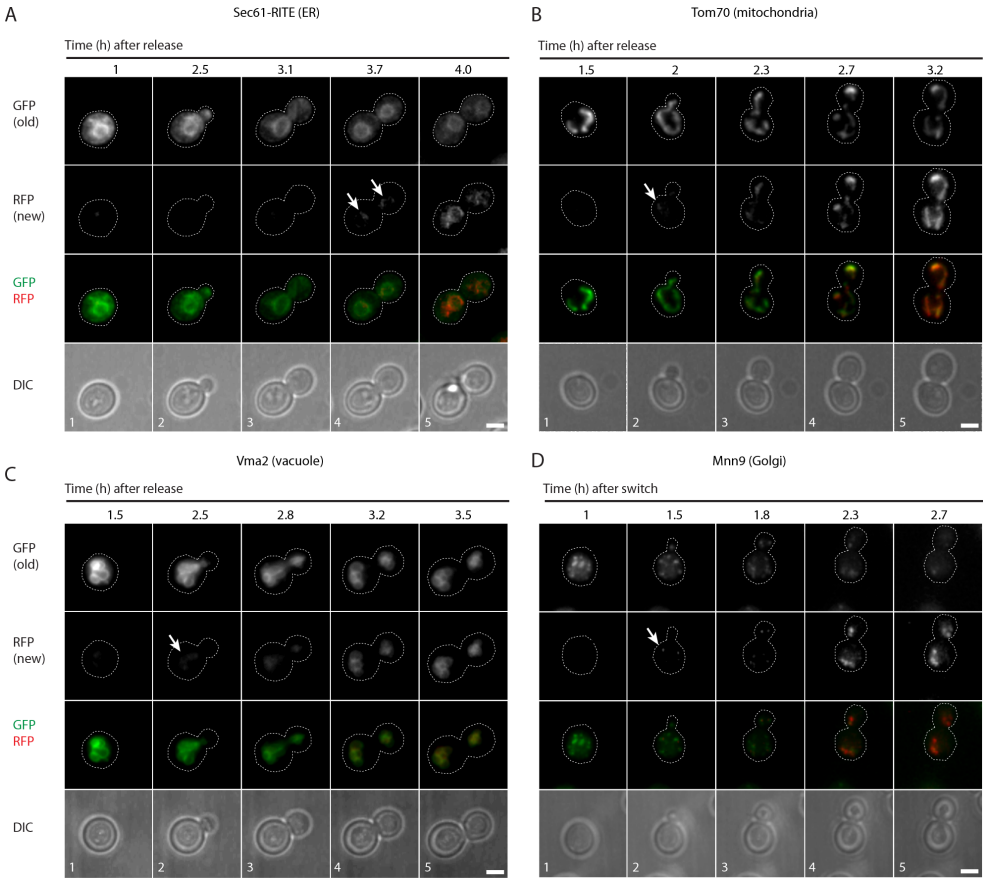
Fig. S4. Time-lapse imaging of the inheritance of ER, mitochondria, vacuole, and Golgi.
Selected time frames from time-lapse recordings of Sec61-RITE (A),Tom70-RITE (B), Vma2-RITE (C), and Mnn9-RITE (D). Live-cell imaging was initiated 1 h postrelease, after a switch performed in stationary phase (A–C) or in log phase (D). Images were taken at 10-min intervals over 3.5 h. The selected frames correspond to the following cell-cycle stages: (1) start, (2) bud emergence, (3) bud growth, (4) nuclear division, and (5) anaphase, and the cell-cycle stages (1–5) are indicated at the bottom. The time (h) elapsed since the release is indicated by the numbers above the frames. The arrows indicate the areas where new (RFP) proteins appear. Dashed lines represent the cell boundaries based on DIC images. (Scale bars, 2 μm.)
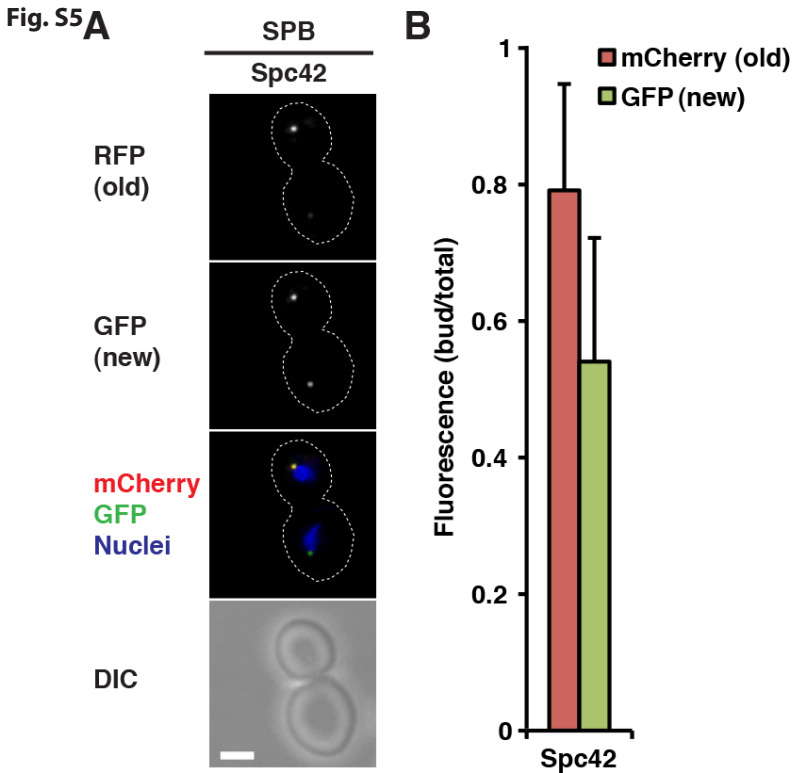
Fig. S5. Duplication and inheritance of Spc42, shown with an alternative RITE cassette, characterized by an epitope switch from mCherry to GFP.
(A) Representative images of Spc42-reRITE 3 h postrelease. Dashed lines represent the cell boundaries based on DIC images. SPB, spindle pole body. (Scale bar, 2 μm.) (B) Quantification of old (mCherry) and new (GFP) Spc42 in mother and daughter cells at 3 h postrelease. Values are average ± SD (n = 24 dividing cells).

Table. S1

	Recombination efficiency (%)	
Strain:	Pre	Post
Nop56	21	90
Sec61	4	92
Tom70	19	77
Vma2	8	88
Mnn9	14	56
Pex3	12	91
Nup188	18	94
Spc42	17	95

Table S1. Recombination efficiency from all of the RITE clones in the RT-qPCR experiment (Fig. S2)
An aliquot from the cells used for RT-PCR was plated before the switch (Pre) and at time 0, just before the release in fresh media (Post). The spontaneous recombination (Pre) and the recombination efficiency (Post) were calculated as indicated in Fig. S1.

67

Chapter   Four

Chapter 4:

N-terminal acetylation and replicative age affect proteasome localization and cell fitness during aging

Sjoerd J. van Deventer[1], Victoria Menendez-Benito[1],
Fred van Leeuwen[2], Jacques Neefjes[1]

4

[1] Division of Cell Biology 2 and
[2] Division of Gene Regulation,
Netherlands Cancer Institute, Amsterdam, The Netherlands

Abstract

Specific degradation of proteins is essential for virtually all cellular processes and is carried out predominantly by the proteasome. The proteasome is important for clearance of damaged cellular proteins. Damaged proteins accumulate over time and excess damaged proteins can aggregate and induce the death of old cells. In yeast, the localization of the proteasome changes dramatically during aging, possibly in response to altered proteasome activity requirements. We followed two key parameters of this process: the distribution of proteasomes in nuclear and cytosolic compartments, and the formation of cytoplasmic aggregate-like structures called proteasome storage granules (PSGs). Whereas replicative young cells efficiently relocalized proteasomes from the nucleus to the cytoplasm and formed PSGs, replicative old cells were less efficient in relocalizing the proteasome and had less PSGs. By using a microscopy-based genome-wide screen, we identified genetic factors involved in these processes. Both relocalization of the proteasome and PSG formation were affected by two of the three N-acetylation complexes. These N-acetylation complexes also had different effects on the longevity of cells, indicating that each N-acetylation complex has different roles in proteasome location and aging.

Introduction

The proteasome is a major intracellular protease and controls many processes, including protein quality control. Protein quality control is required to prevent accumulation of damaged proteins during the lifespan of a cell (Amm *et al*., 2014; Koga *et al*., 2011). Insufficient recognition and clearance of damaged proteins can yield harmful protein aggregates (Powers *et al*., 2009; Schmidt and Finley, 2014). A proper functioning ubiquitin-proteasome system (UPS) might prevent protein aggregation and counteract cellular aging.

Several studies report an age-dependent decline in UPS activity in various model systems (Carrard *et al*., 2002; Dasuri *et al*., 2009; Lee *et al*., 1999; Vernace *et al*., 2007a; Vernace *et al*., 2007b). Other studies suggest a causative relation between UPS activity and aging. Enhancing proteasome activity by overexpression of the proteasome assembly chaperone Ump1 improves budding yeast longevity under starvation conditions (Chen *et al*., 2006). Increasing proteasome levels by overexpressing Rpn4, a protein which drives the transcription of the proteasome subunits, also increases the replicative lifespan in *S. cerevisiae* (Kruegel *et al*., 2011). These studies suggest that the UPS system decays with age and limits the lifespan of cells and organisms. Manipulating UPS therefore might have dramatic effects on the aging process.

For several reasons, *S. cerevisiae* is an important model organism to elucidate the molecular basis of processes related to aging. First, cell division is asymmetrical with a distinguishable mother and daughter cell. This allows tracking of a single cell over time, even during division. Second, the number of cell divisions can be quantified by counting the bud scars left on the mother cell after budding of a new generation. The asymmetrical cell division defines two forms of aging; chronological aging and replicative aging (Kaeberlein, 2010; Jazwinski *et al*., 1989). Chronological aging is defined as the time between the budding from the mother, the birth, until the daughter cell dies. This aging is usually addressed on a

population level by measuring the viability of a liquid culture upon starvation (Kaeberlein, 2010). Replicative aging is aging as a result of cell division and defined by the number of daughter cells produced by an individual mother cell. Replicative aging in yeast is used to model aging of mitotically active mammalian cells (Kaeberlein, 2010; Mortimer and Johnston, 1959). Chronological and replicative aging are overlapping processes (Delaney *et al*., 2013; Kennedy *et al*., 1994; Murakami *et al*., 2012), exemplified by the observation that, during starvation of a liquid yeast culture, the replicative age of a cell at the start of starvation highly affects the chronological age that will be reached (Allen *et al*., 2006; Aragon *et al*., 2008). The studies in yeast have revealed many insights into the various molecular processes underlying aging and is expected to provide handles to manipulate aging-related diseases such as neurodegenerative disorders (Clay and Barral, 2013; Tenreiro and Outeiro, 2010).

Here, we followed two proteasome-related processes that occur during chronological aging in yeast: nuclear-cytoplasmic relocalization of proteasomes, and the formation of cytoplasmic proteasome storage granules (PSGs). PSGs are aggregate-like structures that contain the proteasome and form early during yeast starvation (Laporte *et al*., 2008). The replicative age of cells had a major effect on these processes. Replicative young cells efficiently relocalized the proteasome from the nucleus and formed PSGs, unlike replicative old cells. A genome-wide knockout screen revealed that proteasome relocalization and PSG formation involves two of the three N-acetylation complexes, each having a particular effect on proteasome localization. The N-acetylation complexes were found to affect cell fitness in different ways. One N-acetylation complex, NatC, both affected proteasome location and fitness of old cells.

Results

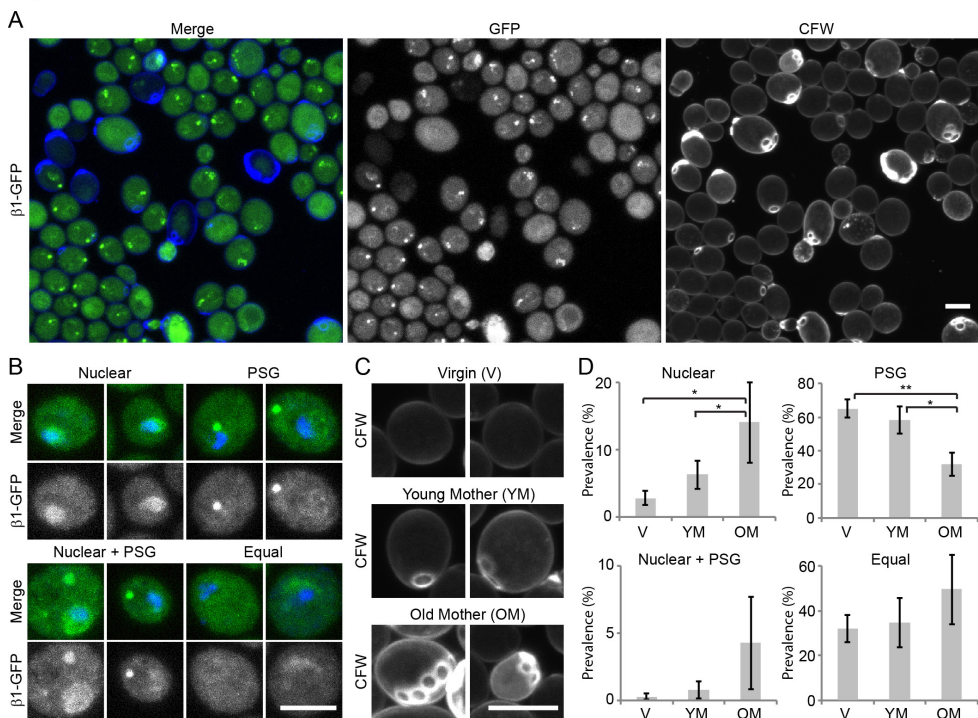### Proteasome localization during starvation correlates with replicative age

Proteasomes equally distribute over the nucleus and cytoplasm in mammalian cells (Reits *et al*., 1997). In the budding yeast *Saccharomyces cerevisiae*, proteasomes accumulate in the nucleus when cells have sufficient nutrients (Russell *et al*., 1999). This changes when yeast cells exhaust glucose in the growth medium, a process that leads to starvation. During starvation, cells relocalize their proteasome from the nucleus into the cytosol and form cytoplasmic PSGs (Laporte *et al*., 2008). Starvation is apparently a factor controlling the intracellular distribution of proteasomes.

We visualized proteasomes in live yeast cells by tagging the catalytically active β1 subunit (Pre3) of the proteasome with GFP. Efficient and quantitative introduction of the β1–GFP in 20S proteasomes was confirmed by native gel electrophoresis (supplementary material Fig. S1). The GFP-labeled proteasomes had a similar distribution during starvation as reported for non-modified proteasomes previously (Laporte *et al*., 2008). We observed that cells in starvation show a wide heterogeneity in proteasome localization (Fig. 1A). Based on proteasome localization, we defined four localization phenotypes: (1) cells with proteasome accumulation in the nucleus (Nuclear); (2) cells displaying dots of cytoplasmic proteasome clusters (PSG); (3) cells displaying both PSGs and a nuclear accumulation of proteasomes (Nuclear + PSG); and (4) cells without any of these phenotypes, where proteasomes are approximately equally distributed between the cytoplasmic and nuclear compartments (Equal) (Fig. 1B). In a typical 5-day starvation experiment the majority of the cells are either PSG or Equal, whereas a small portion of the cells is Nuclear or Nuclear

+ PSG.

Given that these cells are genetically identical and grow under identical conditions, it is expected that other factors should be responsible for this heterogeneity. These could include replicative aging. Replicative aging results from asymmetrical cell division of budding yeasts in which damaged cell components are typically retained in the mother cell (Kaeberlein, 2010). After each cell division, chitinous scar tissue is left on the cell wall of the mother, which is called a bud scar. The number of bud scars can be visualized with Calcofluor White (CFW), which marks the replicative age (Pringle, 1991). CFW staining distinguishes three age groups: (1) virgin cells without bud scars; (2) young mother cells with one or two bud scars, and (3) old mothers with more than two bud scars (Fig. 1C). We quantified the respective proteasome localization phenotypes per age group. PSG formation inversely related to age as ~30% of the old mothers, ~60% of the young mothers

Figure 1

Fig. 1: Proteasome localization in nutrient-starved cells correlates with replicative age
(A) Live cell microscopy of yeast cells in starvation shows various 20S proteasome localizations as is visualized by endogenous expression of β1(Pre3)-GFP. Cells were stained with CalcoFluor White to assess the replicative age of individual cells. (B) β1-GFP localization and Hoechst staining define four different phenotypes: cells with cytosolic Proteasome Storage Granules (PSG), cells with nuclear enrichment of proteasomes (Nuclear), cells that display both (Nuclear + PSG) and cells without a clear enrichment of proteasomes in PSGs or nuclei (Equal). (C) Based on Calcofluor White staining of bud scars, three different replicative age groups were defined; Virgin daughter cells without bud scars (V), Young Mothers with 1-2 bud scars (YM) and Old Mothers with more than two bud scars (OM). (D) The prevalence of the different proteasome phenotypes in living cells from each age group was calculated by dividing the number of cells with a certain phenotype in a particular age group over the total number of cells in this age group. Values and standard deviations are based on three independent experiments and significance was calculated with a paired, two-tailed t-test (* = p<0.05, ** = p<0.01). (Scale bars, 5 μm)

and ~65% of the virgin cells displayed this phenotype (Fig. 1D). Nuclear accumulation of proteasomes correlated with replicative age in the small population of yeast where this phenotype was observed. This suggests that impairment of proteasome relocalization and/or PSG formation can be associated with replicative age. The prevalence of the other two phenotypes did not differ significantly between the different age groups. Similar results were found in yeasts expressing proteasomes labeled through another 20S subunit [α2–GFP (Pre8)] or a 19S subunit (Rpn1–GFP) (supplementary material Fig. S2).

Identification of genes affecting proteasome localization during starvation

To identify genetic factors controlling proteasome localization during starvation, we performed a microscopy-based yeast knockout screen. We considered two explanations for the maintenance of nuclear enrichment of the proteasome during starvation: altered proteasome biogenesis in the nucleus or altered nuclear retention of the proteasome. Therefore, we tagged the β1 subunit (Pre3) of the proteasome with a fluorescent Recombination-Induced Tag Exchange (RITE) cassette (Verzijlbergen *et al*., 2010), to differentially label new and old proteasomes. Integration of the RITE cassette behind the β1 gene results in a GFP-tagged proteasome produced before tag exchange, whereas new proteasomes (produced after tag exchange due to translocation of an estrogen receptor (ER)-coupled Cre-recombinase to the nucleus after addition of β-estradiol (Verzijlbergen *et al*., 2010)) will be labeled with mRFP. The genetic GFP-for-mRFP swapping is permanent and induced after two days of starvation. When recombination was induced at this time point little or no synthesis of proteasomes was detected in wild-type (WT) cells. Similar results have been obtained by Menendez-Benito *et al*. for several other proteins in these starvation conditions (Menendez-Benito *et al*., 2013).

To obtain a screening library, the β1–RITE strain was crossed with the MATa haploid knockout (KO) collection (Thermo Scientific) using SGA technology (Tong *et al*., 2001) (Fig. 2A1). This high-throughput crossing yielded 4263 knockout strains containing a RITE-tagged proteasome. These strains were subjected to a 5-day starvation protocol, including the induction of tag exchange (switch) at day 2 (Fig. 2A2). To efficiently analyze thousands of samples by microscopy, cells were fixed, stained with Hoechst 33342 and spotted on an object glass using a DNA microarray printer (Narayanaswamy *et al*., 2006) (Fig. 2A3). Each spot, typically consisting of ~2000 cells, was imaged by confocal microscopy (Fig. 2A4). A CellProfiler image analysis pipeline was designed for quantification of the proteasome phenotypes of interest (Carpenter *et al*., 2006) (Fig. 2A5). This pipeline assessed the nuclear cytosolic distribution of the proteasome by dividing the mean GFP fluorescence in the nucleus over the mean GFP fluorescence in the cytoplasm. Three successive rounds of screening identified three hits with a nuclear retention phenotype of the proteasome: *hul5Δ*, *uba3Δ* and *mak10Δ* (Fig. 2A6; Fig. 2B). These results were verified by repeating the experiment with independently made knockout strains. Loss of HUL5, UBA3 or MAK10 increased the population of cells with nuclear accumulation of proteasomes (Fig. 2C). Little or no synthesis of new (mRFP tagged) β1 was detected in either WT or KO cells, thus implying that the nuclear enrichment is not due to *de novo* synthesis. A plating assay before and after recombination confirmed the successful genetic recombination (GFP to mRFP) in these cells (supplementary material Fig. S3A). When recombination is induced at an earlier time point in starvation (after 1 day), synthesis of new (mRFP tagged) proteasomes could be observed in both WT cells and the three screen hits (supplementary material Fig. S3B). The RITE technology was only used for identifying the hits.

4
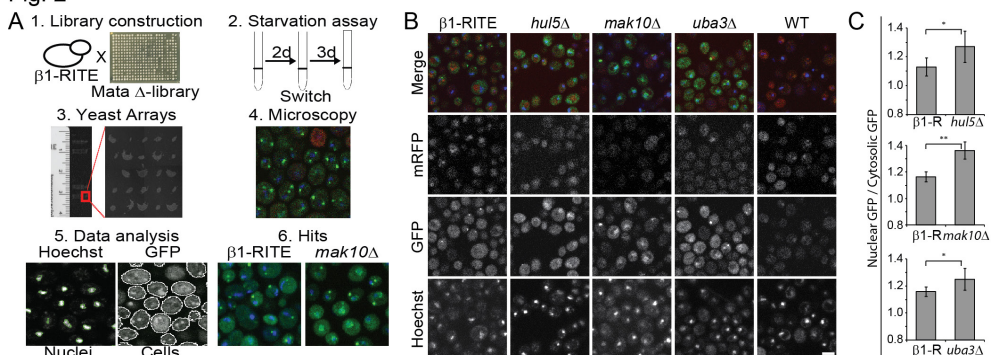
Fig. 2

**Fig. 2: Genome-wide screen identifies genes affecting nuclear proteasome localization during starvation**

(A) Schematic overview of the screening. (1) A yeast knock-out library was crossed with a β1-GFP→mRFP RITE strain. (2) Tag recombination (switch) was performed after two days during a five day starvation experiment. (3) Samples were fixed, stained with Hoechst and printed on yeast arrays. (4) Microscopic imaging of GFP (old proteasomes), RFP (new proteasomes) and Hoechst (nuclei) was performed. (5) Images were analyzed by CellProfiler. (6) mak10Δ was one of the hits for a nuclear proteasome enrichment. (B) Confocal microscopy images of three hits showing nuclear enrichment of GFP labeled proteasome in the nucleus; hul5Δ, mak10Δ and uba3Δ. Only background signal is observed for the mRFP proteasome. (C) Quantification of nuclear/cytosolic ratios of GFP in WT and nuclear retention hits. Values and standard deviations are based on 5 independent experiments and significance was calculated with a paired, two tailed t-test (* = $p<0.05$, ** = $p<0.01$). (Scale bar, 5 μm)

Loss of N-acetylation by NatC causes nuclear enrichment of the proteasome without affecting PSG formation, and both phenotypes are affected by replicative age

The Mak10 protein is a subunit of the N-acetyltransferase C (NatC) complex. NatC associates to the ribosome for co-translational N-terminal acetylation of a subset of proteins (Starheim *et al.*, 2012). The NatC complex further consists of Mak31 and the catalytic subunit Mak3 (Polevoda and Sherman, 2000). In our screening, Mak3 and Mak31 were just below the threshold, but independently generated knockouts of all three individual NatC subunits showed increased nuclear retention of proteasomes during starvation, whereas the number of cells displaying PSGs was not significantly altered (Fig. 3A,C; supplementary material Fig. S4A,B), indicating a specific role for the NatC complex in the nuclear enrichment of the proteasome. The presence of cells with both nuclear enrichment of proteasomes and cytoplasmic PSGs means that PSG formation has been uncoupled from the nuclear-to-cytosolic relocalization of proteasomes (Fig. 3A,B). A catalytically inactive NatC mutant (Mak3 N123A and Y130A) (Polevoda and Sherman, 2000) showed the same phenotype (Fig. 3A,B). NatC activity is apparently involved in the nuclear-to-cytosolic relocalization of proteasomes under starvation conditions. CFW staining was used to assess a potential correlation of proteasome localization with replicative age. Nuclear enrichment of proteasomes correlated with replicative age, whereas PSG formation correlated negatively with replicative age (Fig. 3C,D). Cells displaying both nuclear enrichment and PSG formation also showed a weak correlation, but 'Equal' cells did not. Similar results with respect to the correlation between replicative age and proteasome localization and the effect of NatC deficiency were found for α2– GFP- (Pre8) and Rpn1–GFP-expressing cells (supplementary material Fig. S2). These results

Figure 3
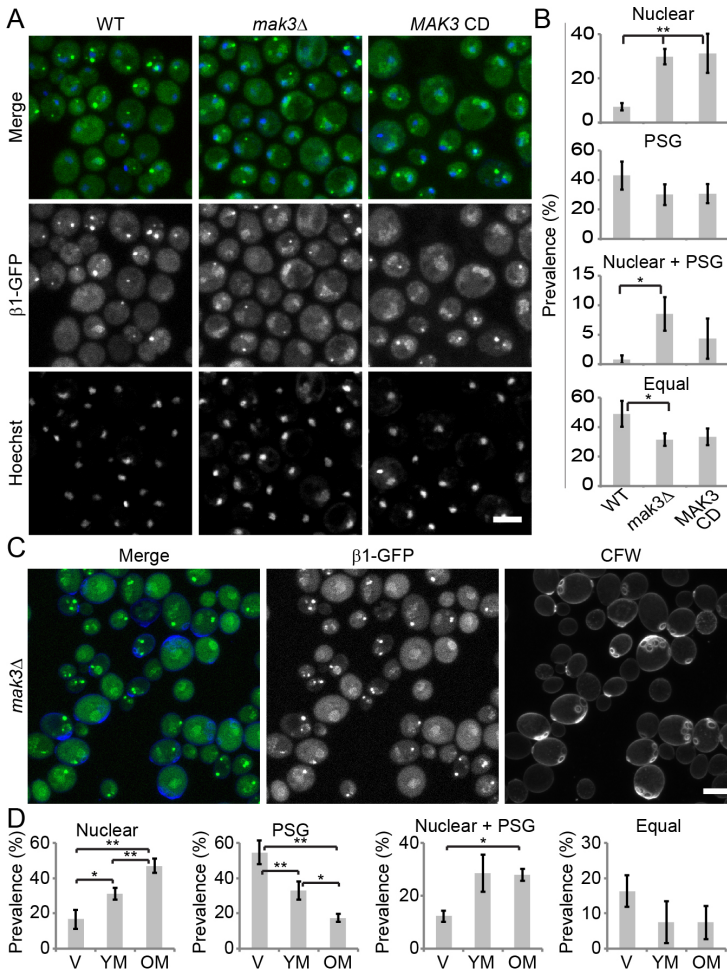
Fig. 3: Loss of N-acetylation by NatC causes nuclear retention of the proteasome without affecting PSG formation; both phenotypes are affected by replicative age

(A) Fixed cell microscopy of Hoechst stained *mak3Δ* cells or cells expressing a catalytically inactive Mak3 (MAK3-CD) shows an increased population of cells displaying nuclear retention of proteasomes after a five day starvation period. (B) The prevalence of the different phenotypes in the total population was scored in three independent experiments. (C) Live cell microscopy of *mak3Δ* cells stained with Calcofluor White after a five day starvation period. (D) The prevalence of each proteasome phenotype in living cells was scored in three different age groups. Quantifications are based on three independent experiments and significance was calculated with paired two-tailed t-tests (* = p<0.05, ** = p<0.01). (Scale bars, 5 μm)

are similar to those observed for WT cells (Fig. 1D), indicating that NatC does not affect aging-related relocalization of proteasomes.
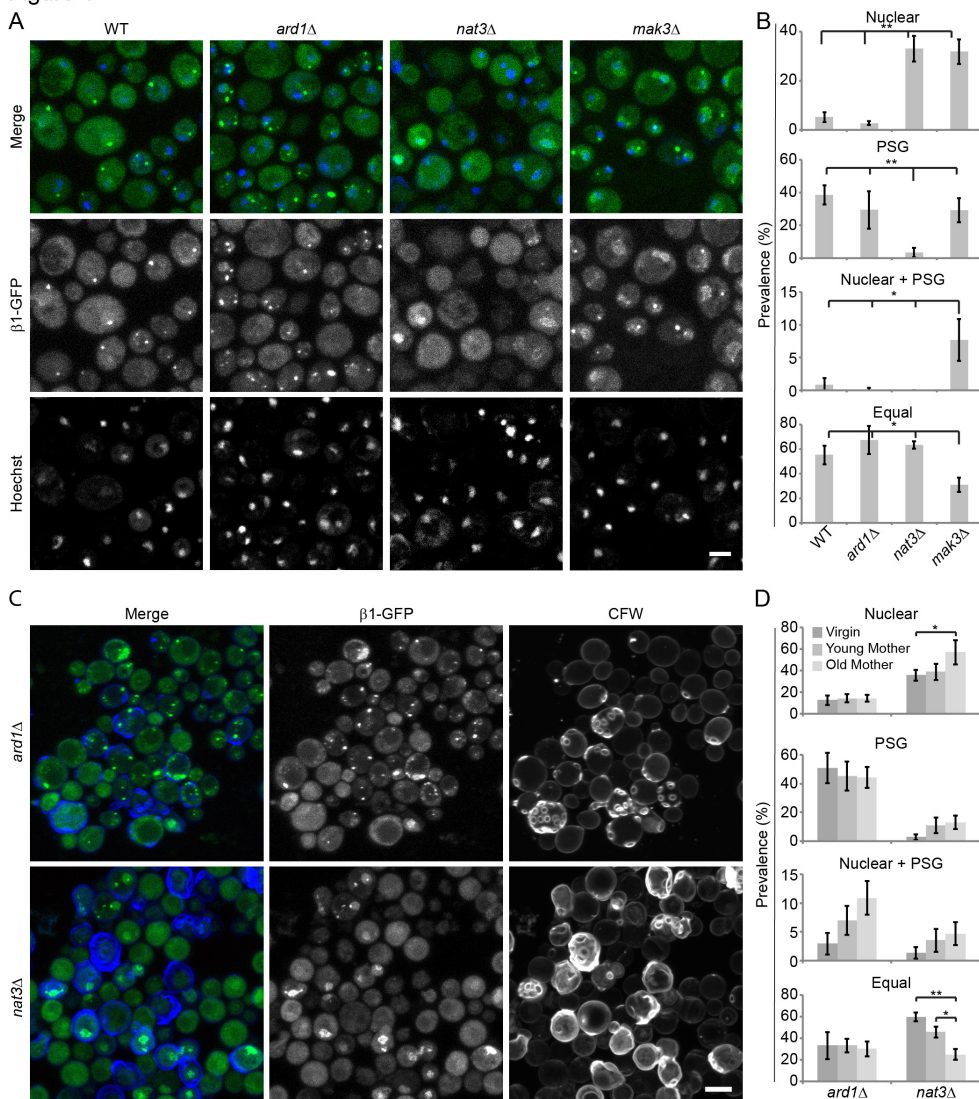
Nuclear-to-cytosolic relocalization of the proteasome during starvation requires NatB and NatC, PSG formation requires only NatB

The main N-terminal acetyltransferases in yeast are NatA, NatB and NatC, contributing to respectively ~50%, ~20% and ~20% of the N-terminal acetylome. Each of these complexes recognizes specific substrates depending on their N-terminal sequences (Starheim *et al.*, 2012). To test whether nuclear enrichment of proteasomes only depends on NatC-mediated N-acetylation, the subunits of the NatA (Ard1, Nat1 and Nat5) and the NatB (Nat3 and Mdm20) complex were knocked out. Deficiency of NatA subunits did not alter proteasome distribution following starvation (Fig. 4A,B;supplementary material Fig. S4C,D). However, deletion of the various NatB subunits increased the population with nuclear proteasomes and reduced the cells displaying PSGs (Fig. 4A,B; supplementary material Fig. S4E,F). Although both NatB and NatC knockouts induced nuclear proteasome

Figure 4

Fig. 4: Nuclear-cytosolic relocalization of the proteasome during starvation requires N-acetylation by NatB and NatC

(A) Fixed cell microscopy of starved *ard1Δ* (NatA deficient), *nat3Δ* (NatB deficient) and *mak3Δ* (NatC deficient) cells. Nuclei were visualized with a Hoechst staining. (B) Prevalence of the different proteasome localization phenotypes was scored in the total population. Values and standard deviations are based on a biological triplicate. (C) Live cell imaging of starved *ard1Δ* and *nat3Δ* cells. Cells were stained with CalcoFluor White to assess their replicative age. (D) Prevalence of the different proteasome phenotypes in the three age groups in living cells was quantified in three independent experiments and significance was calculated with a paired two-tailed T-test. (* = p<0.05, ** = p<0.01) (Scale bars, 5 μm)

enrichment, they had different effects on the cytoplasmic proteasome pool. NatC inactivation still allowed PSG formation, whereas NatB inactivation prevented formation of PSGs (Fig. 4A,B; supplementary material Fig. S4C–F). This suggests a specific role of the NatB complex in PSG formation. Cells with both PSGs and nuclear retention were hardly detected among NatB-knockout cells (Fig. 4B). As for WT and NatC-deficient cells, nuclear enrichment induced by NatB inactivation correlated with replicative age, whereas the prevalence of 'Equal' cells decreased with replicative age. (Fig. 4C,D; compare to Fig. 3D). Surprisingly, NatA-deficient cells did show a WT-like prevalence of the different proteasome phenotypes in the total population, but there was no correlation of these phenotypes with replicative age.

These results would suggest that the mechanism underlying the different proteasome localizations in cells involves selective N-acetylation and can be (at least partially) uncoupled from aging effects that also require N-acetylation. NatB and NatC, unlike NatA, are involved in the effects on proteasome distribution. Their combined inactivation might further accelerate these effects, and a NatB+NatC double knockout strain was made. This double knockout (unlike the single knockouts) had severe growth defects, preventing a fair comparison with the single knockout strains. Given that the effects on nuclear enrichment of the proteasome were specific to NatB and NatC, N-acetylation of one or more NatB and NatC substrates must be involved in nuclear-to-cytosolic proteasome distribution. Based on the N-terminal sequence requirements of each Nat complex a list of potential substrates were defined in the yeast proteome (Arnesen *et al.*, 2009; Polevoda and Sherman, 2003). The role of N-acetylation of selected candidate substrates was tested by making an N-terminal MX- to MP- (X2P) mutation, resulting in an N-terminus that cannot be N-acetylated (Polevoda and Sherman, 2003). Preventing N-acetylation of α5 (Pup2), α6 (Pre5), Rpn9, Fub1, Avo2, Hul5 or Nup100 failed to phenotypically mimic cells lacking NatB or NatC (supplementary material Fig. S4G). Whether NatB and NatC act on proteasome distribution by modifying a single target or many, is as yet unclear.

NatA and NatB control general cell fitness during starvation and NatC fitness of old cells only

As proteasome composition and activity was found to influence longevity in starvation, we wondered whether proteasome localization would also correlate with cell fitness. Cellular fitness in starvation can be determined by assaying the ability of cells to restart their cell cycle when nutrients are added. This is determined by plating equal numbers of cells and quantifying the number of colony-forming units (CFUs). When grown in the presence of sufficient nutrients, the reproductive capacity of NatA- and NatC-deficient cells is similar to WT cells, whereas NatB-deficient cells show a lower reproductive capacity (Fig. 5A) (Polevoda *et al.*, 1999). After a 5-day starvation period, both NatA- and NatB-deficient cells showed lower CFUs than wild-type cells, whereas the reproductive capacity in NatC-deficient cells seemed to be unaffected (Fig. 5B). Proteasome localization in NatA-deficient cells was similar to WT, unlike that in NatB-deficient cells. Given that NatA and NatB deficiency both decrease the number of CFUs measured, proteasome localization cannot be directly related to reproductive capacity in starvation.

Given that NatC-deficient cells show a strong correlation of proteasome localization with replicative age, we wondered whether NatC also affected reproductive capacity in an age-dependent manner. We determined the fitness of old versus young cells in a starved population of the various mutant yeast strains by staining the yeast cells with CFW and

then separating young and old yeast cells by FACS sorting (Pringle, 1991). Microscopy on the sorted populations verified separation of virgin and old mother cells (Fig. 5C). Equal numbers of cells from the different populations were subsequently plated and the number of CFUs determined. About 75% of the young WT cells and ~30% of the old WT cells were able to form colonies upon plating (Fig. 5D). This correlation between replicative age and cell fitness is similar to results previously reported by Allen *et al.* (Allen *et al.*, 2006). The low number of CFUs measured for old as well as young NatA- and NatB-deficient cells was expected, based on their general effects on cell fitness (Fig. 5B) and is in agreement

Fig. 5
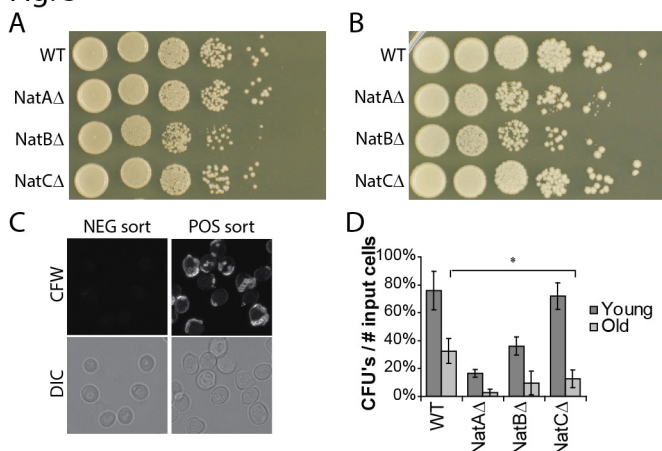
Fig. 5: In starvation, loss of NatA and NatB has a general effect on reproductive capacity, whereas loss of NatC specifically affects old cells

The reproductive capacity of the different strains in log phase (A) and starvation (B) was assessed by a plating assay. Loss of NatA and NatB compromised reproductive capacity in starved cells, whereas loss of NatC did not. Representative plating assay from three independent experiments. (C) After Calcofluor White (CFW) staining of a starved culture, the cells with the lowest (negative) and highest (positive) CFW signal were sorted to obtain populations of virgin cells and old mothers, respectively. The CFW image is the maximum projection of a 5 µm Z-stack, the DIC image is a single scan in the middle of the Z-stacks. (D) CFUs were counted for old and young cells. Loss of NatC affects the reproductive capacity of old cells, while loss of NatA and NatB reduces the reproductive capacity of both young and old cells. Values and standard deviations are based on three independent experiments. Significance was calculated with a paired two-tailed T-test. (* = $p<0.05$, ** = $p<0.01$)

with findings for NatA by Aragon *et al.* (Aragon *et al.*, 2008). Surprisingly, WT and NatC-knockout young cells were equally fit, whereas the fitness of the old NatC-knockout cells was reduced to only 30% of old WT cells. NatC deficiency not only affected localization of proteasomes in replicative old cells, but it also had a selective effect on the fitness of old mothers.

Discussion

The proteasome is located in both the cytosol and nucleosol. Its subunits are made in the cytosol where proteasomes are assembled in precursor complexes that can be imported into the nucleus for full formation of the complex (Lehmann *et al.*, 2002). Nuclear import and export of mature proteasomes is a very slow process in mammalian cells and the details of this process are poorly understood (Reits *et al.*, 1997). Given that the nuclear

envelope disintegrates during mitosis in mammalian cells, the boundary between the two pools of proteasomes is lost and nuclear proteasomes mix with cytosolic proteasomes. Nuclear proteasomes could thus have a cytosolic origin and vice versa. This should be different in budding yeast, where the nuclear envelope is maintained during cell division and proteasomes tend to accumulate in the nucleus. However, nuclear-to-cytosolic relocalization of proteasomes is observed upon glucose exhaustion, which is followed by rapid nuclear import of mature proteasomes upon re-addition of nutrients. It would therefore be expected that proteasome distribution is under some kind of control (Laporte *et al.*, 2008).

We report that nuclear-to-cytosolic relocalization of the proteasome upon starvation correlates with the replicative age of yeast cells. Young cells are better capable of relocalizing the proteasome from the nucleus and of forming cytosolic PSGs, whereas old mother cells usually fail to do so. This correlation might be due to an age-dependent defect in the proteasome relocalization machinery, but could also be due to asymmetrical division of damaged cell components upon cell division. In general, damaged protein accumulates in mother cells leaving daughter cells with a fresh set of proteins (Henderson and Gottschling, 2008; Kaeberlein, 2010; Nyström and Liu, 2014). Perhaps a low amount of damaged proteins allows young cells to store their proteasomes in PSGs, whereas old cells might need to maintain a larger pool of active proteasomes to handle accumulated protein damage at the cost of PSGs. A nuclear enrichment of the proteasome might help replicative old cells to handle protein stress in the nucleus (Gardner *et al.*, 2005) but it might also contribute to protein quality control in the cytosol (Heck *et al.*, 2010; Prasad *et al.*, 2010).

The reported association between the capacity of the ubiquitin-proteasome system and viability during aging (Carrard *et al.*, 2002; Kruegel *et al.*, 2011; Tonoki *et al.*, 2009; Vernace *et al.*, 2007b) suggests that the localization of the proteasome also affects viability. This can only be tested in a system where proteasome localization can be manipulated during the aging process. We performed a microscopy-based screen to identify proteins that control proteasome localization in yeast cells. We identified two of the three complexes involved in N-terminal acetylation of proteins as controlling nuclear-to-cytosolic relocalization of the proteasome. About half of the yeast proteome can be N-acetylated by these complexes (Starheim *et al.*, 2012). N-acetylation can both stabilize and de-stabilize proteins as well as affect the intracellular localization and activity of proteins (Arnesen, 2011; Hwang *et al.*, 2010; Scott *et al.*, 2011). Given that the acetylation complexes NatB and NatC but not NatA control the nuclear-to-cytosolic relocalization of proteasomes, a selective set of substrates rather than the general N-acetylation process seems to be responsible. The different phenotypes for the NatB and NatC knockouts allowed testing of the link between nuclear-to-cytosolic relocalization of proteasomes and the formation of PSGs. Although NatC-deficient old mother cells accumulated significantly more nuclear proteasomes, the prevalence of cytosolic PSGs was unaffected. In addition, a population of cells with both nuclear retention and PSG formation was observed. Both observations suggest that nuclear accumulation of proteasomes in older mothers does not necessarily prevent formation of cytosolic PSGs. This suggests that the mere enrichment of proteasomes in the cytosolic compartment is not a prerequisite for PSG formation.

As proteasome localization during aging can be manipulated by inactivation of either NatB or NatC, the effect on cell fitness during aging can be determined. Although NatA and NatB deficiency strongly affected cell fitness in all age groups tested, NatC deficiency

4

selectively affected fitness of old mothers. As for the localization of the proteasome, the different Nat complexes affected cell fitness in a Nat-complex-specific manner. Whether this is the result of modification of part of the proteome or of one defined substrate, is at present unclear. We excluded some proteins that were potentially involved, like Hul5 (supplementary material Fig. S4G), another hit in our screening, as single candidates but that does not exclude other proteins.

Acetylation of lysine side chains of various proteins has been connected to the aging process. This is exemplified by the yeast deacetylase Sir2. Sir2 reduces lifespan upon deletion and prolongs it upon overexpression (Wierman and Smith, 2014). Homologs of Sir2 in several other organisms, including the SIRT proteins in mammals, have been linked to aging and age-related diseases (Donmez and Guarente, 2010). Furthermore, calorific restriction can increase age and has been associated with altered acetylation status of many mitochondrial proteins (Hebert *et al.*, 2013), which has been extensively studied in neurodegeneration diseases (Guedes-Dias and Oliveira, 2013). These examples indicate a role of acetyl modifications of lysine side chains in processes associated with aging. Here, we have shown that N-terminal acetylation, a different, stable and often co-translational modification with the same chemical group, is associated with proteasome distribution and fitness during aging. The mechanisms controlling proteasome localization and fitness at old age involve specific N-acetylation complexes and result in a further expansion of the role of the small acetyl modification.

Materials and Methods

Yeast strains and plasmids

With the exception of the strains used for screening, all strains were derived from NKI4103 (Verzijlbergen *et al.*, 2010). Gene knockouts were made by PCR-mediated gene disruption based on pRS plasmids (Baker Brachmann *et al.*, 1998). N-terminal mutations were made by PCR amplification of the pYM-N10 and pYM-N11 plasmids using the S1 and S4 primers extended with 40 bp of sequence homologous to the endogenous sequence (Janke *et al.*, 2004). The N-terminal mutation was introduced in the 40 bp endogenous sequence. The two mutations for the catalytically inactive N123A-Y130A-Mak3 were generated by Delitto Perfetto technology (Storici and Resnick, 2006). All strains are described in supplementary material Table S1.

Growth Conditions

Yeast cells were grown in liquid YEPD cultures of 5 ml at 30°C. To prevent recombination of the RITE cassette, cells were grown in presence of Hygromycin (200 µg/ml, Invitrogen). Liquid cultures were starved by inoculating 5 ml of YEPD with 0.5 ml of an overnight culture followed by a 5-day starvation period.

Library construction

NKI4103 (Verzijlbergen *et al.*, 2010) was crossed with the MATa haploid knockout collection (ThermoScientific) by Synthetic Genetic Array analysis (Tong and Boone, 2006) using a RoToR HAD (Singer Instruments) with the following modifications. After mating, diploids were selected and kept on Hygromycin, G418 and CloNat triple selection on rich medium for 1 night. After 2 weeks on sporulation medium, MATa haploid clones containing both a gene knockout and the RITE tagging system were selected. The first

two rounds of selection generated haploid MATa cells (YC-His+Can+SAEC) (van Leeuwen and Gottschling, 2002). The next two selection rounds selected the knockout and the RITE system (YC-His+Can+SAEC+MSG+ Hygromycin, G418 and CloNat).

Microscopy and image analysis

Fixed microscopy samples were prepared by fixing ~10^8 cells in 4% formaldehyde and mounted in Vectashield (Vector Laboratories) on ConA-coated coverslips. Live-cell samples were prepared by resuspending ~10^8 cells in 100 µl 40°C 1% UltraPure™ LMP Agarose (Invitrogen) in PBS which is squeezed between a cover glass and an object glass. Imaging was performed at room temperature within 1 hour after mounting. Hoechst 33342 (Invitrogen, 1 µg/ml) or Calcofluor White (CFW, Sigma-Aldrich, 2 µg/ml) staining was performed before mounting the sample. Images were made on a Leica SP5 (Leica Microsystems), using a 63× objective and a 405-nm laser to excite Hoechst 33342 and CFW, a 488 nm laser for GFP and 561 nm for mRFP. 5 µm thick Z-stacks were made with 15 slides. Image analysis was performed on maximum Z-projections by scoring different phenotypes, counting 200–500 cells per biological replicate.

Screening

The screening of the β1-RITE + KO library was performed in batches of 384 strains. A RoToR HAD (Singer Instruments) was used to transfer the strains from 384-well glycerol stocks to a YEPD+Hygromycin agar plate. 120 µl start cultures in 96-well plates were inoculated from the YEPD plate, grown overnight and used to start a 4 ml culture. A 2-day starvation period was followed with a switch assay as described by Verzijlbergen *et al*. (Verzijlbergen *et al*., 2010) and another 3-day starvation period. Samples were then fixed in 4% formaldehyde, stained with Hoechst and spotted on a yeast array (Narayanaswamy *et al*., 2006). Microscopic analysis was performed on a Leica AOBS LSCM (Leica Microsystems) using 405-, 488- and 561-nm laser light to excite Hoechst 33342, GFP and mRFP respectively. High-throughput image analysis was performed using CellProfiler software (Carpenter *et al*., 2006). The screening results of selected candidates were validated by two additional rounds of analysis and independent generation of the knockout yeast strains.

Flow-based sorting of old and young cells

To isolate replicative old and young cells, ~2×10^7 cells of a starved culture were stained with CFW and FACS sorted on a MoFlo-Astrios (Beckman Coulter) using 405 nm excitation and collecting fluorescence emission with a 450 nm (30-nm bandpass) filter. The 2.5% of the cells with the highest and lowest CFW signal were isolated and ~250 yeasts were subsequently plated on YEPD plates (Allen *et al*., 2006). CFUs were counted after 3 days culture at 30°C.

Protein extraction and native gel analysis

Native protein samples were made by washing a cell pellet of ~10^8 cells in PBS plus protease inhibitors (1 mM PMSF, 5 mM benzamidine, 1 µg/ml pepstatin, 1 µg/ml leupepting) and resuspended in buffer A (20 mM Tris-HCl pH 7.4, 5 mM MgCl2, 1 mM DTT, 1 mM ATP) plus protease inhibitors. Cells were lysed in buffer A by using glass beads, which were removed before addition of a blue loading buffer (5×; 50% glycerol and Bromophenol Blue). Samples were loaded on a NativePAGE™ 3–12% Bis-Tris gel (Life Technologies) and ran in NativePAGE™ running buffer (Life Technologies). GFP fluorescence was visualized on

a ProXPRESS (Perkin Elmer) machine with 480 nm (30-nm bandpass) excitation and 550 nm (40-nm bandpass) emission filters. To visualize untagged proteasomes, the gel was incubated with 100 µM suc-LLVY-AMC (Enzo Life Sciences) in the presence of 1 mM ATP, 1 mM DTT and 0.02% SDS (Elsasser *et al.*, 2005). Gel scans were made with 390 nm (70-nm bandpass) excitation and 450 nm (20-nm bandpass) emission filters.

Acknowledgements

References

Allen, C., Buttner, S., Aragon, A., Thomas, J., Meirelles, O., Jaetao, J., Benn, D., Ruby, S., Veenhuis, M., Madeo, F. *et al*. (2006). Isolation of quiescent and nonquiescent cells from yeast stationary-phase cultures. J Cell Biol 174, 89-100.

Amm, I., Sommer, T. and Wolf, D. (2014). Protein quality control and elimination of protein waste: The role of the ubiquitin proteasome system. Biochim Biophys Acta 1843, 182-196.

Aragon, A. D., Rodriguez, A. L., Meirelles, O., Roy, S., Davidson, G. S., Tapia, P. H., Allen, C., Joe, R., Benn, D. and Werner-Washburne, M. (2008). Characterization of Differentiated Quiescent and Nonquiescent Cells in Yeast Stationary-Phase Cultures. Molecular Biology of the Cell 19, 1271-1280.

Arnesen, T. (2011). Towards a Functional Understanding of Protein N-Terminal Acetylation. PLoS Biol 9, e1001074.

Arnesen, T., Van Damme, P., Polevoda, B., Helsens, K., Evjenth, R., Colaert, N., Varhaug, J., Vandekerckhove, J., Lillehaug, J., Sherman, F. *et al*. (2009). Proteomics analyses reveal the evolutionary conservation and divergence of N-terminal acetyltransferases from yeast and humans. PNAS 106, 8157-8162.

Baker Brachmann, C., Davies, A., Cost, G., Caputo, E., Li, J., Hieter, P. and Boeke, J. (1998). Designer deletion strains derived from *Saccharomyces cerevisiae* S288C: A useful set of strains and plasmids for PCR-mediated gene disruption and other applications. Yeast 14, 115-132.

Carpenter, A., Jones, T., Lamprecht, M., Clarke, C., Kang, I., Friman, O., Guertin, D., Chang, J., Lindquist, R., Moffat, J. *et al*. (2006). CellProfiler: image analysis software for identifying and quantifying cell phenotypes. Genome Biol 7, R100.

Carrard, G., Bulteau, A., Petropoulos, I. and Friguet, B. (2002). Impairment of proteasome structure and function in aging. Int J Biochem Cell Biol 34, 1461-1474.

Chen, Q., Thorpe, J., Dohmen, J., Li, F. and Keller, J. (2006). Ump1 extends yeast lifespan and enhances viability during oxidative stress: Central role for the proteasome? Free Radic Biol Med 40, 120-126.

Clay, L. and Barral, Y. (2013). New approaches to an age-old problem. Current Opinion in Biotechnology 24, 784-789.

Dasuri, K., Zhang, L., Ebenezer, P., Liu, Y., Fernandez-Kim, S. and Keller, J. (2009). Aging and dietary restriction alter proteasome biogenesis and composition in the brain and liver. Mech Ageing Dev 130, 777-783.

Delaney, J., Murakami, C., Chou, A., Carr, D., Schleit, J., Sutphin, G., An, E., Castanza, A., Fletcher, M., Goswami, S. *et al*. (2013). Dietary restriction and mitochondrial function link replicative and chronological aging in *Saccharomyces cerevisiae*. Exp Geront 48, 1006-1013.

Donmez, G. and Guarente, L. (2010). Aging and disease: connections to sirtuins. Aging Cell 9, 285-290.

Elsasser, S., Schmidt, M. and Finley, D. (2005). Characterization of the Proteasome Using Native Gel Electrophoresis. In Methods in Enzymology, vol. Volume 398 (ed. J. D. Raymond), pp. 353-363: Academic Press.

Gardner, R., Nelson, Z. and Gottschling, D. (2005). Degradation-Mediated Protein Quality Control in the Nucleus. Cell 120, 803-815.

Guedes-Dias, P. and Oliveira, J. (2013). Lysine deacetylases and mitochondrial dynamics in neurodegeneration. Biochim Biophys Acta 1832, 1345-1359.

Hebert, A., Dittenhafer-Reed, K., Yu, W., Bailey, D., Selen, E., Boersma, M., Carson, J., Tonelli, M., Balloon, A., Higbee, A. *et al*. (2013). Calorie Restriction and SIRT3 Trigger Global Reprogramming of the Mitochondrial Protein Acetylome. Mol Cell 49, 186-199.

Heck, J., Cheung, S. and Hampton, R. (2010). Cytoplasmic protein quality control degradation mediated by parallel actions of the E3 ubiquitin

ligases Ubr1 and San1. PNAS 107, 1106-1111.

Henderson, K. and Gottschling, D. (2008). A mothers sacrifice: what is she keeping for herself? Current Opinion in Cell Biology 20, 723-728.

Hwang, C., Shemorry, A. and Varshavsky, A. (2010). N-Terminal Acetylation of Cellular Proteins Creates Specific Degradation Signals. Science 327, 973-977.

Janke, C., Magiera, M., Rathfelder, N., Taxis, C., Reber, S., Maekawa, H., Moreno-Borchart, A., Doenges, G., Schwob, E., Schiebel, E. *et al*. (2004). A versatile toolbox for PCR-based tagging of yeast genes: new fluorescent proteins, more markers and promoter substitution cassettes. Yeast 21, 947-962.

Kaeberlein, M. (2010). Lessons on longevity from budding yeast. Nature 464, 513-519.

Kennedy, B. K., Austriaco, N. R. and Guarente, L. (1994). Daughter cells of *Saccharomyces cerevisiae* from old mothers display a reduced life span. J Cell Biol 127, 1985-1993.

Koga, H., Kaushik, S. and Cuervo, A. (2011). Protein homeostasis and aging: The importance of exquisite quality control. Ageing Research Reviews 10, 205-215.

Kruegel, U., Robison, B., Dange, T., Kahlert, G. and Delaney, J. (2011). Elevated Proteasome Capacity Extends Replicative Lifespan in *Saccharomyces cerevisiae*. PLoS Genet, 1371.

Laporte, D., Salin, B., Daignan-Fornier, B. and Sagot, I. (2008). Reversible cytoplasmic localization of the proteasome in quiescent yeast cells. J Cell Biol 181, 737-745.

Lee, C., Klopp, R., Weindruch, R. and Prolla, T. (1999). Gene Expression Profile of Aging and Its Retardation by Caloric Restriction. Science 285, 1390-1393.

Lehmann, A., Janek, K., Braun, B., Kloetzel, P. and Enenkel, C. (2002). 20 S proteasomes are imported as precursor complexes into the nucleus of yeast. J Mol Biol 317, 401-413.

Menendez-Benito, V., van Deventer, S. J., Jimenez-Garcia, V., Roy-Luzarraga, M., van Leeuwen, F. and Neefjes, J. (2013). Spatiotemporal analysis of organelle and macromolecular complex inheritance. Proceedings of the National Academy of Sciences 110, 175-180.

Michal Jazwinski, S., Egilmez, N. K. and Chen, J. B. (1989). Replication control and cellular life span. Experimental Gerontology 24, 423-436.

Mortimer, R. K. and Johnston, J. R. (1959). Life Span of Individual Yeast Cells. Nature 183, 1751-1752.

Murakami, C., Delaney, J., Chou, A., Carr, D., Schleit, J., Sutphin, G., An, E., Castanza, A., Fletcher, M., Goswami, S. *et al*. (2012). pH neutralization protects against reduction in replicative lifespan following chronological aging in yeast. Cell Cycle 11, 3087-3096.

Narayanaswamy, R., Niu, W., Scouras,

A., Hart, G. T., Davies, J., Ellington, A., Iyer, V. and Marcotte, E. (2006). Systematic profiling of cellular phenotypes with spotted cell microarrays reveals mating-pheromone response genes. Genome Biol 7, R6.

Nystrom, T. and Liu, B. (2014). The mystery of aging and rejuvenation; a budding topic. Current Opinion in Microbiology 18, 61-67.

Polevoda, B., Norbeck, J., Takakura, H., Blomberg, A. and Sherman, F. (1999). Identification and specificities of N-terminal acetyltransferases from *Saccharomyces cerevisiae*. The EMBO Journal 18, 6155-6168.

Polevoda, B. and Sherman, F. (2000). N-terminal Acetylation of Eukaryotic Proteins. J Biol Chem 275, 36479-36482.

Polevoda, B. and Sherman, F. (2003). N-terminal Acetyltransferases and Sequence Requirements for N-terminal Acetylation of Eukaryotic Proteins. J Mol Biol 325, 595-622.

Powers, E., Morimoto, R., Dillin, A., Kelly, J. and Balch, W. (2009). Biological and Chemical Approaches to Diseases of Proteostasis Deficiency. Annu Rev Biochem 78, 959-991.

Prasad, R., Kawaguchi, S. and Ng, D. (2010). A Nucleus-based Quality Control Mechanism for Cytosolic Proteins. Mol Biol Cell 21, 2117-2127.

Pringle, J. (1991). [52] Staining of bud scars and other cell wall chitin with Calcofluor. In Methods in Enzymology Guide to Yeast Genetics and Molecular Biology, (ed. G. Christine Guthrie), pp. 732-735: Academic Press.

Reits, E., Benham, A., Plougastel, B., Neefjes, J. and Trowsdale, J. (1997). Dynamics of proteasome distribution in living cells. EMBO J 16, 6087-6094.

Russell, S., Steger, K. and Johnston, S. (1999). Subcellular Localization, Stoichiometry, and Protein Levels of 26 S Proteasome Subunits in Yeast. J Biol Chem 274, 21943-21952.

Schmidt, M. and Finley, D. (2014). Regulation of proteasome activity in health and disease. Biochim Biophys Acta 1843, 13-25.

Scott, D., Monda, J., Bennett, E., Harper, J. W. and Schulman, B. (2011). N-Terminal Acetylation Acts as an Avidity Enhancer Within an Interconnected Multiprotein Complex. Science 334, 674-678.

Starheim, K., Gevaert, K. and Arnesen, T. (2012). Protein N-terminal acetyltransferases: when the start matters. Trends Biochem Sci 37, 152-161.

Storici, F. and Resnick, M. (2006). The Delitto Perfetto Approach to *In Vivo* Site Directed Mutagenesis and Chromosome Rearrangements with Synthetic Oligonucleotides in Yeast. In Methods in Enzymology DNA Repair, Part B, (ed. L. C. Judith), pp. 329-345: Academic Press.

Tenreiro, S. and Outeiro, T. (2010). Simple is good: yeast models of neurodegeneration. FEMS Yeast Research 10, 970-979.

4

Tong, A. and Boone, C. (2006). Synthetic genetic array analysis in *Saccharomyces cerevisiae.* Methods Mol Biol 313:171-92.

Tong, A., Evangelista, M., Parsons, A., Xu, H., Bader, G., Pag, N., Robinson, M., Raghibizadeh, S., Hogue, C., Bussey, H. *et al*. (2001). Systematic Genetic Analysis with Ordered Arrays of Yeast Deletion Mutants. Science 294, 2364-2368.

Tonoki, A., Kuranaga, E., Tomioka, T., Hamazaki, J., Murata, S., Tanaka, K. and Miura, M. (2009). Genetic Evidence Linking Age-Dependent Attenuation of the 26S Proteasome with the Aging Process. Mol Cel Biol 29, 1095-1106.

van Leeuwen, F. and Gottschling, D. (2002). Assays for gene silencing in yeast. In Methods in Enzymology
Guide to Yeast Genetics and Molecular and Cell Biology - Part B, (ed. C. G. a. Gerald), pp. 165-186:

Academic Press.

Vernace, V., Arnaud, L., Schmidt-Glenewinkel, T. and Figueiredo-Pereira, M. (2007a). Aging perturbs 26S proteasome assembly in Drosophila melanogaster. FASEB J 21, 2672-2682.

Vernace, V., Schmidt-Glenewinkel, T. and Figueiredo-Pereira, M. (2007b). Aging and regulated protein degradation: who has the UPPer hand? Aging Cell 6, 599-606.

Verzijlbergen, K., Menendez-Benito, V., van Welsem, T., van Deventer, S., Lindstrom, D., Ovaa, H., Neefjes, J., Gottschling, D. and van Leeuwen, F. (2010). Recombination-induced tag exchange to track old and new proteins. PNAS 107, 64-68.

Wierman, M. and Smith, J. (2014). Yeast sirtuins and the regulation of aging. FEMS Yeast Research 14, 73-88.

Supplemental Figures:
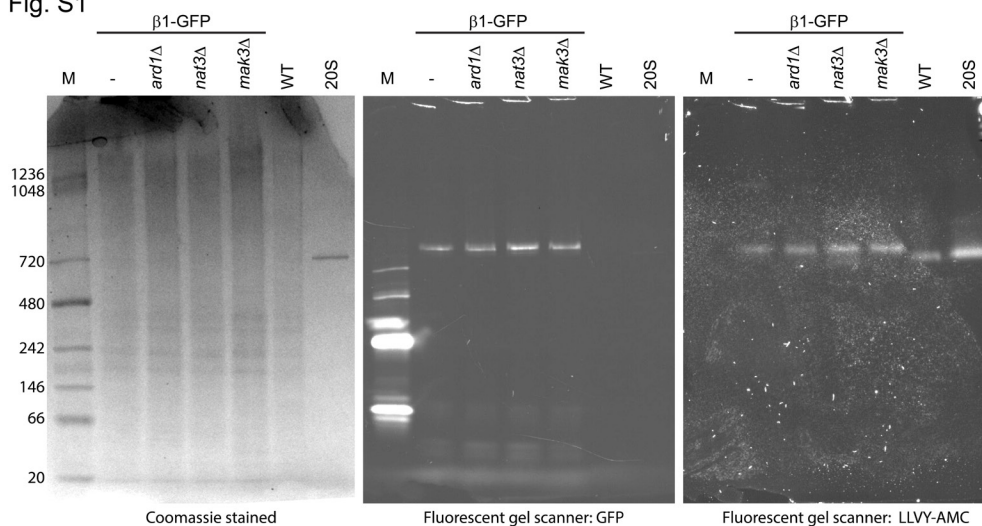
Fig. S1

Fig S1: β1-GFP is efficiently incorporated in the 20S proteasome in WT and NatA, B or C deficient cells
A fluorescent gel scan of a native gel shows one GFP fluorescent band around 720 kDa for both β1-GFP and NatA, B or C deficient starved cells. This band runs at the same height as a purified 20S control (Mouse 20S proteasome, Boston Biochem) and is also present in a WT sample without GFP as was visualized by incubating the gel with a suc-LLVY-AMC (Enzo Life Sciences) proteasome activity probe. The marker (M) was visualized by Coomassie staining of the same gel. We conclude that the presence of the GFP tag on β1 doesn't induce the presence of proteasome assembly intermediates or a pool of unincorporated substrates in β1-GFP or NatA, B or C deficient cells.
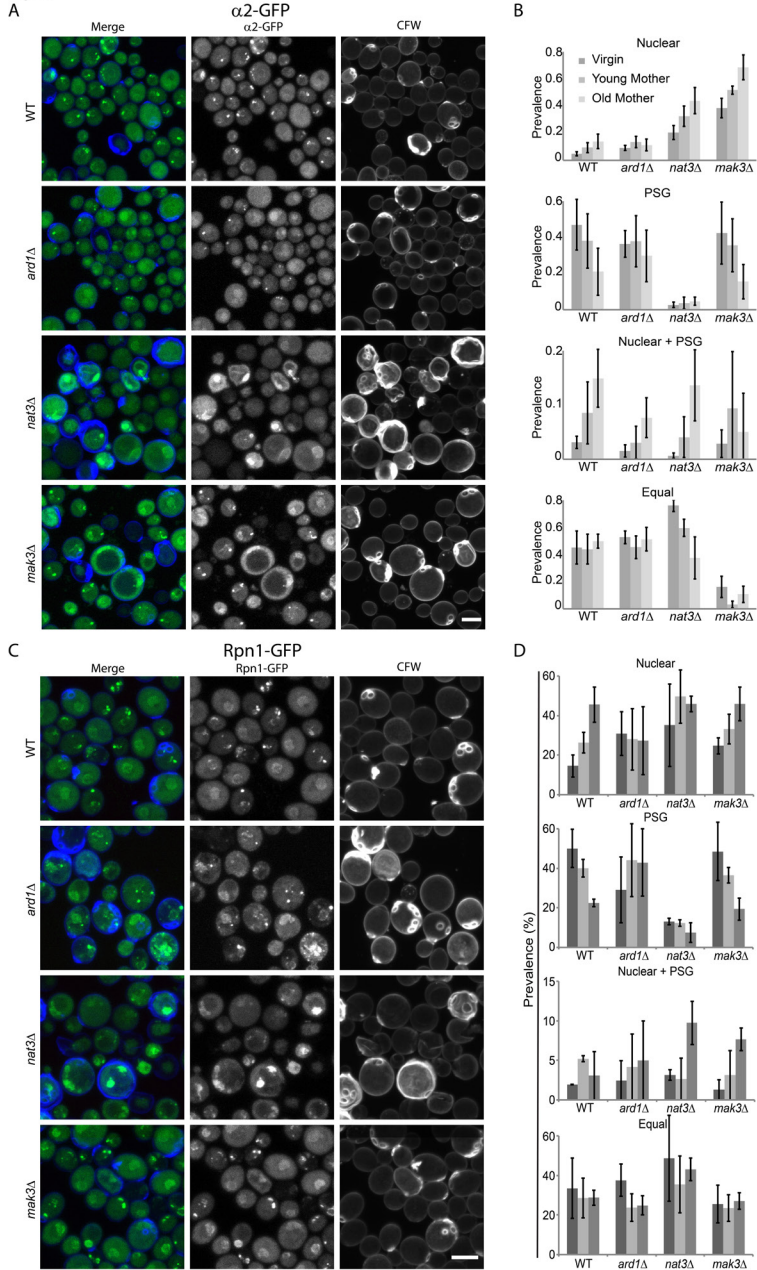
**Fig S2: GFP tagged α2 (Pre8) and Rpn1 show the same proteasome localization as β1-GFP in WT and NatA,B or C deficient cells**

(A) Live cell microscopy of starved WT and NatA (*ard1Δ*), NatB (*nat3Δ*) or NatC (*mak3Δ*) deficient cells endogenously expressing α2(Pre8)-GFP. Cells were stained with CalcoFluor White to asses replicative age. (B) The prevalence of the different phenotypes in the different age groups was scored in two independent experiments (~200 live cells per replicate). (C) The same experiment as in (A), but now with cells endogenously expressing RPN1-GFP, a component of the 19S base particle. (D) Prevalence of the different proteasome phenotypes in the three age groups of living cells. (Scale bars, 5 μm)
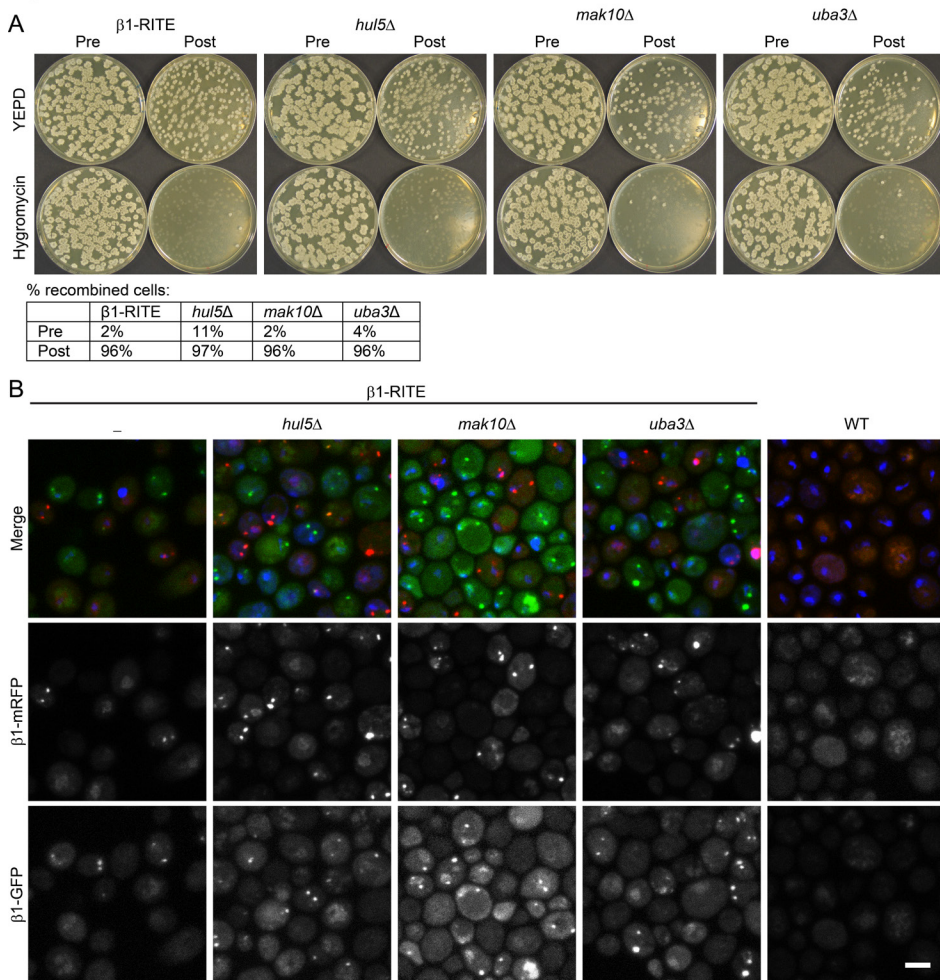
Fig. S3

Fig S3: Plating assay confirms efficient recombination in hul5Δ, mak10Δ and uba3Δ cells
(A) Genetic recombination of the RITE cassette results in the loss of Hygromycin resistance, which can be used to assess the percentage of cells that underwent a recombination event as described by (Verzijlbergen *et al.*, 2010). Samples were taken just before (Pre) and ~16h after (Post) recombination was induced. In both WT and mutant cells the recombination without induction is low and the induced recombination is high. (B) Live cell microscopy of WT cells and the three nuclear retention hits. Images were taken after 5 days starvation, but the recombination was induced after one day starvation instead of two days. Under those conditions synthesis of new (mRFP-tagged) proteasome can be detected, thereby validating the RITE tool in starvation conditions. (Scale bar, 5 μm)
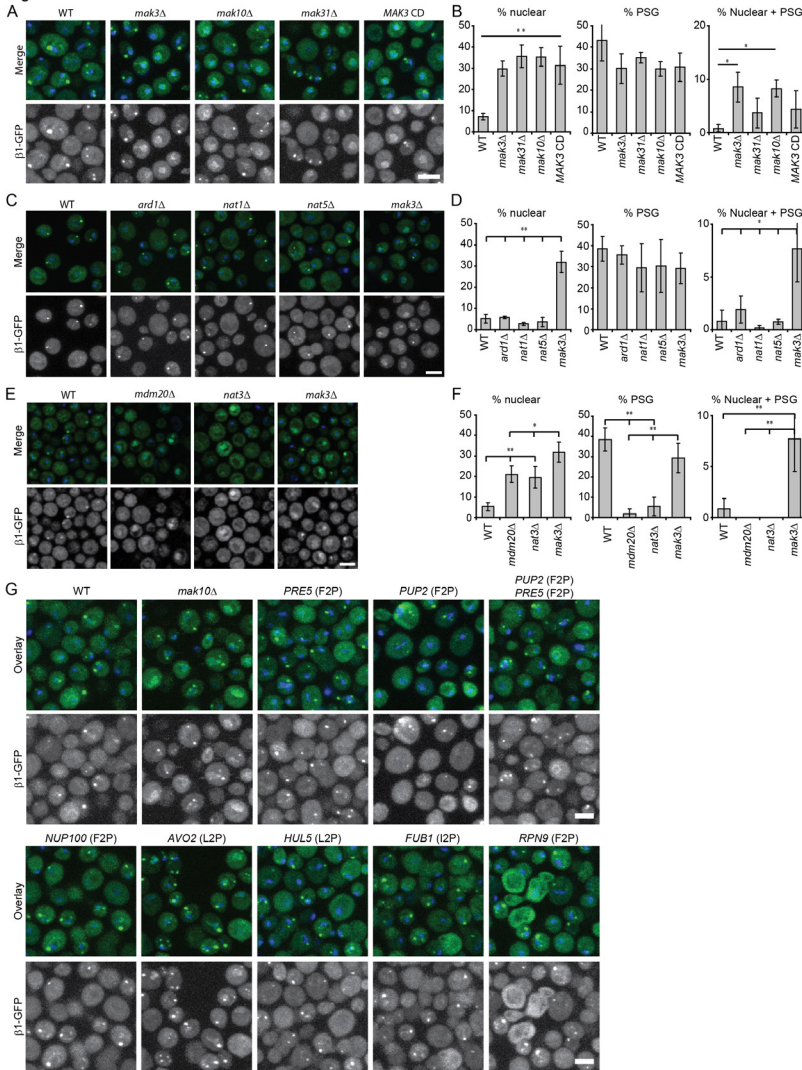
Fig S4: Loss of the non-catalytic subunits of the different N-acetylation complexes results in the same phenotype as loss of the catalytic subunit and N-acetylation status of defined proteins did not affect the localization of the proteasome in starved cells

(A) Loss of NatC activity by knockout of one of its subunits (Mak3, Mak10 and Mak31) or exchange for a catalytic inactive Mak3 leads to an altered proteasome localization after a five day starvation period. (B) Cells showing nuclear retention, PSGs or a combination of both were scored in three independent experiments. Approximately 200 cells were scored in two independent samples per condition. Significance was calculated with a non-paired, two-tailed t-test (* = $p < 0.05$, ** = $p < 0.01$). (C) Loss of any single NatA subunit (Nat1, Nat5 and Ard1) does not lead to different proteasome localization after a five day starvation period. (D) Quantification as in (B). (E) Loss of any single NatB subunit (Nat3 and Mdm20) alters proteasome localization after a five day starvation period. (F) Quantification as in (B). (G) Several predicted NatC substrate proteins were N-terminally mutated to test whether their N-acetylation status was important for proteasome localization in starvation. An X2P mutation was made of α6 (Pre5), α5 (Pup2), Nup100, Avo2, Hul5, FUB1 and RPN9 and these strains were subjected to a five day starvation period. All X2P mutants showed a proteasome localization similar to the WT and can thus be excluded as a NatC substrate influencing proteasome localization. (Scale bars, 5 μm)

Supplementary Table 1:

List of used strains:

Strain:	Genotype:
NKI4103*	MAT@ can1d::STE2pr-Sp_his5 lyp1d his3d1 leu2d0 ura3d0 met15d0 LYS2+ pre3::PRE3-V5-loxP-HA-yEGFP-HYG-loxP-T7-mRFP lyp1d::NATMX-GPD_CRE_EBD78
NKI5537	NKI4103 + mak3Δ::URA3
NKI5538	NKI4103 + mak31Δ::LEU2
NKI5539	NKI4103 + mak10Δ::KanMX4
NKI5540	NKI4103 + nat3Δ::URA3
NKI5541	NKI4103 + mdm20Δ::URA3
NKI5542	NKI4103 + ard1Δ::URA3
NKI5543	NKI4103 + nat1Δ::URA3
NKI5544	NKI4103 + nat5Δ::URA3
NKI5545	NKI4103 + mak3Δ::KanMX4, nat3Δ::URA3
NKI5546	NKI4103 + mak3::MAK3(N123A,Y130A)
NKI4101*	MAT@ can1d::STE2pr-Sp_his5 lyp1d his3d1 leu2d0 ura3d0 met15d0 LYS2+ pre3::PRE3-V5-loxP-HA-yEGFP-HYG-loxP-T7-mRFP
NKI5547	NKI4101 + pre5::NatNT2-PCYC1-PRE5(F2P)
NKI5548	NKI4101 + pup2::NatNT2-PCYC1-PUP2 (F2P)
NKI5549	NKI4101 + pre5::NatNT2-PCYC1-PRE5(F2P) pup2::KanMX4-PCYC1-PUP2(F2P)
NKI5550	NKI4101 + nup100::KanMX4-PCYC1-NUP100(F2P)
NKI5551	NKI4101 + avo2::NatNT2-PCYC1-AVO2(L2P)-3xFlag-KanMX4
NKI5552	NKI4101 + hul5::NatNT2-PCYC1-HUL5(L2P)
NKI5553	NKI4101 + fub1::NatNT2-PCYC1-FUB1(I2P)
NKI5554	NKI4101 + rpn9::NatNT2-PCYC1-RPN9(L2P)
NKI4105	MAT@ can1d::STE2pr-Sp_his5 lyp1d his3d1 leu2d0 ura3d0 met15d0 LYS2+ pre8::PRE8-V5-loxP-HA-yEGFP-HYG-loxP-T7-mRFP lyp1d::NATMX-GPD_CRE_EBD78
NKI5555	NKI4105 + ard1Δ::URA3
NKI5556	NKI4105 + nat3Δ::URA3
NKI5557	NKI4105 + mak3Δ::URA3
NKI4121	MAT@ can1d::STE2pr-Sp_his5 lyp1d his3d1 leu2d0 ura3d0 met15d0 LYS2+ rpn1::RPN1-V5-loxP-HA-yEGFP-HYG-loxP-T7-mRFP lyp1d::NATMX-GPD_CRE_EBD78
NKI5558	NKI4121 + ard1Δ::URA3
NKI5559	NKI4121 + nat3Δ::URA3
NKI5560	NKI4121 + mak3Δ::URA3

* As described in Verzijlbergen *et al* 2009

4

Chapter　Five

Chapter 5:

How is the proteasome degraded?

Sjoerd J. van Deventer[1], Victoria Menendez-Benito[1],
Martje Erkelens[1], Fred van Leeuwen[2], Jacques Neefjes[1]

Manuscript in preparation

5

[1] Division of Cell Biology 2 and
[2] Division of Gene Regulation,
Netherlands Cancer Institute, Amsterdam, The Netherlands

Abstract

To maintain cellular fitness and functionality throughout its lifetime, a cell needs to maintain the quality of its proteins. Cells therefore employ the ubiquitin-proteasome system (UPS) to specifically degrade damaged proteins. Still, protein damage tends to accumulate during cellular aging and is implicated in several age-related diseases, which suggests limiting UPS activity. One reason for limiting UPS activity may be that proteasomes get damaged and then become less effective. Therefore, analogous to damaged proteins, one would expect that damaged proteasomes would be specifically cleared from the cell. The scope and mechanism of such a proteasome quality control system, however, remain to be determined. In this Chapter, we present arguments for lysosomal degradation of proteasomes in budding yeast and mammalian HeLa cells. Also, our data is consistent with specificity towards damaged proteasomes, as a quality control system requires. Our observations may thus represent the first sketches of a quality control system for the proteasome. A deeper understanding of such system may yield new insights in aging and the treatment of age-related diseases.

Introduction

To survive as a single cell or to function within a multicellular organism, a cell needs to maintain its fitness and functionality throughout its lifetime. An important aspect thereof is the maintenance of a functional pool of cellular proteins. To keep their proteins in optimal condition, cells continuously synthesize new proteins and repair or degrade damaged proteins. In fact, synthesis, repair and degradation processes keep the pool of cellular proteins in a constant flux. Tight regulation of these processes allows the cell to maintain a functional pool of proteins under a variety of different conditions, like altering nutrient conditions, stress conditions and signaling [1,2]. Despite the cells efforts to maintain protein fitness, damaged proteins do accumulate during the lifetime of a cell. Accumulation of damaged proteins is a hallmark of cellular aging and has been implicated in several age-related diseases [3,4].

To prevent harmful accumulation of damaged proteins, cells have to degrade proteins that cannot be repaired. Degradation of damaged proteins is mediated by two degrading entities; the lysosome and the proteasome [5]. The lysosome is a membrane-enclosed compartment filled with proteases. Proteins to be degraded by this compartment can be targeted by a process called autophagy, of which several types exist. The most common type is macro-autophagy, which involves the formation of a double membrane structure (the autophagosome) around the substrate proteins. The autophagosome subsequently fuses with the lysosome followed by degradation of its content [6]. Another type of autophagy is micro-autophagy, which entails the endocytosis of substrates by the lysosome [7]. Autophagy in general was long considered to be a non-specific bulk degradation process of (damaged) cytoplasmic proteins and organelles [8]. However, increasing specificity and diversity is assigned to this process, such as the specific degradation of ribosomes and mitochondria [8,9].

The other protein degrading entity in cells is the proteasome. The proteasome is a protein complex that can be divided into two sub-complexes; the 20S core particle (20S) and one or two 19S regulatory particles (19S). The 20S and the 19S together form

the active 26S proteasome [10]. The 20S is the degrading part of the proteasome and is formed by the stacking of four protein rings (each containing seven subunits) into a tube-shaped structure. Inside this tube, the catalytic activity is conveyed by two sets of three catalytically active subunits [11]. For substrate proteins to be degraded inside the 20S they need to be unfolded and pushed into the 20S tube, a task mediated by the 19S complex that caps one or both ends of the 20S tube. The 19S complex recognizes proteasome substrates by their poly-ubiquitin tail, which is removed before the substrate is degraded [12]. Poly-ubiquitination of substrate proteins is mediated by an enzymatic cascade of ubiquitin-activating (E1), ubiquitin-conjugating (E2) and ubiquitin-ligating (E3) enzymes. Together, these enzymes form the ubiquitination machinery, which selectively targets (damaged) proteins for degradation by the proteasome [13]. The proteasome and the ubiquitination machinery together form the ubiquitin-proteasome system (UPS). By selective degradation of damaged proteins, the UPS plays an important role in the cell's defense against the accumulation of damaged proteins during its lifetime [14].

The accumulation of damaged proteins during cellular aging suggests that the degrading activity of the cell can become limiting and correlates with the decrease in proteasome activity observed in several aging model organisms [15–18]. Decreasing proteasome activity is suggested to be a causative factor in the aging process [19,20] and enhanced activity of the proteasome is found to correlate with longer longevity in several organisms including humans [21,22]. These observations fuel a growing interest in ways to enhance proteasome activity as a potential treatment for neurodegenerative and other age-related diseases [4]. Finding the causes underlying this age-related decrease in proteasome activity, may provide new modalities of treatment for age-related diseases.

Several factors are proposed to play a role in the age-related decrease of proteasome activity, including decreased proteasome levels, altered proteasome conformation or decreased efficiency of proteasomes. Decreasing proteasome levels are observed in several model organisms, often deduced from lower expression of proteasome subunits [15,17]. The reason for this counterintuitive decrease in expression levels is unclear. Conformational changes in proteasomes during aging are observed in *Drosophila* and budding yeast, which show an age-dependent decline in 26S proteasomes in favor of the less active 20S forms [18,23]. In human lymphocytes on the other hand, levels and conformation of the proteasome are stable during aging and still they show a decreasing proteasome activity. This decreasing activity correlates with an increasing number of post-translational modifications of the proteasomes (glycation and conjugation with lipid peroxidation products), suggesting that these modifications damage the proteasome and make it less efficient [24]. A model in which damage to the proteasome compromises its efficiency is also consistent with several *in vitro* and *in vivo* studies showing decreased proteasome activity upon treatment with oxidizing agents like nitric oxide [15,25]. Although none of these studies shows the actual oxidative damage to the proteasome, it is likely that proteasomes obtain oxidative damage during their lifetime, given their long half-life [26–28] and the increased oxidative stress in aging cells as a result of malfunctioning mitochondria [29]. Another reason for age-dependent decreasing efficiency of the proteasome may be that they may get 'clogged' by certain substrates [15].

To prevent the accumulation of less functional proteasomes, cells are expected to employ a 'proteasome quality control system'. The action of such a quality control system would be of particular importance for long-lived non-dividing cells, like neurons. This type of cells cannot simply 'dilute' their malfunctioning proteasomes by cell division and since

5

they are long-lived they will need exquisite proteasome activity to maintain proteome fitness during their entire lifetime. The relevance of optimal proteasome activity in these cells is highlighted by the accumulation of damaged proteins in many neurodegenerative disorders [3]. Elucidation of the mechanism involved in proteasome quality control may therefore yield important insights in the pathology of neurodegenerative and other age-related diseases.

Two issues should be considered for proteasome quality control; recognition of damaged proteasomes and a degradation mechanism. Nothing is known about the first, though there are hints for mechanisms involved in the latter. The first evidence for *in vivo* degradation of proteasomes came from pulse-chase experiments in HeLa cells with tritium labeled leucine. In this study a half-life of 5-6 days was found for the 19S 'prosome', which was later identified as the 20S core particle [26,30]. Pulse-chase experiments in adult rats yielded half-lifes ranging from 4 to 15 days for the 20S particle in the liver and 8 days for the 20S particle in rat brain [27,28,31]. These pulse-chase experiments show that the 20S proteasome is remarkably stable in both dividing (HeLa) and non-dividing (rat brain and liver) cells, but do not provide mechanistic insights.

The first mechanistic insights came from a study with isolated lysosomes from the liver of adult rats. Incubation of purified proteasomes with broken rat lysosomes at pH 5 at 37°C showed that proteasomes can be degraded under lysosomal conditions. Furthermore, proteasomes were detected in lysosomes isolated from starved and/or leupeptin treated rats, whereas they could not be detected in lysosomes of normally fed rats [28]. This suggests that proteasomes can be degraded by lysosomes *in vivo* and the correlation with starvation may suggest that autophagy plays a role in the delivery of the proteasome to the lysosome. Proteasome delivery to the lysosome was shown in an *in vitro* model for micro-autophagy, which may be indicative for the involvement of micro-autophagy *in vivo* [28].

In this Chapter, we extend the above findings to model systems more suitable for in-depth analysis of the mechanisms underlying proteasome degradation; budding yeast and HeLa cells. In both model systems we find indications for lysosomal degradation of the proteasome and our findings in HeLa cells are consistent with autophagic delivery of damaged proteasomes to the lysosome. Our findings may thus provide the first sketches of a proteasome quality control system.

Results

Proteasomes can be detected in yeast vacuoles, but degradation cannot be detected by RITE

To study degradation of proteasomes in budding yeast, the catalytically active β1 subunit (Pre3) of the proteasome was tagged endogenously with a GFP tag. β1-GFP is efficiently and quantitatively incorporated in functional 20S core particles [32]. A potential role of the vacuole, the yeast homologue of the lysosome, is best studied in starved yeast cells as they have one big central vacuole. Electron microscopy after a five-day starvation showed immunogold labeling of GFP in the vacuolar compartment (Fig1A). GFP was found both in the vacuolar lumen and in membrane-enclosed structures that may resemble the final stages of autophagosomes. Analogous to the findings in rat livers, this suggests a role for the vacuole in the degradation of the proteasome and a possible role for autophagy.

To further study the potential factors involved in proteasome degradation, the β1 subunit
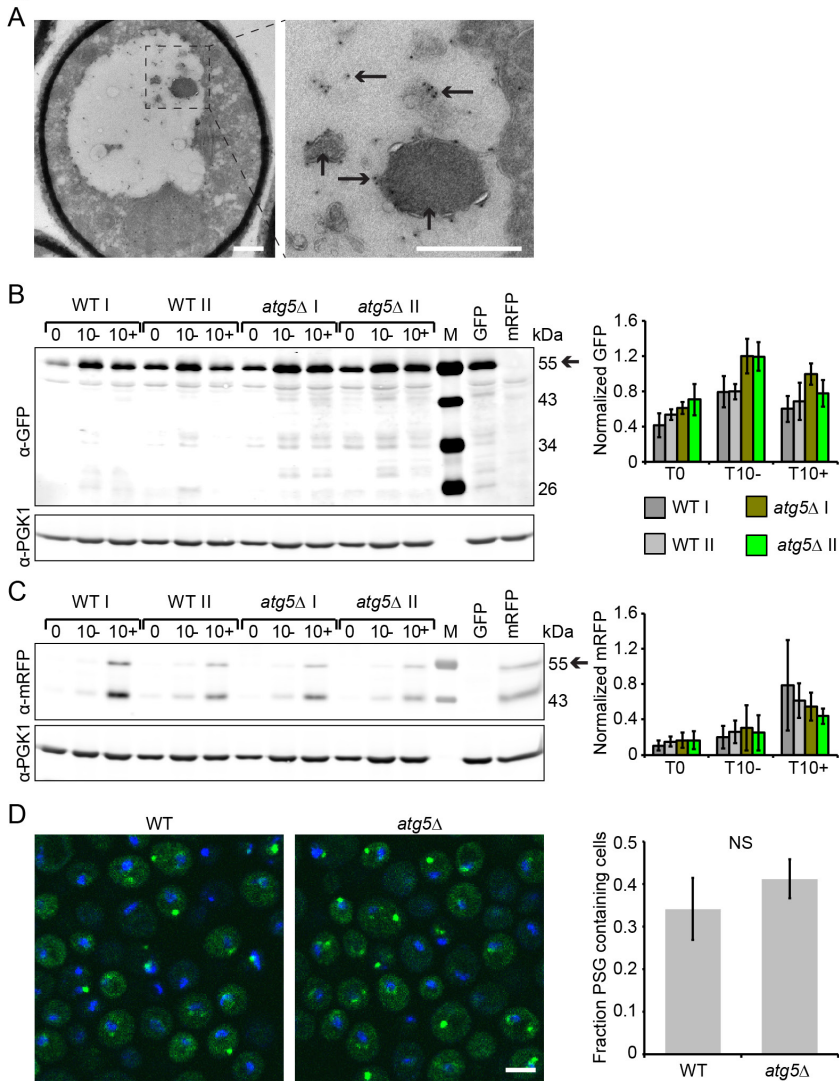
Figure 1

Figure1: Proteasomes can be detected in yeast vacuoles, but degradation cannot be detected by RITE
A) Immunolocalization of yeast 20S proteasomes by EM in starved yeast cells expressing β1-GFP. Samples were stained with a primary antibody against GFP and a secondary antibody coupled to 10-nm gold particles. Examples of gold particles are highlighted with a horizontal arrow. Potential remainders of autophagosomes are highlighted with a vertical arrow. Scale bar: 500 nm. B) Detection of old proteasomes (β1-GFP, ~55 kDa) in total lysates of two WT and two autophagy-deficient (*atg5Δ*) yeast strains expressing β1-RITE. Samples were taken after 2 days in starvation (T0), when the recombination was induced and 10 days later in both non-recombined (T10-) and recombined (T10+) cultures. Full length β1-GFP is indicated with an arrow and the housekeeping enzyme Pgk1 was used as a loading control. Values and standard deviations of the quantification are based on a biological triplicate and normalized to a strain expressing β1-GFP. C) The same samples used for B) were also probed and quantified for new proteasomes (β1-mRFP, ~55 kDa and a degradation band at ~43 kDa). D) Single plane confocal images of 5 day starved β1-GFP expressing WT and autophagy-deficient cells. Hoechst was used as nuclear counter staining. Scale bar: 5 μm. The prevalence of cells containing PSG is quantified by cell counting. Values and standard deviations are based on a biological triplicate.

of the yeast proteasome was endogenously tagged with a fluorescent Recombination-Induced Tag Exchange (RITE) cassette. The RITE cassette behind the β1 gene results in a fusion protein, which initially expresses as β1-GFP. However, an irreversible hormone-induced DNA recombination event results in expression of β1-mRFP. This system defines an old population of proteasomes, produced before the recombination event (green), and a new population produced after the recombination event (red) [33]. Degradation of the proteasome can now be detected by a decrease in the old (GFP-tagged) population of proteasomes (like in a classical pulse-chase), whereas synthesis of proteasomes can be addressed by an increasing level of new (mRFP-tagged) proteasomes.

Since cell divisions will cause a decrease in the old protein population by dilution, degradation of the old proteasome pool can best be detected in conditions with little or no proliferation. These conditions can be met by growing a liquid yeast culture until the carbon source gets depleted and cells enter a starvation induced quiescent state [34]. In our experiments, the recombination of the RITE cassette was induced after a two day growth of a liquid culture, when cell division has almost ceased (Fig S1). At this time point ~5% of the cells had already undergone (non-induced) recombination, whereas adding the hormone β-estradiol in these conditions resulted in recombination in ~90% of the cells (Fig S1).

To assess a role for autophagy in proteasome degradation, the proteasome was RITE tagged in two WT and two autophagy-deficient (atg5Δ) yeast strains. Yeast strains lacking Atg5, are deficient for macro-autophagy and hampered in micro-autophagy [7]. After a two day starvation of WT and atg5Δ cells, recombination was induced and the cells were kept in this low-dividing state for an additional 10 days to allow them to degrade their proteasomes. A parallel culture without induction of recombination served to assess the changes in overall proteasome levels. Recombination and growth characteristics are not significantly different between both strains, which allows their comparison (Fig S1).

The levels of old (GFP-tagged) proteasome were assessed by the levels of β1-GFP (~55 kDa) in cell lysates made at the time of recombination (T0) and 10 days after that, either with (T10+) or without (T10-) recombination (Fig 1B). The housekeeping enzyme Pgk1 served as a loading control. The β1-GFP levels did not show a decrease between T0 and T10+ for either WT or atg5Δ cells, indicating that there was no detectable proteasome degradation. Neither was fast proteasome degradation detected by the accumulation of free GFP (~25 kDa), as was previously reported for the starvation-induced degradation of ribosomal subunits by autophagy [9,35]. The β1-GFP levels do show that overall proteasome levels were higher for atg5Δ cells in both T0 and T10-, which may suggest that the loss of autophagic activity in these cells was compensated by increased proteasome activity. Also, comparing the β1-GFP levels of T0 with T10- shows that overall proteasome levels increase during the starvation process in both WT and atg5Δ cells. Increasing overall proteasome levels in the population of cells that did not perform the recombination (~10%) may also explain the slight increase in β1-GFP levels observed between T0 and T10+. Detection of β1-mRFP (~55kDa and a degradation band at ~43 kDa) in the same lysates yielded information about the synthesis of new proteasomes during starvation (Fig 1C). As expected, the β1-mRFP levels were low for T0 and T10- and the higher levels in T10+ are consistent with the overall increase in proteasome levels. Overall, we can conclude that RITE technology was not able to detect degradation of the proteasome in this system. This can be due to insufficient sensitivity of this technology or the absence of proteasome degradation in starved yeast cells.

A very slow, or even absent, degradation of the proteasome in starving yeast cells may be caused by the presence of Proteasome Storage Granules (PSGs). These starvation-induced cytoplasmic clusters of proteasomes were found in respectively ~35% of the WT and 40% of the *atg5Δ* cells (Fig 1D) and suggested to be important for proteasome storage under starvation conditions [36]. Our data is consistent with a model in which proteasomes in PSGs are protected from degradation. Given this hypothesis, we decided not to pursue the study of proteasome degradation in starved budding yeast and move on to another model system; mammalian cell lines.

Figure 2
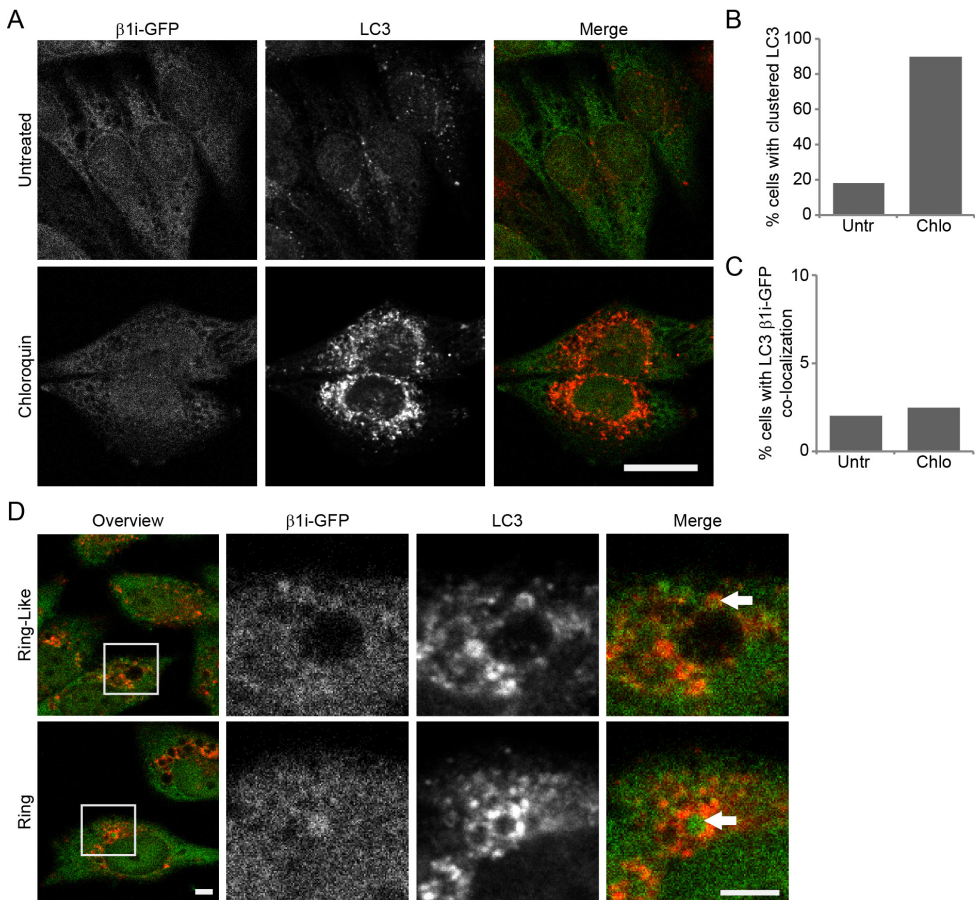
Figure 2: Proteasomes can be detected in autophagosomes in HeLa cells
A) Single plane confocal images of methanol-fixed β1i-GFP overexpressing HeLa cells either treated or non-treated for 16h with chloroquin to inhibit lysosomal degradation. β1i-GFP was visualized by direct fluorescence and immunofluorescent staining was used to visualize LC3, which marks autophagosomal membranes. Scale bar: 10 μm. B) The percentage of cells with a clustered LC3 phenotype was scored in the experiment depicted in panel A. 150 cells were scored per condition. C) The percentage of cells with one or more co-localization events between LC3 and the proteasome was scored in the experiment depicted in A). A co-localization event is defined as proteasome enrichment surrounded (Ring) or partially surrounded (Ring-like) by LC3 staining. 150 cells were scored per condition. D) Representative confocal images of the two types of proteasome-LC3 co-localization found: ring-like and ring. Scale bar: 10 μm.

Proteasomes are substrates of autophagosomes in HeLa cells

To visualize proteasomes in HeLa cells, a GFP-tagged β1i (LMP2) (immuno-) proteasome subunit was stably over expressed. β1i-GFP is efficiently and quantitatively incorporated in the 20S core particle and thus a bona fide marker for proteasome localization [37]. If the proteasome is indeed targeted for degradation by autophagy, one would expect to find co-localization with autophagosomal membranes. These membranes can be visualized by immuno-fluorescent staining for LC3 [38], which showed a punctate pattern in untreated HeLa cells (Fig 2A). In these cells, one or two LC3 β1i-GFP co-localization events were observed in ~2% of the cells (Fig 2C). A co-localization event is defined as proteasome enrichment surrounded (Ring) or partially surrounded (Ring-like) by LC3 staining (Fig 2D). Ring and ring-like co-localization may represent different stages in the internalization of proteasomes in the autophagosome. The low incidence of this co-localization can either be caused by a low incidence of proteasome degradation or by the high rate of the autophagic flux. Autophagosomes and their internalized substrates have a relatively short half-life, as they will fuse with lysosomes and thereby get degraded. This short half-life decreases the chance of finding co-localization of autophagosomes and their substrates, but can be prolonged by inhibition of lysosomal degradation. Lysosomal degradation can be inhibited by the addition of chloroquin [39], which neutralizes the lysosomal pH and results in a strong increase in the number and clustering of LC3 positive vesicles (Fig 2A-B). Despite a strong increase in LC3 positive vesicles, the number of cells with LC3 β1i-GFP co-localization increased very modestly from ~2% under untreated conditions to ~3% after a 16h treatment with chloroquin (Fig 2C). This modest increase suggests that the uptake of the proteasome by autophagosomes is a process with a low flux under normal conditions.

Proteasome uptake by autophagosomes is induced by covalent proteasome inhibitors

If the observed uptake of proteasomes in autophagosomes is part of a quality control system, one would expect that damage to the proteasome would increase the flux of this process. To damage proteasomes, cells were treated with the covalent proteasome inhibitor MV151, which targets an active site of proteasomes and has a fluorescent group [40]. HeLa cells overexpressing β1i-GFP were treated with MV151 for 2h and proteasome localization was observed 16h after thoroughly washing the cells. Treatment with MV151 alone resulted in a modest increase in LC3 β1i-GFP co-localization, though an additional 16h treatment with chloroquin resulted in a strong increase (Fig 3AC). This suggests an increased autophagic flux of the proteasome upon inhibition with MV151. Other covalent proteasome inhibitors, like epoxomycine and lactacystin had a similar effect (data not shown). Unlike these inhibitors, MV151 has a fluorescent group, which allows visualization of the inhibited proteasome. The presence of MV151 within the ring or ring-like LC3 staining showed the internalization of mature inhibited proteasomes (Fig 3B). However, since MV151 signal co-localized with β1i-GFP throughout the cell we cannot tell whether this internalization is specific (excluding not inhibited proteasomes). The overall co-localization of MV151 with β1i-GFP, suggests that the (partial) proteasome inhibition by MV151 not necessarily renders the proteasome useless for the cell. Still our data suggests an increased autophagic flux of the proteasome following covalent inhibition.

Fig 3
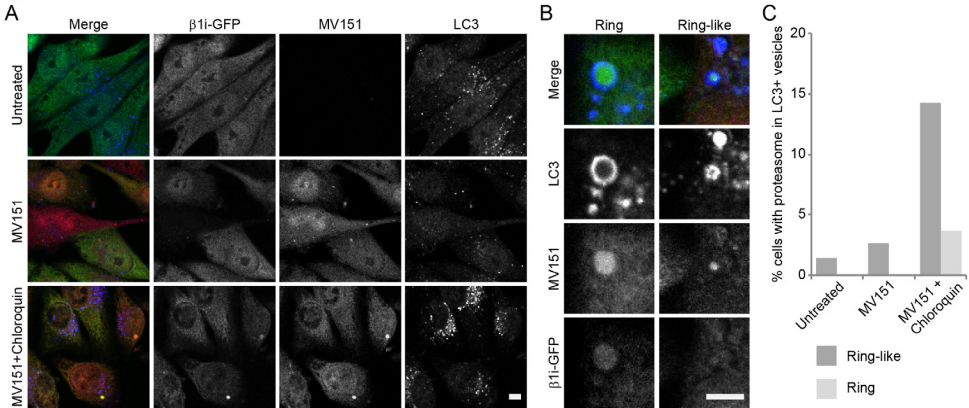
Figure 3: Proteasome uptake by autophagosomes is induced by covalent proteasome inhibition
A) Single plane confocal images of formaldehyde-fixed β1i-GFP overexpressing HeLa cells 16h after a 2h treatment with the covalent and fluorescent proteasome inhibitor MV151. β1i-GFP and MV151 are visualized by direct fluorescence and LC3 by immunofluorescent staining. Chloroquin was added to inhibit lysosomal degradation. Scale bar: 10 μm. B) Single plane confocal images of ring-like and ring LC3 staining around the proteasome. Scale bar: 10 μm. C) Prevalence of cells showing ring and rind-like LC3 staining around the proteasome 16h after the MV151 pulse of the experiment shown in A). Values are based on ~150 cells per condition.

Inhibited proteasomes are degraded

The data presented above suggests that the degradation of the proteasome can be enhanced by its covalent inhibition. To test whether inhibited proteasomes are degraded, HeLa cells were pulsed with the covalent and fluorescent proteasome inhibitor MV151 for 2h and chased for three days. Proteasome subunits bound to MV151 are visualized in total lysates by fluorescent scan of a SDS-PAGE gel (Fig 4A). Tubulin staining after protein transfer to a nitrocellulose membrane shows the increasing number of cells during the assay (Fig 4A). The decrease of proteasome-associated MV151 signal in cell lysates, as determined by fluorescent gel scan, showed that inhibited proteasomes are indeed degraded (Fig 4A,B). Whether this degradation is enhanced by (and thus selective for)

5
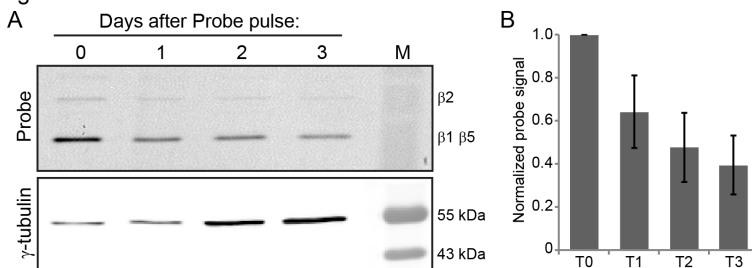
Figure 4

Figure 4: Inhibited proteasomes are degraded
A) Fluorescent gel scan of a pulse-chase experiment with the covalent and fluorescent proteasome inhibitor MV151 in HeLa cells. Cells were pulsed for 2h with MV151, washed extensively and chased for three days. Proteasome subunits bound to MV151 are visualized in total lysates by fluorescent scan of a SDS-PAGE gel. Tubulin staining after protein transfer to a nitrocellulose membrane shows the increasing number of cells during the assay. B) Quantification of four independent experiments. Values were normalized to T0 and standard deviations were calculated.

covalent inhibition cannot be concluded since the turnover of un-inhibited proteasomes was not addressed in this experiment. However, the observed decrease in proteasome-associated MV151 signal suggests a half-life of ~2 days, which is shorter than the reported half-life of ~5 days of non-inhibited proteasomes in HeLa cells [26].

Conclusions and Discussion

To maintain sufficient proteasome activity throughout their lifespan, cells are expected to employ quality control mechanisms on the proteasome. Insufficient activity of such mechanisms could result in a pool of damaged proteasomes and may lead to an (age-dependent) decrease in proteasome activity and (harmful) accumulation of damaged proteins. Unraveling the mechanisms underlying proteasome quality control may therefore yield valuable new insights in the process of aging and the onset of age-related diseases like Alzheimer's disease.

An important aspect of proteasome quality control would be the specific degradation of damaged proteasomes. In this study we detected proteasomes in the vacuole of starving budding yeast and in LC3-coated vesicles in HeLa cells. This suggests degradation of the proteasome by the autophagy-lysosome system in these model systems as was also suggested for proteasomes in rat livers [28]. Degradation of another macromolecular complex, the ribosome, has been shown to be mediated by a specific form of macro-autophagy [9]. Whether this is also true for degradation of proteasomes remains unclear, since LC3-containing vesicles are implicated in both macro-autophagy and in several forms of micro-autophagy [7]. Possibly, both types of autophagy are involved like for peroxisomes and mitochondria [8].

For proteasome degradation to be part of quality control it needs to be specific for damaged proteasomes. The observation that only few LC3-containing vesicles contain proteasomes, may suggest specific targeting of proteasomes by autophagy instead of being a bycatch of other (non-specific) autophagic events. Specificity for damaged proteasomes is consistent with the increased internalization of proteasomes upon their covalent inhibition. Pulse-chase experiments with MV151 clearly showed the degradation of inhibited proteasomes. Although the half-life of these proteasomes is lower than has been reported for untreated proteasomes, we cannot claim that this means specificity as we did not study the latter.

Specific degradation of damaged proteasomes implies that the cell can recognize them. This can be mediated by post-translational modifications (PTMs) or associated proteins that mark damaged proteasomes for degradation. A myriad of different PTMs and associated proteins have been assigned to the proteasome [41,42], though as a rule it is unclear whether their presence is damage induced. Age-related PTMs of proteasomes (glycation and conjugation with lipid peroxidation products) are reported in human lymphocytes, though it is unclear whether they signal damage [24]. A more direct link between proteasome damage and PTMs on the proteasome has been reported by Besche *et al*. They reported that *in vivo* and *in vitro* treatment with various proteasome inhibitors leads to selective poly-ubiquitination of a ubiquitin receptor of the 19S (Rpn13) by the proteasome-associated ubiquitin ligase Ube3c/Hul5. Poly-ubiquitination of Rpn13 strongly inhibits the degradation of proteasome substrates, supposedly by occupying the ubiquitin binding sites of the 19S proteasome [43]. The authors suggest that this mechanism evolved to prevent binding of ubiquitinated proteins to (temporarily) impaired proteasomes, but it

may also serve as a mark for the degradation of these impaired proteasomes. Although this is an interesting possibility, the exact signal for degradation of damaged proteasomes remains to be identified.

In this Chapter we present the RITE tool, which seems fit for further study of this degradation signal. In-depth mass spectrometry analysis of old and new proteasomes isolated from dividing yeast cells is likely to yield proteasome modifications that are dependent on the 'age' of the proteasome. These age-dependent modifications are potential degradation signals, but may also give indications for the proteasome damage that induces these signals. Although we recognize the potential of this approach, we considered it outside the scope of this study.

In summary, we can conclude that our data in budding yeast and HeLa cells is consistent with a model of (damaged) proteasome degradation by autophagy and the lysosome. Our data adds two new model systems to the proteasome degradation research and could represent the first sketches of a proteasome quality control system.

Materials and Methods

Yeast strains and growth conditions

The *Saccharomyces cerevisiae* strains used in this study were NKI4103 [33] and an *atg5Δ* derivative of this strain. The atg5 gene knockout was made by PCR-mediated gene disruption based on pRS plasmids [44]. Yeast cells were grown at 30°C in 5 ml liquid YEPD cultures. Unwanted recombination of the RITE cassette was prevented by the addition of Hygromycin B (200 µg/ml, Invitrogen). Liquid cultures were starved by inoculating 5 ml of YEPD with 0.5 ml of an overnight culture followed by 12 days of incubation without medium refreshment. Recombination of the RITE cassette was induced after 2 days of starvation as described by Verzijlbergen *et al* [33].

5

Cell culture and treatments

β1i-GFP overexpressing HeLa cells [37] were cultured in DMEM (Invitrogen) supplemented with 10% FCS and 250 µg/ml Neomycin (BioConnect) under standard culturing conditions. Cells were treated with 50 µM chloroquin (Sigma) to inhibit lysosomal degradation and 100 nM MV151 to inhibit the proteasome. A pulse-chase experiment with MV151 was performed by a 2h incubation of cells with MV151 followed by three PBS washes and the reseeding of the cells in different wells for each time point.

Immunoelectron microscopy

Yeast cells were washed in PBS, fixed for 2h (2% paraformaldehyde and 0.2% glutaraldehyde in 60 mM PIPES, 25 mM HEPES, 2 mM $MgCl_2$, 10 mM EGTA, pH 6.9) and processed for ultrathin cryosectioning [45]. Before immunolabeling, sample sections were blocked by incubation with 0.15 M glycine in PBS for 10 min, followed by 10 min incubation with 1% BSA in PBS. The blocked sections were then incubated with a polyclonal rabbit anti-GFP antibody [46] and a secondary goat anti-rabbit antibody coupled to 10 nm protein-A conjugated colloidal gold (EMlab, University of Utrecht). The immune-stained sections were embedded in uranylacetate and methylcellulose and examined with a Philips CM 10 electron microscope (FEI Eindhoven, The Netherlands).

Microscopy sample preparation and microscopy

To prepare yeast cells for microscopic imaging they were washed in PBS and fixed in 4% formaldehyde for 5 min. The fixed cells were washed, stained with 1 µg/mL Hoechst 33342 (Invitrogen) for 15 min and washed again. Samples were mounted with Vectashield (VectorLaboratories) onto Con A-coated coverslips. HeLa cells were grown on coverslips and fixed for 2 min in 4% formaldehyde or ice-cold methanol. This methanol treatment was also used to permeabilize formaldehyde fixed cells. Fixed and permeabilized cells were blocked at room temperature in 0,5% BSA (Sigma) in PBS for 30-60 min. Blocked cells were incubated for 60 min with rabbit anti-LC3 (Novus Biologicals) in 0.5% BSA, washed with PBS and subsequently incubated for 30 min with goat anti-rabbit coupled to a 647 nm fluorescent dye (Invitrogen). After a final wash step, samples were mounted in Prolong containing DAPI (Life Technologies). Samples were analyzed using a 63x objective on a Leica SP5 confocal microscope, equipped with LAS-AF software (Leica). Single plane images were made using sequential scanning settings and a 405 nm laser for DAPI and Hoechst, 488 nm for GFP labeled proteins, 561 nm for MV151 and 633 nm for secondary antibodies with a 647 nm dye.

Biochemical analysis

Yeast cell lysates were made of 1×10^8 cells, which were washed in cold TE supplemented with 2 mM PMSF and stored at -80°C before further processing. Lysis was performed as described in Terweij *et al* [47]. Samples were run in a 12% polyacrylamide gel and blotted on a 0.45 µm nitro-cellulose membrane. Membranes were blocked with 4% skim milk powder (Oxoid) in PBS + 0.1% Tween. Primary antibody incubations were performed at RT for 1h in blocking buffer using mouse anti-3-PGK (1:5000, Invitrogen) and rabbit anti-GFP or rabbit anti-mRFP (1:2000; 46). Secondary antibody staining was performed for 45 min at RT using the goat anti-rabbit (700 nm) and the goat anti-mouse (800 nm) LI-COR Odyssey IRDyes (1:10.000; LI-COR). Membranes were scanned with a LI-COR Odyssey IR Imager (Biosciences) and analyzed with the associated software package.

HeLa cells were lysed in 1x sample buffer with 5% β-mercaptoethanol and subsequently sonicated and boiled for 5 min at 96°C. HeLa lysates were separated on gel as described for the yeast cell lysates. A fluorescence scan was made of the gel on a ProXpress fluorescence scanner (Perkin Elmer), using 550/30 nm excitation and 590/35 nm emission. Gels were blotted and blocked as described before and stained with mouse anti-tubulin (1:5000; Sigma) and the goat anti-mouse (700 nm) LI-COR Odyssey IRDye (LI-COR; 1:10.000).

References

1. Hartl, F. U., Bracher, A. & Hayer-Hartl, M. Molecular chaperones in protein folding and proteostasis. Nature 475, 324–32 (2011).

2. Balch, W. E., Morimoto, R. I., Dillin, A. & Kelly, J. W. Adapting proteostasis for disease intervention. Science 319, 916–9 (2008).

3. Vilchez, D., Saez, I. & Dillin, A. The role of protein clearance mechanisms in organismal ageing and age-related diseases. Nat. Commun. 5, 5659 (2014).

4. Schmidt, M. & Finley, D. Regulation of proteasome activity in health and disease. Biochim. Biophys. Acta 1843, 13–25 (2014).

5. Ciechanover, A. Intracellular protein degradation: from a vague idea through the lysosome and the ubiquitin-proteasome system and onto human diseases and drug targeting. Bioorg. Med. Chem. 21, 3400–10 (2013).

6. Feng, Y., He, D., Yao, Z. & Klionsky, D. J. The machinery of macroautophagy. Cell Res. 24, 24–41 (2014).

7. Li, W., Li, J. & Bao, J. Microautophagy: lesser-known self-eating. Cell. Mol. Life Sci. 69, 1125–36 (2012).

8.   Reggiori, F. & Klionsky, D. J. Autophagic processes in yeast: mechanism, machinery and regulation. Genetics 194, 341–61 (2013).

9.   Kraft, C., Deplazes, A., Sohrmann, M. & Peter, M. Mature ribosomes are selectively degraded upon starvation by an autophagy pathway requiring the Ubp3p/Bre5p ubiquitin protease. Nat. Cell Biol. 10, 602–10 (2008).

10. Tomko, R. J. & Hochstrasser, M. Molecular architecture and assembly of the eukaryotic proteasome. Annu. Rev. Biochem. 82, (2013).

11. Chen, P. & Hochstrasser, M. Biogenesis, structure and function of the yeast 20S proteasome. EMBO J. 14, 2620–30 (1995).

12. Liu, C.-W. & Jacobson, A. D. Functions of the 19S complex in proteasomal degradation. Trends Biochem. Sci. 38, 103–10 (2013).

13. Hershko, a & Ciechanover, a. The ubiquitin system for protein degradation. Annu. Rev. Biochem. 61, 761–807 (1992).

14. Glickman, M. H. & Ciechanover, A. The Ubiquitin-Proteasome Proteolytic Pathway : Destruction for the Sake of Construction. Physiol. Rev. 82, 373–428 (2002).

15. Carrard, G., Bulteau, A.-L., Petropoulos, I. & Friguet, B. Impairment of proteasome structure and function in aging. Int. J. Biochem. Cell Biol. 34, 1461–1474 (2002).

16. Dasuri, K. et al. Aging and dietary restriction alter proteasome biogenesis and composition in the brain and liver. Mech. Ageing Dev. 130, 777–83 (2009).

17. Lee, C., Klopp, R. G., Weindruch, R. & Prolla, T. A. Gene Expression Profile of Aging and Its Retardation by Caloric Restriction. Science (80-.). 285, 1390–1393 (1994).

18. Vernace, V. A., Arnaud, L., Schmidt-glenewinkel, T. & Figueiredo-, M. E. Aging perturbs 26S proteasome assembly in Drosophila melanogaster. Faseb J 21, 2672–2682 (2012).

19. Chen, Q., Thorpe, J., Dohmen, J. R., Li, F. & Keller, J. N. Ump1 extends yeast lifespan and enhances viability during oxidative stress: central role for the proteasome? Free Radic. Biol. Med. 40, 120–6 (2006).

20. Kruegel, U. et al. Elevated proteasome capacity extends replicative lifespan in Saccharomyces cerevisiae. PLoS Genet. 7, e1002253 (2011).

21. Chondrogianni, N., Petropoulos, I., Franceschi, C., Friguet, B. & Gonos, E. . Fibroblast cultures from healthy centenarians have an active proteasome. Exp. Gerontol. 35, 721–728 (2000).

22. Aragon, A. D. et al. Characterization of differentiated quiescent and nonquiescent cells in yeast stationary-phase cultures. Mol. Biol. Cell 19, 1271–80 (2008).

23. Bajorek, M., Finley, D. & Glickman, M. H. Proteasome Disassembly and Downregulation Is Correlated with Viability during Stationary Phase. Curr. Biol. 13, 1140–1144 (2003).

24. Carrard, G., Dieu, M., Raes, M., Toussaint, O. & Friguet, B. Impact of ageing on proteasome structure and function in human lymphocytes. Int. J. Biochem. Cell Biol. 35, 728–739 (2003).

25. Glockzin, S. Activation of the Cell Death Program by Nitric Oxide Involves Inhibition of the Proteasome. J. Biol. Chem. 274, 19581–19586 (1999).

26. Hendil, K. B. The 19 S multicatalytic "prosome" proteinase is a constitutive enzyme in HeLa cells. Biochem. Int. 17, 471–478 (1988).

27. Tanaka, K. Half-Life of Proteasomes (Multiprotease Complexes) in Rat Liver '. Biochem. Biophys. Res. Commun. 159, 1309–1315 (1989).

28. Cuervo, M., Palmer, A., Rivett, J. & Knecht, E. Degradation of proteasomes by lysosomes in rat liver. Eur. J. Biochem. 227, 792–800 (1995).

29. Balaban, R. S., Nemoto, S. & Finkel, T. Mitochondria, oxidants, and aging. Cell 120, 483–95 (2005).

30. Arrigo, A. ., Tanake, K., Goldberg, A. L. & Welch, W. J. Identity of the 19S "prosome" particle with the large multifunctional protease complex of mammalian cells (the proteasome). Nature 331, 192–194 (1988).

31. Price, J. C., Guan, S., Burlingame, A., Prusiner, S. B. & Ghaemmaghami, S. Analysis of proteome dynamics in the mouse brain. PNAS 107, 14508–14513 (2010).

32. Van Deventer, S. J., Menendez-Benito, V., van Leeuwen, F. & Neefjes, J. N-Terminal Acetylation And Replicative Age Affect Proteasome Localization And Cell Fitness During Aging. J. Cell Sci. (2014).

33. Verzijlbergen, K. F. et al. Recombination-induced tag exchange to track old and new proteins. PNAS 107, 64–68 (2010).

34. Gray, J. V et al. Sleeping Beauty : Quiescence in Saccharomyces cerevisiae. Microbiol. Mol. Biol. Rev. 68, 188–202 (2004).

35. Cheong, H. et al. Atg17 Regulates the Magnitude of the Autophagic Response. Mol. Biol. Cell 16, 3438–3453 (2005).

36. Laporte, D., Salin, B., Daignan-Fornier, B. & Sagot, I. Reversible cytoplasmic localization of the proteasome in quiescent yeast cells. J. Cell Biol. 181, 737–45 (2008).

37. Reits, E., Benham, M., Plougastel, B., Neefjes, J. & Trowsdale, J. Dynamics of proteasome distribution in living cells. EMBO J. 16, 6087–94 (1997).

38. Klionsky, D. J., Cuervo, A. M. & Seglen, P. O. Methods for Monitoring Autophagy from Yeast to Human. Autophagy 3, 181–206 (2007).

39. Seglen, P. O., Grinde, B. & Solheim, a E. Inhibition of the lysosomal pathway of protein degradation in isolated rat hepatocytes by ammonia, methylamine, chloroquine and leupeptin. Eur. J. Biochem. 95, 215–225 (1979).

40. Verdoes, M. et al. A fluorescent broad-spectrum

proteasome inhibitor for labeling proteasomes *in vitro* and *in vivo*. Chem. Biol. 13, 1217–26 (2006).

41. Leggett, D. S. *et al*. Proteasome Structure and Function. Mol. Cell 10, 495–507 (2002).

42. Wang, X. *et al*. Mass Spectrometric Characterization of the Affinity-Purified Human 26S Proteasome Complex. Biochemistry 46, 3553–3565 (2007).

43. Besche, H. C. *et al*. Autoubiquitination of the 26S Proteasome on Rpn13 Regulates Breakdown of Ubiquitin Conjugates. EMBO J. 33, 1159–1176 (2014).

44. Brachmann, C. B. *et al*. Designer deletion strains derived from *Saccharomyces cerevisiae* S288C: A useful set of strains and plasmids for PCR-me-diated gene disruption and other applications. Yeast 14, 115–132 (1998).

45. Calafat, B. J. *et al*. Human Monocytes and Neutrophils Store Transforming Growth Factor-a in a Subpopulation of Cytoplasmic Granules. Blood 90, 1255–1267 (1997).

46. Rocha, N. *et al*. Cholesterol sensor ORP1L contacts the ER protein VAP to control Rab7-RILP-p150 Glued and late endosome positioning. J. Cell Biol. 185, 1209–25 (2009).

47. Terweij, M. *et al*. Recombination-induced tag exchange (RITE) cassette series to monitor protein dynamics in *Saccharomyces cerevisiae*. G3 3, 1261–72 (2013).

Supplemental Figures:

Figure S1
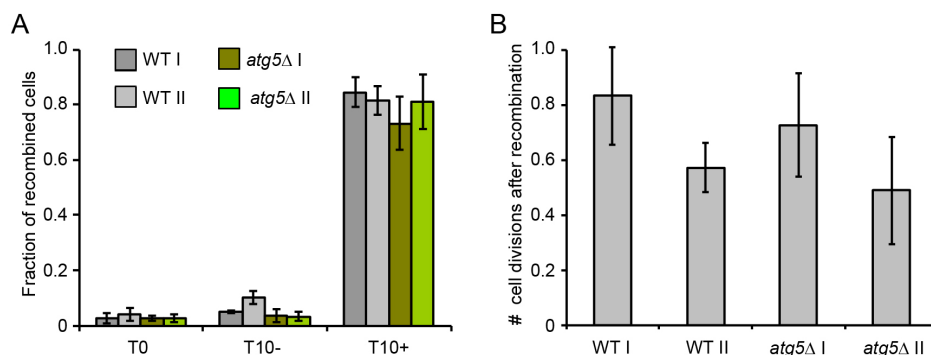
Figure S1: WT and autophagy-deficient cells have similar recombination and growth characteristics
A) Fraction of cells with a recombined RITE cassette as determined by plating assay [33]. Limited non-induced recombination can be observed before recombination is induced (T0) and ten days after that without recombination (T10-). Hormone-induced recombination can be observed ten days after the recombination event (T10+). Non-induced and hormone-induced recombination is not significantly different for WT and autophagy-deficient cells. Values and standard deviations are based on a biological triplicate. B) The number of cell divisions between the time of the recombination (T0) and the end of the experiment (T10) was assessed by FACS-based cell counting. No significant differences were observed between WT and autophagy-deficient cells. Values and standard deviations are based on a biological triplicate.

5

Chapter Six

Chapter 6:

Conclusions and Discussion

6

Conclusions and Discussion

When proteins would have been static entities, instead of the highly dynamic entities they are, life would never have evolved. It is the complex interplay of protein synthesis, repair, degradation, modification, movement and interactions that makes a cell a living entity instead of a bag full of proteins. The ability to monitor these protein dynamics is therefore crucial for the discovery of the cellular processes underlying life.

The RITE tool to monitor protein dynamics

To study cellular processes, monitoring the dynamics of the total pool of a protein is informative. However, more detailed information can often be obtained by monitoring specific sub-populations within the total pool. A decrease in the overall level of a protein, for example, may be caused by enhanced degradation or decreased synthesis. These possibilities can be distinguished when one can track the dynamics of a sub-population of this protein, e.g. by labeling a defined population with radioactive labeled amino acids as one does in a pulse-chase assay. Sub-populations may also be defined by functional differences. The overall levels of a kinase, for example, may not change upon a certain stimulus, whereas the sub-population of phosphorylated (and thus activated) kinases may. Antibodies specific for the (un) phosphorylated form are therefore of great additive value to study the dynamics of kinases.

To distinguish sub-populations of proteins based on their age (synthesized long ago versus recently), we developed a technique that we named Recombination-Induced Tag Exchange (RITE) [1,2]. RITE allows the distinction and simultaneous tracking of old and new proteins and has been successfully used to address the exchange of histones in chromatin [1], inheritance of histones and plasma-membrane proteins [3,4], synthesis and inheritance of organelles and macromolecular complexes [5], and the origin of nuclear proteasomes [6]. Here we discuss the strong and weak points of this technique as encountered in this Thesis as well as some future perspectives.

A strong point of the RITE technique is that it allows tracking of old and new proteins simultaneously. Amongst others, this capability enabled us to distinguish *de novo* and template-based synthesis of peroxisomes and nuclear enrichment of proteasomes due to localized synthesis or retention of existing proteasomes [5,6]. Whereas these studies relied on fluorescent tags, a series of different RITE cassettes and the modular design of these cassettes allows easy adjustment of the tags to the experimental needs [2]. In Chapter 2, for example, epitope tags are used for immunodetection and purification of old and new histones [1]. Old and new proteins may also be distinguished by using tags with a different size. This allows simultaneous Western-blot detection with a single antibody (e.g. against LoxP or the tagged protein), which enables quantitative comparison of the levels of old and new proteins [2]. Adequate detection of old and new proteins in this Thesis is supported by a high recombination efficiency of the RITE cassette upon induction and low levels of non-induced background recombination. Application of RITE in these studies is further strengthened by the endogenous expression of the tagged proteins and the lack of a non-tagged (WT) protein pool. The genomic integration of the RITE cassette and the efficient and irreversible recombination make RITE suitable for many downstream applications including high-throughput screening. This was successfully exploited in a microscopy-based screening for factors involved in proteasome dynamics and a CHIP-Seq based screening for factors modulating histone turnover in the chromatin [6,7].

A limitation of RITE is the time needed to complete recombination in the total population of cells, which is ~2 h under both nutrient-rich and starvation conditions [1,2]. This makes RITE less suitable to track fast protein dynamics, since synthesis of RITE tagged proteins during this time period will yield proteins with both new and old tags. In this Thesis we minimized this problem by inducing the recombination in nutrient-starved cells, which show only limited transcription and translation [8]. In this system the old protein pool is mainly produced before nutrient starvation and a pool of new proteins is emerging slowly after recombination when starvation is prolonged. On the other hand, a strong increase in new proteins can be observed when releasing cells in nutrient rich medium, which quickly induces new transcription and translation. Recombination under starved conditions and release in fresh medium not only expands the 'age-gap' between old and new proteins, but also results in a more or less synchronized first cell division. This principle was used in Chapter 3 to study the inheritance of organelles and macromolecular complexes.

Whereas RITE was successfully used in Chapter 3 and 4 to address the localization and synthesis of old and new proteins, it was unable to detect degradation of old proteasomes in Chapter 5. This may be due to a very high stability of the proteasome and/or insufficient sensitivity of the RITE technique. The sensitivity of RITE is probably higher for synthesis then for degradation, as synthesis adds new signal to a small population and degradation removes signal from a big population. Still, there is no reason to suspect that RITE cannot be used to address the degradation of other (less stable) proteins. In fact, RITE has been successfully used to detect the disappearance of old histones from the chromatin in growth arrested yeast cells [1,7].

All in all, we can conclude that RITE is a valuable tool to distinguish and simultaneously track old and new proteins with a variety of different read-outs under a variety of different conditions. Especially its compatibility with screening methods makes it an interesting tool to further study factors involved in the dynamics of specific proteins, protein complexes and organelles. In this Thesis, we present applications of RITE in budding yeast only. However, the universal nature of the RITE cassettes and the available Cre-recombinases for other organisms make RITE in principle applicable to a broad range of model systems. The emergence of techniques to tag proteins endogenously in higher eukaryotes will even further increase the potential of RITE in these model systems [9].

6

Organelle dynamics upon cell division
In Chapter 3 we applied RITE to make a comprehensive analysis of the synthesis and inheritance of organelles and macromolecular complexes upon cell division. The inheritance of old and new components of these structures can be addressed by RITE and may be important to define lineage differences. Furthermore, RITE can address the biogenesis of these structures, as it is able to distinguish *de novo* and template-based synthesis. Here we discuss the general conclusions from this analysis and some organelle specific issues.

Our comprehensive analysis shows that, in general, old and new components of organelles and macromolecular complexes are symmetrically inherited upon cell division [5]. Apparently the age of these components does not play a role in asymmetric inheritance or lineage differences. This suggestion is supported by the observed mixing of old and new components in all tested organelles and the nucleolus [5]. The mixing of old and new components of mitochondria, in particular, illustrates this notion as yeast cells do show asymmetrical inheritance and lineage differences based on the functionality of this

organelle [10,11]. An interesting exception to the generally observed mixing of old and new components is the nuclear pore complex (NPC). Since the NPC is formed *de novo* and is very stable, the age of its components reflects the age of the entire complex and may thus influence its functionality and inheritance [12]. Still we find symmetrical inheritance of old and new NPCs, suggesting that the age of the complex is unconnected to its inheritance. Symmetrical NPC inheritance also resolves ongoing debates about whether or not daughter cells obtain their nuclear pores by synthesis and inheritance or by *de novo* synthesis only [13,14]. Our data based on two RITE tagged subunits of the nuclear pore strongly support the first model and was later strengthened by similar observations for three other subunits [15]. All in all we can conclude that symmetrical inheritance of old and new components of organelles and macromolecular complexes is a common rule in budding yeast. Whether this is also the case in mammalian cells remains an interesting question.

An interesting exception to this common rule is the spindle pole body (SPB), the yeast centrosome, which shows an unexpected mode of asymmetrical inheritance [5,16]. Based on our data, we propose the following model. Upon cell division, a small portion of this macromolecular complex splits to initiate the duplication process. New components are added to this template to build a new SBP and a similar amount of new components is added to the existing SPB, which is therefore bigger. Interestingly, the bigger SPB (containing the majority of the old components) is inherited by the daughter cell (the younger lineage), whereas the smaller SPB (containing mostly new components) stays in the mother [5]. Apparently the old components of the SPB contain functionalities that are favorable for the daughter cell or the daughter needs a bigger SPB. As a consequence of this inheritance pattern, the SPB in the mother cell will shrink after each cell division. Whether a shrinking SPB is limiting the replicative potential of a mother cell or whether mother cells synthesize new components to compensate for this loss at a later time point is an interesting question for further research.

Another aspect that we addressed in our RITE-based analysis of organelles and macromolecular complexes is whether they are synthesized *de novo* or template-based. Template-based synthesis is known or expected for most membrane containing organelles [17], though is still debated for peroxisomes [18,19]. In our RITE assays, template-based synthesis should result in mixing of old and new components within the same compartment. This was indeed observed in the nucleolus and all membrane containing organelles, including the peroxisome. Our data not only supports a model of template-based synthesis of peroxisomes, but also excludes *de novo* synthesis since no peroxisomes were observed with only new components. In summary, our work suggests that all membrane containing organelles are synthesized in a template-based manner in budding yeast.

The macromolecular complexes in our analysis displayed more variation, since the nucleolus and the SPB showed template-based synthesis and the NPC showed *de novo* synthesis. *De novo* synthesis of NPCs is apparent since old and new NPC components do not co-localize in our assays, although they are present in the same nucleus. Even several divisions after the recombination of the RITE cassette, old components appear to exclude new components indicating that the tagged subunits do not exchange visibly in these very stable complexes. Interestingly, old and new nuclear pores appear to cluster in their own areas on the nuclear envelope. The reason for this phenomenon is unknown, but may be related to the assembly of this complex. The clustering of NPCs and their stability across generations is, unlike their *de novo* synthesis, most likely not conserved in mammalian

cells, since these cells completely disassemble their nuclear envelope and NPCs during cell division [12].

Overall we can conclude that template-based growth and symmetric distribution of old and new components upon cell division are common aspects of organelle and macromolecular complex dynamics. Two important exceptions are the nuclear pore complex, that is formed *de novo*, and the spindle pole body, that showed asymmetric inheritance.

PSGs; storage granules or protein quality control compartments?

In Chapter 4 and 5 we used budding yeast to address novel aspects of proteasome dynamics [6]. A characteristic aspect of this dynamics in yeast is the sequestration of proteasomes in cytoplasmic foci upon glucose depletion (starvation). These foci are stable when starvation is prolonged, though when nutrients are re-added they rapidly dissolve to restore the normal (non-starved) proteasome localization. These observations made the initial discoverers suggest that the main function of these foci is storage of the proteasome, hence they named them Proteasome Storage Granules (PSGs) [20]. However, when the term PSG was coined, another research group reported stress-induced cytoplasmic proteasome foci that they named JUxta-Nuclear Quality control (JUNQ) compartments. JUNQ compartments are induced by protein stress and are suggested to enhance Protein Quality Control (PQC) by sequestering proteasomes and their substrates in the same compartment [21]. The discovery of JUNQ compartments raised the question whether PSGs are indeed storage compartments (as initially suggested) or compartments with high PQC activity (like JUNQ compartments) [22]. Although a definite answer to this question is missing, the data presented in this Thesis strongly favors the storage function of PSGs.

First of all, it is unlikely that JUNQ compartments and PSGs represent the same structure induced under different conditions (protein stress and glucose depletion respectively). One reason is that JUNQ compartments are in close proximity to the nuclear or ER membrane [21], whereas PSGs do not show any membrane association [20] (and our unpublished results). Another reason is that JUNQ compartments show a strictly mother-biased segregation upon cell division [21,23], which is not compatible with the higher prevalence of PSGs in virgin cells that we observed [6]. However, so far there are no reports on the presence of marker proteins (BLM10 for PSG [24] and HSP104 and soluble misfolded proteins for JUNQ compartments [21]) in both structures.

Although it is unlikely that PSGs are JUNQ compartments, they may still represent compartments with high PQC activity. If so, one would expect to find active proteasomes in PSGs. The presence of both 20S and 19S (base and lid) subunits in the same PSGs suggests the presence of (active) 26S proteasomes [20,25]. However, native gel analysis of starved yeast cells yields conflicting data. Whereas Laporte *et al* shows predominantly 26S proteasomes in these cells, Weberuss *et al* convincingly shows PSG-containing cells with predominantly 20S proteasomes [20,24]. Starvation-induced 26S proteasome dissociation was also observed by Bajorek *et al* and suggested to be caused by a drop in ATP levels [26]. On the other hand, a subunit of the 19S lid complex was found to be required for PSG formation, which suggests sequestering of intact 26S proteasomes [27]. Also, proteasome dissociation does not appear to be required for PSG formation [27,28]. These apparently conflicting data may suggest a model in which the dissociation of the 26S and the formation of PSGs are independent processes.

6

Other than discussing proteasome conformation in PSGs, the issue of whether or not proteasomes are active in PSGs may also be addressed by using model substrates. Simply assessing the decreasing levels of these substrates is not informative; since it cannot be excluded that the proteasomes outside the PSGs are responsible for the observed degradation. A rapid exchange of (fluorescent) model substrates between PSGs and its surroundings or ubiquitin dependent recruitment of substrates to the PSGs, may be a better indication of active proteasomes [21].

Two additional observations argue against PSGs as compartments with high PQC activity. First, if the proteasome would be sequestered with high amounts of substrates one would expect their degradation before proteasomes are released from the PSGs. This seems incompatible with the rapid release of proteasomes (within 10 minutes) upon addition of fresh nutrients [20,24] (our unpublished results). A second argument relates to the drop in cellular ATP levels during the starvation process. This could lead to 26S disassembly [26], but may also necessitate the cell to shut down the energy consuming activity of the UPS in favor of less energy consuming processes, like autophagy or the sequestration of damaged proteins by small Heat Shock Proteins [8,29]. It may therefore very well be that PSGs convey PQC activity when cells have sufficient energy, but that this activity ceases rapidly during the starvation process.

Whereas it is not trivial to identify PQC functionalities of PSGs, PSGs show many similarities with known protein storage compartments in budding yeast. Several metabolic enzymes, a histone deacetylase and F-actin are known to form cytoplasmic foci upon the depletion of specific nutrients during yeast starvation [30–33]. Like PSGs, these cytoplasmic foci do not show any association with membranes and rapidly dissolve upon re-addition of nutrients. The formation of these foci, as for PSGs, is suggested to be induced by a drop in cytosolic pH that accompanies starvation due to glucose limitation [25,32]. The storage function of these foci is deduced from their very high stability in starvation and their rapid dissociation when the cell gets re-activated with new nutrients.

As reported for other storage compartments, we found a very high stability of PSGs since their prevalence hardly decreases during a two week starvation period (our unpublished results). Also, RITE experiments presented in Chapter 5 are consistent with a very high stability of the proteasome during starvation. This may suggest that storage in PSGs protects proteasomes from degradation. This hypothesis is also consistent with the positive correlation between PSG prevalence and proteasome abundance in starvation, which was found when studying a yeast knock-out library (our unpublished results).

The term 'storage' entails that the stored proteins are functional once released from their storage compartment. In many studies, including those describing PSGs [20,31,33], the functionality of stored proteins after release is deduced from their re-localization to their original (non-starved) location. Application of the RITE technology provided us with more direct evidence of the functionality of proteasomes after release from PSGs. When recombination of the RITE cassette was induced after two days of starvation, little or no synthesis was detected in the following three days and the old proteasome was sequestered in PSGs. Upon addition of fresh medium, PSGs rapidly dissolve and proteasomes regain their nuclear localization while cells prepare to start a new cell division. New proteasomes were only detected during this first cell division, indicating that the activity of the old (stored) proteasomes was at least sufficient to support this first cell cycle, for which they should be active (our unpublished results).

The data presented in this Thesis shed new light on the question whether PSGs are storage

compartments or PQC compartments. First, the higher prevalence of PSGs in virgin cells, as presented in Chapter 4, argues against being a PQC compartment. Second, application of RITE technology suggests that PSGs are bona fide storage compartments.

A role for proteasome localization and quality control in aging cells?

Accumulation of damaged proteins is a hallmark of cellular aging and implicated in several age-related diseases [34,35]. This suggests that the degradation of damaged proteins gets limiting during cellular aging. Limiting degradation of damaged proteins may (in part) be caused by the age-dependent decline in proteasome activity, as observed in several aging model systems [36–38]. Increasing proteasome activity may solve the limiting degradation during aging and is therefore expected to attenuate cellular aging. The validity of this idea was proven in budding yeast [39,40] and fuelled a growing interest in ways to enhance proteasome activity as potential treatment for neuro-degenerative and other age-related diseases [41]. In this Thesis we addressed novel aspects of proteasome dynamics that may also play a role during cellular aging; proteasome localization and proteasome quality control. Here we discuss their potential role in cellular aging.

In Chapter 4 we report a correlation between the localization of the proteasome and replicative age in starving budding yeast. This observation may indicate a role for proteasome localization in cellular aging. During the starvation process, budding yeast transports its nuclear proteasomes to the cytoplasm and stores them in cytoplasmic PSGs. Whereas this scheme applies to most replicative young cells during starvation, old cells are more likely to maintain their nuclear proteasome pool and not to form PSGs [6]. This may be caused by an age-dependent defect in the proteasome re-localization machinery, but may also reflect a response to the reported accumulation of protein damage in old cells [42,43]. Perhaps damage accumulation requires the maintenance of a larger pool of active proteasomes in old cells, which would be consistent with the low prevalence of PSGs. The nuclear enrichment of the proteasome may help old cells to clear protein damage in the nucleus [44,45], but may also support protein quality control in the cytoplasm [46,47]. The latter is especially important for quality control of (partially) unfolded cytoplasmic proteins, since one of the dominant E3s of this pathway (San1) is localized in the nucleus [46,47]. In summary, the data presented in Chapter 4 are consistent with a model in which the proteasome localization is adapted to the load of protein damage during aging. The exact nature of this damage and possible conservation of the age-related localization of the proteasome in mammalian cells requires further study.

Mammalian cells harbor proteasomes in both the nucleus and the cytosol [48,49], while not showing the nuclear enrichment as observed in budding yeast [50]. Similar to the situation in yeast, nuclear proteasomes in mammalian cells are implicated in nuclear protein quality control [45,51], as well as the degradation of misfolded cytosolic proteins [52]. The conservation of these processes may underlie conservation of age-related proteasome localization. However, proteasome localization in mammalian cells is more difficult to address than in budding yeast. Not only does a substantial population of free 20S proteasomes exist in several mammalian cell lines, there is also a compartment-dependent attachment of different regulatory particles [53,54]. Assessing proteasome localization therefore requires tracking of both the 20S and its regulatory particles. This principle has been illustrated by a study of age-dependent proteasome localization in human liver samples. Whereas the localization of several 20S subunits does not correlate with age, the cytoplasmic levels of the 11S complex (a regulatory particle like the 19S) specifically drop in the cytoplasm and

6

not the nucleus [55]. Another study showed a correlation between the nuclear localization of both 20S and 19S subunits and the neuronal vulnerability for Alzheimer's Disease and Creutzfeld-Jacobs Disease in human brains [56]. These correlations and our data in budding yeast justify a more extensive study on proteasome localization during aging in mammalian cells.

In Chapter 5 we present the first sketches of a potential quality control system for the 20S proteasome. Such a system is likely to play a role in the aging of long-lived non-dividing cells, like neurons, since its limiting activity could lead to a less functional pool of proteasomes. This, in turn, may contribute to the accumulation of damaged proteins that is implicated in cellular aging and several age-related neurodegenerative diseases. The data presented in Chapter 5 is consistent with a model in which damaged proteasomes are degraded by some form of autophagy. The specifics and specificity of this autophagic degradation remain to be established and may yield new insights in the mechanisms underlying cellular aging

Knowledge of the proteasome quality control mechanisms may also yield new treatment modalities for age-related diseases. Currently the idea of treating these diseases by enhancing proteasome activity gets increasing attention [57]. Potential compounds for these treatments are IU1, a small molecule inhibitor of the proteasome associated de-ubiquitination enzyme USP14 [58], and sulforaphane, which induces the expression of proteasome subunits by inducing the transcription factor Nrf2 [59]. An alternative for these methods to enhance proteasome activity may be enhancing the quality control mechanisms of the proteasome, which therefore deserve further attention.

Degradation of 20S proteasomes is also interesting from a more philosophical point of view. Not only because this complex is very stable, but also considering the protease activity inside the 20S. During 20S assembly, protease activity is only activated inside the 20S barrel when the complex assembly has been completed, thus assuring that the cell is protected from unwanted and uncontrolled protein degradation [60]. The mechanisms degrading the 20S can be expected to involve similar precautions. In the proteasome degradation mechanism that we propose in Chapter 5, this requirement is met since the proteasome is degraded inside the lysosome as the result of an autophagy-like process. The acidic conditions in a lysosome may then support unfolding of the 20S proteins as a prelude to complete destruction. The requirement for a protection mechanism makes proteasome degradation by another proteasome unlikely, since this would entail disassembly of the complex before degradation of its subunits. Also, so far no chaperones have been identified that would facilitate 20S disassembly. For the same reasons, it is unlikely that (damaged) subunits within the 20S are turned over individually instead of turnover of the complex as a whole. Whole complex turnover is also consistent with the very similar half-lifes found for the individual subunits of the 20S in mouse brains [61].

All in all, we uncovered novel aspects of proteasome dynamics that may play a role in cellular aging. Our data justifies further research on the role of proteasome localization and proteasome quality control in aging and age-related diseases.

N-acetylation in proteasome dynamics and aging
In Chapter 4 we show the involvement of three N-terminal acetylation complexes (NatA, NatB and NatC) in proteasome localization and fitness during aging of budding yeast [6]. Deletion of different Nat complexes has different effects on proteasome localization and longevity, implying that the N-terminal acetylation of specific (subsets of) proteins is

important for these phenotypes. This may suggest that acetylation of protein N-termini, like acetylation of lysine residues [62,63], is important in age-related processes. The relevant substrate(s) of these Nat complexes and the conservation of a role for N-terminal acetylation in aging in mammalian cells remain to be established.

Like in budding yeast, the major N-acetylation complexes in mammalian cells are NatA, B and C. Their subunit composition and their specificities for certain N-terminal sequences is largely conserved from yeast to human [64,65]. Also, the functionality of N-terminal acetylation shows many conserved aspects. One conserved aspect of N-terminal acetylation is being a modulator of the N-end rule. The N-end rule describes the influence of the N-terminal amino acid and its post translational modifications on the stability of the protein. Proteins can be stabilized by N-terminal acetylation of a (destabilizing) N-terminal amino acid in both yeast and mammalian cells [65,66]. On the other hand, for some proteins in yeast, N-terminal acetylation may also represent a destabilizing signal [67]. A mammalian version of this destabilizing signal remains to be characterized. Other conserved functions of N-terminal acetylation include preventing other N-terminal modifications and mediating protein-protein and protein-membrane interactions [65,68]. Although the Nat complexes and the functionality of N-terminal acetylation seem to be conserved from yeast to human, the very N-termini of substrate proteins are generally not conserved. Therefore it may be necessary to evaluate the N-terminal acetylation status of specific proteins rather than the Nat complexes themselves when considering conserved roles of N-acetylation in proteasome localization and aging.

To further address the (conservation of the) role of N-terminal acetylation in proteasome localization and aging, identification of the relevant Nat substrates would be very helpful. Several substrates tested negative in Chapter 4, but that does not exclude involvement of other (groups of) substrates or may indicate functional redundancy. In principle, loss of a Nat complex can affect proteasome localization by affecting its translocation machinery or by inducing protein damage. Induction of protein damage may also directly affect fitness during aging. A 'damage-induced model' would lead to the following hypotheses on how the different Nat complexes affect proteasome localization and aging.

A population of starved NatC-deficient cells showed WT-like prevalence of PSGs and higher prevalence of nuclear enrichment of the proteasome. Whereas PSGs were most prevalent in replicative young cells, old cells were more likely to retain their proteasomes in the nucleus. Enhanced nuclear retention in NatC-deficient cells may be caused by induction of nuclear protein damage or cytoplasmic protein misfolding. Mother-biased inheritance of this protein damage may allow replicative young cells to store their proteasomes in PSGs. Old cells on the other hand, may need their proteasome in the nucleus to cope with the enhanced load of damage. Enhanced protein damage in old, but not in young, cells may also explain the observed decrease in fitness during the aging of replicative old cells. Loss of NatB activity strongly reduced the prevalence of PSGs in starved cells, whereas nuclear retention of the proteasome was more prevalent then in WT cells. The higher prevalence of nuclear proteasomes in replicative old cells suggests that the mother-biased inheritance of protein damage is intact when NatB activity is lost. Still the low prevalence of PSGs in replicative young cells suggests that the load of protein damage does not allow them to store their proteasomes in PSGs. Increased levels of protein damage in both young and old cells is also consistent with the observed drop in the fitness of both old and young cells.

Unlike NatC and NatB, loss of the NatA complex did not affect the localization of the

6

proteasome in the total population. This suggests that NatA deficiency does not affect the levels of nuclear protein damage or cytosolic protein misfolding. However, the mother-biased inheritance of this damage appeared to be affected, since no correlation between proteasome localization and replicative age was observed in NatA-deficient cells. The lower fitness of both young and old NatA-deficient cells may suggest a higher load of cell damage in both groups, but apparently not of the kind that affects the localization of the proteasome.

In summary, the model of 'damage-induced proteasome localization' is consistent with the data presented in Chapter 4, though further research will be necessary to validate this model. Our data suggest a role for N-terminal acetylation in proteasome localization and fitness during aging. The exact underlying mechanisms remain to be established and may yield novel insights in proteasome dynamics and aging.

Overall summary

In this Thesis we addressed two important aspects of protein dynamics; protein synthesis and distribution upon cell division and the dynamics of the protein degradation machinery. To analyze protein synthesis and distribution upon cell division, one needs to distinguish and simultaneously track old and new proteins. Therefore we developed Recombination-Induced Tag Exchange (RITE) in Chapter 2. In Chapter 3 we used RITE to make a comprehensive analysis of the synthesis and inheritance of all organelles and the major macromolecular complexes in budding yeast. We conclude that most of these large cell structures are synthesized by template-based growth and show symmetric distribution of old and new components upon cell division. Two important exceptions are the nuclear pore complex, that is formed *de novo*, and the spindle pole body, that showed asymmetric inheritance of its components.

The dynamics of the protein degradation machinery is of interest since it is implicated in aging and age-related diseases. In Chapter 4 and 5 we addressed two novel aspects of proteasome dynamics that may be of interest for aging research; proteasome localization and quality control of the proteasome. In Chapter 4 we showed that the localization of the proteasome, like its activity, correlates with fitness during aging. Also, genetic factors involved in proteasome localization and longevity in budding yeast were identified in a genome-wide screening. In Chapter 5 we presented data that is consistent with lysosomal degradation of damaged proteasomes, which may represent the first sketches of a quality control system for the proteasome.

References

1. Verzijlbergen, K. F. *et al*. Recombination-induced tag exchange to track old and new proteins. PNAS 107, 64–68 (2010).

2. Terweij, M. *et al*. Recombination-induced tag exchange (RITE) cassette series to monitor protein dynamics in *Saccharomyces cerevisiae*. G3 3, 1261–72 (2013).

3. Radman-Livaja, M. *et al*. Patterns and mechanisms of Ancestral Histone protein inheritance in Budding yeast. PLoS Biol. 9, (2011).

4. Thayer, N. H. *et al*. Identification of long-lived proteins retained in cells undergoing repeated asymmetric divisions. PNAS 111, 14019–26 (2014).

5. Menendez-Benito, V. *et al*. Spatiotemporal analysis of organelle and macromolecular complex inheritance. PNAS 110, 175–180 (2012).

6. Van Deventer, S. J., Menendez-Benito, V., van Leeuwen, F. & Neefjes, J. N-Terminal Acetylation And Replicative Age Affect Proteasome Localization And Cell Fitness During Aging. J. Cell Sci. (2014).

7. Verzijlbergen, K. F. *et al*. A barcode screen for epigenetic regulators reveals a role for the NuB4/HAT-B histone acetyltransferase complex in histone turnover. PLoS Genet. 7, 18–24 (2011).

8. Gray, J. V *et al*. Sleeping Beauty : Quiescence in *Saccharomyces cerevisiae*. Microbiol. Mol. Biol. Rev. 68, 188–202 (2004).

9. Dambournet, D., Hong, S. H., Grassart, A. & Drubin, D. G. Tagging Endogenous Loci for Live- Cell Fluorescence Imaging and Molecule Counting Using ZFNs , TALENs , and Cas9. Methods Enzymol. 546, 139–160 (Elsevier Inc., 2014).

10. Higuchi, R. *et al*. Actin dynamics affect mitochondrial quality control and aging in budding yeast. Curr. Biol. 23, 2417–22 (2013).

11. McFaline-Figueroa, J. R. *et al*. Mitochondrial quality control during inheritance is associated with lifespan and mother-daughter age asymmetry in budding yeast. Aging Cell 10, 885–95 (2011).

12. Fernandez-Martinez, J. & Rout, M. P. Nuclear pore complex biogenesis. Curr. Opin. Cell Biol. 21, 603–612 (2009).

13. Khmelinskii, A., Keller, P. J., Lorenz, H., Schiebel, E. & Knop, M. Segregation of yeast nuclear pores. Nature 466, E1 (2010).

14. Shcheprova, Z., Baldi, S., Frei, S. B., Gonnet, G. & Barral, Y. A mechanism for asymmetric segregation of age during yeast budding. Nature 454, 728–734 (2008).

15. Colombi, P., Webster, B. M., Fröhlich, F. & Patrick Lusk, C. The transmission of nuclear pore complexes to daughter cells requires a cytoplasmic pool of Nsp1. J. Cell Biol. 203, 215–232 (2013).

16. Pereira, G., Tanaka, T. U., Nasmyth, K. & Schiebel, E. Modes of spindle pole body inheritance and segregation of the Bfa1p-Bub2p checkpoint protein complex. EMBO J. 20, 6359–6370 (2001).

17. Cerveny, K. L., Tamura, Y., Zhang, Z., Jensen, R. E. & Sesaki, H. Regulation of mitochondrial fusion and division. Trends Cell Biol. 17, 563–9 (2007).

18. Motley, A. M. & Hettema, E. H. Yeast peroxisomes multiply by growth and division. J. Cell Biol. 178, 399–410 (2007).

19. Hoepfner, D., Schildknegt, D., Braakman, I., Philippsen, P. & Tabak, H. F. Contribution of the endoplasmic reticulum to peroxisome formation. Cell 122, 85–95 (2005).

20. Laporte, D., Salin, B., Daignan-Fornier, B. & Sagot, I. Reversible cytoplasmic localization of the proteasome in quiescent yeast cells. J. Cell Biol. 181, 737–45 (2008).

21. Kaganovich, D., Kopito, R. & Frydman, J. Misfolded proteins partition between two distinct quality control compartments. Nature 454, 1088–95 (2008).

22. Enenkel, C. Proteasome dynamics. Biochim. Biophys. Acta 1843, 39–46 (2014).

23. Liu, B. *et al*. The polarisome is required for segregation and retrograde transport of protein aggregates. Cell 140, 257–67 (2010).

24. Weberruss, M. H. *et al*. Blm10 facilitates nuclear import of proteasome core particles. EMBO J. 32, 2697–707 (2013).

25. Peters, L. Z., Hazan, R., Breker, M., Schuldiner, M. & Ben-Aroya, S. Formation and dissociation of proteasome storage granules are regulated by cytosolic pH. J. Cell Biol. 201, 663–71 (2013).

26. Bajorek, M., Finley, D. & Glickman, M. H. Proteasome Disassembly and Downregulation Is Correlated with Viability during Stationary Phase. Curr. Biol. 13, 1140–1144 (2003).

27. Saunier, R., Esposito, M., Dassa, E. P. & Delahodde, A. Integrity of the *Saccharomyces cerevisiae* Rpn11 protein is critical for formation of proteasome storage granules (PSG) and survival in stationary phase. PLoS One 8, e70357 (2013).

28. Hanna, J., Waterman, D., Boselli, M. & Finley, D. Spg5 protein regulates the proteasome in quiescence. J. Biol. Chem. 287, 34400–9 (2012).

29. Hartl, F. U., Bracher, A. & Hayer-Hartl, M. Molecular chaperones in protein folding and proteostasis. Nature 475, 324–32 (2011).

30. Narayanaswamy, R., Levy, M., Tsechansky, M. & Stovall, G. M. Widespread reorganization of metabolic enzymes into reversible assemblies upon nutrient starvation. PNAS 106, 10147–10152 (2009).

31. Sagot, I., Pinson, B., Salin, B. & Daignan-Fornier, B. Actin Bodies in Yeast Quiescent Cells : An Immediately Available Actin Reserve ? Mol. Cell. Biol. 17, 4645–4655 (2006).

32. Petrovska, I. *et al*. Filament formation by metabolic enzymes is a specific adaptation to an advanced state of cellular starvation. Elife 1–19 (2014).

33. Liu, I.-C., Chiu, S.-W., Lee, H.-Y. & Leu, J.-Y. The histone deacetylase Hos2 forms an Hsp42-dependent cytoplasmic granule in quiescent yeast cells. Mol. Biol. Cell 23, 1231–42 (2012).

34. Vilchez, D., Saez, I. & Dillin, A. The role of protein clearance mechanisms in organismal ageing and age-related diseases. Nat. Commun. 5, 5659 (2014).

35. Schmidt, M. & Finley, D. Regulation of proteasome activity in health and disease. Biochim. Biophys. Acta 1843, 13–25 (2014).

36. Carrard, G., Bulteau, A.-L., Petropoulos, I. & Friguet, B. Impairment of proteasome structure and function in aging. Int. J. Biochem. Cell Biol. 34, 1461–1474 (2002).

37. Vernace, V. A., Arnaud, L., Schmidt-glenewinkel, T. & Figueiredo-, M. E. Aging perturbs 26S proteasome assembly in Drosophila melanogaster. Faseb J 21, 2672–2682 (2012).

38. Chondrogianni, N., Petropoulos, I., Franceschi, C., Friguet, B. & Gonos, E. . Fibroblast cultures from healthy centenarians have an active proteasome. Exp. Gerontol. 35, 721–728 (2000).

39. Chen, Q., Thorpe, J., Dohmen, J. R., Li, F. & Keller,

J. N. Ump1 extends yeast lifespan and enhances viability during oxidative stress: central role for the proteasome? Free Radic. Biol. Med. 40, 120–6 (2006).

40. Kruegel, U. *et al*. Elevated proteasome capacity extends replicative lifespan in *Saccharomyces cerevisiae*. PLoS Genet. 7, e1002253 (2011).

41. Lindquist, S. L. & Kelly, J. W. Chemical and biological approaches for adapting proteostasis to ameliorate protein misfolding and aggregation diseases: progress and prognosis. Cold Spring Harb. Perspect. Biol. 3, 1–34 (2011).

42. Nyström, T. & Liu, B. The mystery of aging and rejuvenation - a budding topic. Curr. Opin. Microbiol. 18, 61–7 (2014).

43. Aguilaniu, H., Gustafsson, L., Rigoulet, M. & Nyström, T. Asymmetric inheritance of oxidatively damaged proteins during cytokinesis. Science 299, 1751–3 (2003).

44. Gardner, R. G., Nelson, Z. W. & Gottschling, D. E. Degradation-mediated protein quality control in the nucleus. Cell 120, 803–815 (2005).

45. Nielsen, S. V, Poulsen, E. G., Rebula, C. A. & Hartmann-Petersen, R. Protein quality control in the nucleus. Biomolecules 4, 646–661 (2014).

46. Prasad, R., Kawaguchi, S. & Ng, D. T. W. A nucleus-based quality control mechanism for cytosolic proteins. Mol. Biol. Cell 21, 2117–27 (2010).

47. Heck, J. W., Cheung, S. K. & Hampton, R. Y. Cytoplasmic protein quality control degradation mediated by parallel actions of the E3 ubiquitin ligases Ubr1 and San1. PNAS 107, 1106–1111 (2010).

48. Palmer, A. *et al*. Subpopulations of proteasomes in rat liver nuclei , microsomes and cytosol. Biochem. J. 407, 401–407 (1996).

49. Reits, E., Benham, M., Plougastel, B., Neefjes, J. & Trowsdale, J. Dynamics of proteasome distribution in living cells. EMBO J. 16, 6087–94 (1997).

50. Russell, S. J., Steger, K. A. & Johnston, S. A. Subcellular Localization, Stoichiometry, and Protein Levels of 26 S Proteasome Subunits in Yeast. J. Biol. Chem. 274, 21943–21952 (1999).

51. Iwata, A. *et al*. Intranuclear degradation of polyglutamine aggregates by the ubiquitin-proteasome system. J. Biol. Chem. 284, 9796–9803 (2009).

52. Park, S. H. *et al*. PolyQ proteins interfere with nuclear degradation of cytosolic proteins by sequestering the Sis1p chaperone. Cell 154, 134–145 (2013).

53. Brooks, P. *et al*. Subcellular localization of proteasomes and their regulatory complexes in mammalian cells. Biochem. J. 161, 155–161 (2000).

54. Fabre, B. *et al*. Subcellular distribution and dynamics of active proteasome complexes unraveled by a workflow combining *in vivo* complex cross-linking and quantitative proteomics. Mol. Cell. Proteomics 12, 687–99 (2013).

55. Bellavista, E. *et al*. Lifelong maintenance of composition, function and cellular/subcellular distribution of proteasomes in human liver. Mech. Ageing Dev. 141-142C, 26–34 (2014).

56. Adori, C. *et al*. The ubiquitin-proteasome system in Creutzfeldt-Jakob and Alzheimer disease: intracellular redistribution of components correlates with neuronal vulnerability. Neurobiol. Dis. 19, 427–35 (2005).

57. Dantuma, N. P. & Bott, L. C. The ubiquitin-proteasome system in neurodegenerative diseases: precipitating factor, yet part of the solution. Front. Mol. Neurosci. 7, 70 (2014).

58. Lee, B. *et al*. Enhancement of Proteasome Activity by a Small-Molecule Inhibitor of Usp14. Nature 467, 179–184 (2011).

59. Liu, Y. *et al*. Sulforaphane enhances proteasomal and autophagic activities in mice and is a potential therapeutic reagent for Huntington's disease. J. Neurochem. 129, 539–547 (2014).

60. Tomko, R. J. & Hochstrasser, M. Molecular architecture and assembly of the eukaryotic proteasome. Annu. Rev. Biochem. 82, (2013).

61. Price, J. C., Guan, S., Burlingame, A., Prusiner, S. B. & Ghaemmaghami, S. Analysis of proteome dynamics in the mouse brain. PNAS 107, 14508–14513 (2010).

62. Donmez, G. & Guarente, L. Aging and disease: Connections to sirtuins. Aging Cell 9, 285–290 (2010).

63. Hebert, A. S. *et al*. Calorie restriction and SIRT3 trigger global reprogramming of the the mitochondrial protein acetylome. Mol Cell 487, 109–113 (2013).

64. Arnesen, T. *et al*. Proteomics analyses reveal the evolutionary conservation and divergence of N-terminal acetyltransferases from yeast and humans. PNAS 106, 8157–8162 (2009).

65. Starheim, K. K., Gevaert, K. & Arnesen, T. Protein N-terminal acetyltransferases: when the start matters. Trends Biochem. Sci. 37, 152–61 (2012).

66. Sriram, S. M., Kim, B. Y. & Kwon, Y. T. The N-end rule pathway: emerging functions and molecular principles of substrate recognition. Nat. Rev. Mol. Cell Biol. 12, 735–47 (2011).

67. Hwang, C.-S., Shemorry, A. & Varshavsky, A. N-Terminal Acetylation of Cellular Proteins Creates Specific Degradation Signals. Science (80-.). 29, 997–1003 (2012).

68. Arnesen, T. Towards a functional understanding of protein N-terminal acetylation. PLoS Biol. 9, e1001074 (2011).

6

Summary

When proteins would be static entities, instead of the highly dynamic entities they are, life would never have evolved. It is the complex interplay of protein synthesis, folding, degradation, modification, movement and interactions that makes a cell something alive instead of a lifeless bag full of proteins. Understanding these protein dynamics is therefore pivotal to understand life and is essential to understand the causes and treatment of many human diseases. In this Thesis we address two important aspects of protein dynamics; protein synthesis and distribution upon cell division and dynamics of the protein degradation machinery.

Adequate synthesis and distribution of proteins upon cell division is important to make sure that both new cells get enough starting material to support life. This is particularly true for the proteins inside organelles and macromolecular complexes, since these large cell structures are essential for the cell and often synthesized in a template-based manner. Therefore, components of the existing organelles and macromolecular complexes need to be adequately shared between both new cells (inheritance) and complemented with synthesis of new components. Synthesis of organelles and macromolecular complexes can occur either *de novo* or template-based. The mechanisms underlying the inheritance and synthesis of organelles and macromolecular complexes have been extensively studied in budding yeast, yet important questions remained unanswered. Like whether both new cells get an equal share of existing and new components and to what extend some of these structures are synthesized in a *de novo* or template-based manner.

To address these questions one needs to distinguish and simultaneously track old and new proteins. We therefore developed the Recombination-Induced Tag Exchange (RITE) technique in **Chapter 2**. RITE is a genetic method that induces a permanent epitope-tag switch in the coding sequence after a transient hormone-induced activation of Cre recombinase. Old and new proteins can thus be simultaneously tracked by their different tags and the variety of available tags allows detection by a wide range of methods.

In **Chapter 3** we applied RITE to make a comprehensive analysis of the synthesis and inheritance of organelles and macromolecular complexes upon cell division. Asymmetric inheritance of these large cell structures are of interest since they can induce lineage differences and play a role in cell differentiation. Our analysis shows that, in general, old and new components of organelles and macromolecular complexes are symmetrically inherited. Apparently the age of these components does not play a role in asymmetric inheritance and does not induce lineage differences. An interesting exception to this common rule is the Spindle Pole Body (SPB), the yeast centrosome, which shows predominant inheritance of old components in the young daughter cell. The biological consequence of this asymmetrical inheritance remains to be determined. Our RITE-based analysis also shows that all membrane-containing organelles are synthesized in a template-based manner in budding yeast. This was known or expected for most organelles, but still debated for peroxisomes. Also most macromolecular complexes showed a template based synthesis, with the interesting exception of the nuclear pore complex (NPC). Our data not only shows *de novo* synthesis of NPC's, but also suggests that there is no exchange of old for new subunits in this very stable complex over many generations.

The dynamics of the protein degradation machinery is of interest since it affects the

degradation of damaged proteins in aging cells. The accumulation of damaged proteins in aging cells suggests that insufficient protein degradation is an important factor in cellular aging and is implicated in several age-related diseases. An important mechanism for the degradation of damaged proteins is the ubiquitin-proteasome system (UPS). The activity of the UPS is found to decrease during the aging of several model organisms and this decrease is suggested to play a causative role in cellular aging. Also, enhanced UPS activity seems to correlate with enhanced longevity. These observations fueled a growing interest in the role of UPS activity in the aging process and raise the possibility of curing age-related diseases by enhancing this activity.

In **Chapter 4** we present data that suggest that not only the activity of the UPS, but also the localization of this activity may play a role in cellular aging. We found a correlation between the localization of the proteasome and the replicative age of starving budding yeast cells, a frequently used model for cell aging. Also, a genome-wide screening identified a role for N-terminal acetylation in both proteasome localization and fitness during cellular aging. All in all our data justifies further research on the role of proteasome localization in aging and age-related diseases.

One reason for the decrease in UPS activity during aging may be a decreasing 'fitness' of the pool of proteasomes. Being a protein complex itself, the proteasome is vulnerable to protein damage which may compromise its activity. Therefore, analogous to damaged proteins, one would expect damaged proteasomes to be cleared from the cell. The scope and mechanisms of such proteasome quality control however, remained to be determined.

In **Chapter 5** we present the first sketches of a potential proteasome quality control mechanism. Our data is consistent with a model in which damaged proteasomes are degraded by some form of autophagy. The specifics and specificity of this degradation remain to be established and is of high interest since it is likely to play a role in both cellular aging and age-related diseases.

In summary, this Thesis provides a comprehensive analysis of the synthesis and inheritance of organelles and macromolecular complexes upon cell division and uncovers novel aspects of proteasome dynamics that may play a role in cellular aging.

Nederlandse Samenvatting

De Griekse filosoof Heraclitus zei ooit "Panta rhei", oftewel "Alles stroomt". Hoewel hij daarbij waarschijnlijk niet aan eiwitten dacht, is deze spreuk daar zeker op van toepassing. Eiwitten in een cel worden namelijk continu gesynthetiseerd, afgebroken, gemodificeerd, verplaatst en gekoppeld aan andere celcomponenten. Al deze processen samen worden eiwitdynamiek genoemd en zijn essentieel voor het voortbestaan en functioneren van een cel. Het bestuderen van deze dynamiek is belangrijk om de werking van cellen te snappen en om meer inzicht te krijgen in het ontstaan en de behandeling van ziektes. Dit proefschrift gaat over twee belangrijke aspecten van eiwitdynamiek: synthese en verdeling van eiwitten tijdens celdeling en de dynamiek van het eiwitafbraakmechanisme.

De synthese en verdeling van eiwitten tijdens celdeling is belangrijk, omdat beide nieuwe cellen voldoende materiaal moeten krijgen voor een succesvolle start van hun leven. Dit is zeker van belang voor de eiwitten in organellen en macromoleculaire complexen, aangezien deze grote celonderdelen essentieel zijn voor de cel en vaak een stuk van zichzelf nodig hebben voor hun synthese. De eiwitten in de al bestaande organellen en macromoleculaire complexen moeten daarom goed worden verdeeld over beide nieuwe cellen (dit heet overerving) en worden aangevuld met nieuwe eiwitten. Die nieuwe eiwitten kunnen worden toegevoegd aan bestaande structuren (template-based synthese) of een compleet nieuwe structuur maken (*de novo* synthese). De mechanismen die ten grondslag liggen aan de synthese en overerving van organellen en macromoleculaire complexen zijn in het verleden uitgebreid onderzocht in de bakkersgist *Saccharomyces cerevisiae*. Toch bleven er belangrijke aspecten onduidelijk. Zoals de mate waarin sommige organellen template-based danwel *de novo* worden gemaakt en of beide nieuwe cellen evenveel bestaande en nieuw gemaakte eiwitten krijgen. Deze laatste vraag is van belang omdat asymmetrische overerving generatieverschillen kunnen induceren en een rol kunnen spelen bij celdifferentiatie.

Om dit soort vraagstukken te beantwoorden is het belangrijk om oude en nieuwe eiwitten te kunnen onderscheiden en tegelijktertijd te kunnen volgen. In **hoofdstuk 2** wordt daarom Recombination-Induced Tag Exchange (RITE) gepresenteerd, een genetische methode waarbij de labeling van een eiwit op DNA niveau permanent kan worden verandert door het tijdelijk activeren van een Cre recombinase enzym. Oude en nieuwe eiwitten kunnen dan tegelijkertijd worden gevolgd doordat ze een verschillend label hebben. Omdat er heel veel verschillende labels zijn, kun je RITE gebruiken met een breed scala aan detectietechnieken.

Met behulp van de RITE techniek is in **hoofdstuk 3** vervolgens een overzicht gemaakt van de synthese en overerving van alle organellen en de belangrijkste macromoleculaire complexen in bakkersgist. Hieruit blijkt dat oude en nieuwe eiwitten in organellen en macromoleculaire complexen zich tijdens de celdeling in het algemeen gelijk verdelen over beide nieuwe cellen. Blijkbaar speelt de leeftijd van deze eiwitten geen rol bij de overerving en zal dus ook geen generatie verschillen veroorzaken. Een interessante uitzondering op die regel is het centrosoom, waarvan de oude eiwitten bij de celdeling met name in de jonge dochtercel terechtkomen. Of deze assymmetrische overerving ook generatieverschillen veroorzaakt zal verder onderzoek moeten uitwijzen. De resultaten in hoofdstuk 3 maken ook duidelijk dat alle organellen worden gesynthetiseerd op een template-based manier. Dit was al verwacht of aangetoond voor de meeste organellen,

maar was nieuw voor peroxisomen. Ook sommige macromoleculaire complexen, zoals de nucleolus en het centrosoom, gebruiken template-based synthese. Dit in tegenstelling tot kern-poriën, die *de novo* worden gevormd en stabiel zijn gedurende meerdere celdelingen.

De dynamiek van het eiwitafbraakmechanisme in cellen is onder andere belangrijk om de ophoping van beschadigde eiwitten tegen te gaan. Het ophopen van beschadigde eiwitten is een teken van cellulaire veroudering en speelt een belangrijke rol in verouderingsziektes zoals de ziekte van Alzheimer. Een essentieel eiwitafbraakmechanisme is het ubiquitine-proteasoom systeem (UPS). De activiteit van het UPS neemt doorgaans af tijdens het verouderingsproces en het verhogen van deze activiteit kan in sommige modelsystemen veroudering vertragen. Dit suggereerd dat de activiteit van het UPS een dominante factor is in het verouderingsproces van cellen en organismen. Vandaar ook dat er veel onderzoek wordt gedaan naar manieren om deze activiteit te verhogen, om daarmee veroudering af te remmen en verouderingsziektes te behandelen.

De resultaten in **hoofdstuk 4** laten zien dat niet alleen de activiteit van het UPS, maar wellicht ook de localisatie ervan van belang is voor cellulaire veroudering. De localisatie van een belangrijk onderdeel van het UPS, het proteasoom, blijkt namelijk te correleren met de leeftijd van de cel in verouderende bakkersgist. Ook vinden we in dit veelgebruikte onderzoeksmodel voor veroudering een rol voor N-terminale acetylatiecomplexen in zowel proteasoomlocalisatie als de fitheid van een cel tijdens veroudering.

De reden voor afname van de activiteit van het UPS tijdens veroudering is onduidelijk, al zijn er verschillende verklaringen te bedenken. Eén daarvan is dat het proteasoom tijdens veroudering beschadigd raakt en daardoor minder actief wordt. Om te zorgen dat de cel dan voldoende proteasoomactiviteit overhoudt, zou je verwachten dat beschadigde proteasomen worden afgebroken en vervangen door nieuwe, zoals ook gebeurt met beschadigde eiwitten. Het mechanisme van zo'n kwaliteitscontrolesysteem en z'n mogelijke rol in veroudering moet nog worden uitgezocht.

Hoofdstuk 5 van dit proefschrift maakt aannemelijk dat het lysosoom een rol speelt in de afbraak van het proteasoom in bakkersgist en HeLa cellen en dat het proteasoom daar terecht komt door een vorm van autophagy. Daarnaast wijzen de observaties in HeLa cellen er op dat er mogelijk een selectiviteit is voor beschadigde proteasomen. Verder onderzoek moet gaan uitwijzen of we hier de eerste stukjes van een kwaliteitscontrolesysteem voor het proteasoom hebben gevonden.

Curriculum Vitae

Sjoerd van Deventer was born on the 25th of September, 1984, in Apeldoorn. There he enjoyed his secondary school at the Veluws College and passed his final VWO exams in 2003. In the same year he moved to Wageningen to start his study Molecular Sciences at the Wageningen University. After receiving his Bachelor's degree in 2007, with a minor in Biological Chemistry, he continued pursuing this specialization in his Master study. In the first of three Master internships he studied the arms race between RNA viruses and plants in the research group of Prof. dr. Rob Goldbach at the Wageningen University. In his second internship he tried to find genes involved in proteasome dynamics in budding yeast. The research was performed under supervision of dr. Victoria Menendez-Benito in the group of Prof. dr. Jacques Neefjes at the Netherlands Cancer Institute in Amsterdam. After studying the proteasome he decided to study another aspect of protein quality control in his last internship; chaperones. He studied the role of small heatshock proteins in oxidative stress in the lab of dr. Wilbert Boelens at the NCMLS in Nijmegen.

After receiving his Master's degree in 2009, Sjoerd returned to the Netherlands Cancer Institute in Amsterdam to further pursue the research of his internship as a PhD student. In this research he combined the cell biological expertise of the research group of his promotor Prof. dr. Jacques Neefjes with the budding yeast expertise of the research group of dr. Fred van Leeuwen. The results of this research can be found in this Thesis.

List of Publications

N-terminal acetylation and replicative age affect proteasome localization and fitness during aging
S.J. van Deventer, V. Menendez-Benito, F. van Leeuwen and J. Neefjes
Journal of Cell Science, 128(1): 109-117, January 2015

Recombination-Induced Tag Exchange (RITE) Cassette Series to Monitor Protein Dynamics in Saccharomyces cerevisiae
M. Terweij, T. van Welsem, **S.J. van Deventer**, K.F. Verzijlbergen, V. Menendez-Benito, D. Antoso, P. San-Segundo, J. Neefjes and F. van Leeuwen
G3, 3(8) 1261-1272, August 2013

Spatiotemporal analysis of organelle and macromolecular complex inheritance
V. Menendez-Benito, **S. J. van Deventer**, V. Jimenez-Garcia, M. Roy-Luzarraga, F. van Leeuwen and J. Neefjes
PNAS, 110(1): 175-180, January 2013

The Immunoproteasome Cleans up after Inflammation (Preview)
S.J. van Deventer and J. Neefjes
Cell, 142(4): 517-8, August 2010

Recombination-Induced Tag Exchange to track old and new proteins
K.F. Verzijlbergen, V. Menendez-Benito, T. van Welsum, **S.J. van Deventer**, D.L. Lindstrom, H. Ovaa, J. Neefjes, D.E. Gottschling and F. van Leeuwen
PNAS, 107(1): 64-68, Jan 2010

Two Dot1 isoforms in Saccharomyces cerevisiae as a result of leaky scanning by the ribosome
F. Frederiks, G.J. Heynen, **S.J. van Deventer**, H. Janssen and F. Van Leeuwen
Nucleic Acids Research, 37(21): 7047-58, November 2009

Acknowledgements